ISSN 1023-9855

Thoracic Medicine

Volume 38 • Number 1 • March 2023

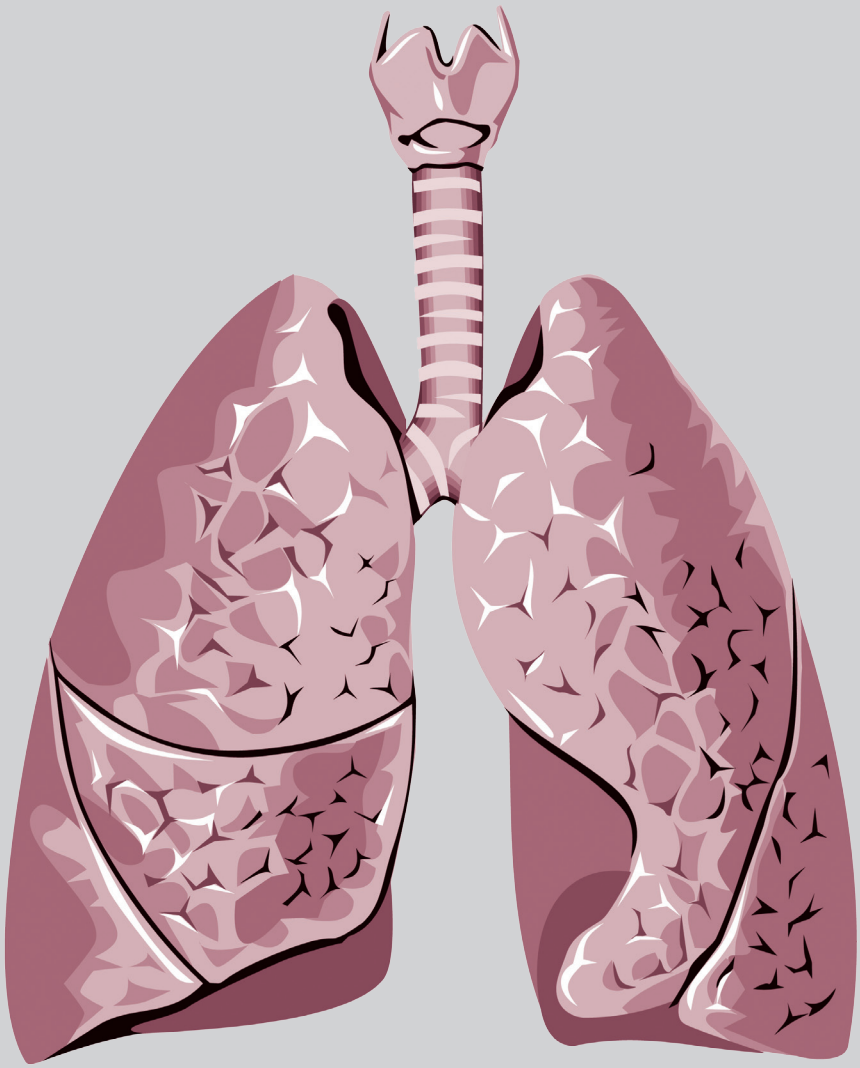

The Official Journal of

Taiwan Society of Pulmonary and Critical Care Medicine

Taiwan Society of Sleep Medicine

Taiwan Society for Respiratory Therapy

Taiwan Society of Tuberculosis and Lung Diseases

Thoracic Medicine

The Official Journal of
Taiwan Society of Pulmonary and Critical Care Medicine
Taiwan Society for Respiratory Therapy
Taiwan Society of Sleep Medicine
Taiwan Society of Tuberculosis and Lung Diseases

Thoracic Medicine

The Official Journal of
Taiwan Society of Pulmonary and Critical Care Medicine
Taiwan Society for Respiratory Therapy
Taiwan Society of Sleep Medicine
Taiwan Society of Tuberculosis and Lung Diseases

Volume 38
Number 1
March 2023

CONTENTS

Orginial Articles

Case Reports

Continuous Positive Airway Pressure Reduces Serum Levels of Alzheimer Disease-Related Proteins in Patients with Obstructive Sleep Apnea

Ching-Shan Luo[1,2], Shang-Yang Lin[3], Sheng-Ming Wu[1,4], Cheng-Yu Tsai[5], Wen-Te Liu[1,3,6], Po-Hao Feng[1,4]

Introduction: Alzheimer disease (AD) is the most common form of dementia, and patients with obstructive sleep apnea (OSA) show significantly high serum levels of AD-related proteins. Because of the high AD prevalence, the heavy burden on the medical system, and the lack of promising pharmacological options, treatments focusing on reducing AD risk must be urgently explored. Hypoxia causes the accumulation of AD-related proteins, and sleep disruption may disturb the clearance process. Continuous positive airway pressure (CPAP) is supposed to improve nocturnal oxygen saturation and sleep quality, thus reducing AD risk.

Methods: The role of short-term CPAP in reducing the serum level of AD-related proteins in patients with OSA was evaluated using immuno-magnetic reduction technology. Twenty-three OSA patients were divided into 4 groups according to whether they had received CPAP or not, and their AD risk was assessed by calculating the product of 2 AD-related proteins. The serum levels of tau and amyloid β (Aβ)42 were determined before and after 3–6 months of CPAP treatment (with a corresponding time for those patients who refused CPAP).

Results: After short-term CPAP treatment, the serum levels of tau and Aβ42 were significantly reduced in the high AD risk group.

Conclusion: Our preliminary result shows that short-term CPAP treatment efficiently reduces the serum level of AD-related proteins in OSA patients with a high AD risk. We highly recommend incorporating hematological biomarker examinations into routine tests for OSA patients, as well as the use of CPAP treatment for patients with a high AD risk. ***(Thorac Med 2023; 38: 1-9)***

Key words: Continuous positive airway pressure, Obstructive sleep apnea, Alzheimer disease, Amyloid beta protein, Tau proteins, Immuno-magnetic reduction assay

[1]Division of Pulmonary Medicine, Department of Internal Medicine, Shuang Ho Hospital, Taipei Medical University, New Taipei City, Taiwan, [2]International Ph.D. Program for Cell Therapy and Regeneration Medicine, College of Medicine, Taipei Medical University, Taipei, Taiwan, [3]School of Respiratory Therapy, Taipei Medical University, Taipei, Taiwan, [4]Division of Pulmonary Medicine, Department of Internal Medicine, School of Medicine, College of Medicine, Taipei Medical University, Taipei, Taiwan, [5]Department of Civil and Environmental Engineering, Imperial College London, London, UK, [6]Sleep Center, Shuang Ho Hospital, New Taipei City, Taiwan
Address reprint requests to: Dr. Po-Hao Feng, Department of Internal Medicine, Shuang Ho Hospital, No.291, Zhongzheng Rd., Zhonghe District, New Taipei City, 23561, Taiwan

Introduction

Alzheimer disease (AD) is the most common cause of dementia (72%), and has become a growing global concern following the changes in worldwide demographics [1]. AD is commonly observed in the older population, and its prevalence has increased exponentially with age, reaching a level of 47.2% in the population >85 years old [2]. According to the World Health Organization, the current global cost of treating and caring for people with dementia is >US$604 billion per year, and Alzheimer Europe (a nongovernmental organization that promotes the rights of people with dementia) estimates that the cost could increase by 43% from 2008 to 2030 [3]. However, so far, the efficacy of AD treatment is controversial. Certain drugs that target cholinergic and glutamatergic neurotransmission are only partly successful, and although they may improve symptoms, their neuro-protective activity is doubtful [4]. Owing to the large amount of manpower required, and the social and economic burden of AD management, identifying AD risks early and developing treatments that reduce those risks are urgently needed.

The mechanism of AD development is unclear, but it usually features an accumulation of extracellular amyloid β (Aβ) plaques and abnormal hyperphosphorylation of the microtubule-associated protein tau, which aggregates into neurofibrillary tangles in the brain [5]. Previously, clinical AD diagnosis involved cerebrospinal fluid (CSF) biomarker sampling [6]. Although such sampling has excellent diagnostic accuracy, obtaining CSF is far more difficult than drawing blood, and is rarely performed during routine hematology tests. Ultrasensitive measurement techniques have made blood biomarkers of neurodegeneration a reality. Immuno-magnetic reduction (IMR) assays can sensitively detect trace proteins (including the proteins tau and Aβ42, which are the greatest contributors to AD) in blood through the measurement of magnetic flux reduction, and these assays have become a commonly used commercial examination for AD patients [7].

In recent years, an increasing number of studies have reported the relationship between sleep and AD. In a randomized clinical trial, sleep deprivation was proved to increase Aβ42 levels [8]. Moreover, combining the results of images obtained through Pittsburgh compound-B positron emission tomography (PiB-PET) and a questionnaire, Aβ burden was found to be reversely associated with sleep duration [9]. Among patients with sleep disorders, obstructive sleep apnea (OSA) syndrome is a common subgroup, and is known as an independent risk factor for several diseases, such as hypertension, cardiovascular disease, cerebrovascular accident, and diabetes mellitus [10]. OSA is also a crucial public health issue due to its relationship to hypersomnolence, traffic accidents, cardiovascular events, metabolic disorder, cognitive impairment, depression, and anxiety [11]. A study showed that OSA patients exhibited considerably higher serum Aβ40, Aβ42, and total Aβ levels than age- and sex-matched controls [12].

In clinical practice, continuous positive airway pressure (CPAP) therapy is the standard treatment for patients with moderate to severe OSA, and studies have shown that it effectively eliminates obstructive respiratory events [13]. This study aims to understand whether CPAP reduces AD-related proteins in OSA patients.

Materials and Methods

Participants

This study was conducted according to human study protocols approved by the Institutional Review Board of Taipei Medical University (approval number: N201709023). Patients aged between 20 and 80 years with at least 2 of the following 5 clinical features were included: (1) daytime sleepiness and fatigue; (2) sleep fragmentation or sleeping difficulty; (3) snoring during sleep; (4) witnessed sleep apnea, and (5) an apnea–hypopnea index (AHI) ≥ 5 times per hour, assessed through polysomnography. Patients with the following medical conditions were excluded: anemia, pregnancy, cancer, severe heart disease (myocardial infarction, heart failure, arrhythmia, etc.), and severe mental or psychological disorders such as dementia. Thirty-two patients gave written informed consent and were enrolled. After conventional CPAP instruction, the patients were assigned to the CPAP or CPAP-free group, based on their own choice, and a first hematological biomarker examination was conducted. Using the examination results, we further divided the patients in both the CPAP and CPAP-free group into high- or low-AD risk subgroups, based on the product of tau and Aβ42 protein levels [greater or less than 382.68 (pg/mL)2] [14]. After 3–6 months of CPAP treatment (with a corresponding time for the CPAP-free group), we conducted a second hematological biomarker examination in all 4 groups, to evaluate the effect of CPAP on the serum level of AD-related proteins. Assays were performed without personally identifiable information and medical records.

Hematological Test

A hematological biomarker examination was conducted by MagQu Co. Ltd. (New Taipei City, Taiwan), using IMR technology. For each patient, 16 mL of whole blood was collected in an EDTA tube, and samples were centrifuged at 2,500 g for 15 min at room temperature within 15 min after the blood had been drawn. Plasma was collected and stored at −80°C. Frozen plasma aliquots were shipped on dry ice to MagQu Co. Ltd. for IMR assays. The reagent of IMR is a solution with magnetic nanoparticles, which are coated with a bio-probe (e.g., antibodies) and oscillated under external magnetic fields. Once these magnetic nanoparticles associate with target antigens, they aggregate and become larger, hence the response to external magnetic fields is much less than that of the original individual ones. The greater the number of target antigens in the reagent, the greater the number of aggregated magnetic nanoparticles, so there is a larger reduction in magnetic flux for the reagents. The reduction in the magnetic property of the reagent precisely indicates the amount of the target antigen in the reagent. The concentration of the target protein is determined based on the reduction in the magnetic field.

Treatment

For the CPAP treatment group, APEX iCH Auto 2 was provided and technologically supported online by APEX Co. (New Taipei City, Taiwan). The CPAP-free group included patients accepting the oral appliance and the pharmacological and surgical treatments, based on the physician's advice.

Statistics

Nine of the participants were excluded because of either loss to follow-up or a lack of compliance (eligible compliance was defined as CPAP use of at least 4 hours a day for more

than 70% of the time during the trial period, based on patient self-report, for example, "greater than 4 hours a day and more than 5 days usage a week"). Twenty-three patients were included in the final analysis. To evaluate the effect of CPAP on AD risk in OSA patients, we used the mean reduction of the tau and Aβ42 protein levels and the product of these 2 values as indicators for AD risk reduction. Kruskal-Wallis (K-W) tests were conducted, and if the results were significant, post hoc Bonferroni-adjusted t-contrasts were computed.

Results

Twenty-three patients were included in the final analysis of this study, and their demographic data are presented in Table 1. All patients were cognitively normal and were assigned to 1 of the 4 groups according to their treatment (CPAP or other treatment) and AD risk (high or low). Age, height, weight, body mass index, neck circumference, and waistline were not significantly different among the 4 groups (K-W test: $p = 0.82$, 0.53, 0.38, 0.44, 0.36, and 0.12, respectively). Furthermore, OSA severity, which was assessed using the AHI, was not significantly different among the 4 groups (K-W test: $p = 0.09$).

Regardless of their treatment program, a hematological biomarker test was conducted again after treatment for 3–6 months. Comparing the first and second test outcomes, we obtained the serum level reductions of tau and Aβ42, and the product of these 2 protein levels. These 3 indexes were all significantly different among the 4 groups (K-W test: $p = 0.0069$, 0.0207, and 0.0068, respectively) (Figure 1(A), 1(B) and 1(C)). Post hoc Bonferroni-adjusted contrasts are presented in Figure 1(D) using capital letters, and the results revealed that patients with high AD risk showed a significant reduction in the product of tau and Aβ42 protein levels after CPAP treatment. Conversely, these indexes in

Table 1. Demographic characteristics of participants. Group 1: Low AD risk with CPAP treatment; Group 2: High AD risk with CPAP treatment; Group 3: Low AD risk with CPAP-free treatment; and Group 4: High AD risk with CPAP-free treatment

	Total	Group 1	Group 2	Group 3	Group 4	*p*
Number	23	4	4	12	3	
Men/Women	17/6	4/0	4/0	6/6	3/0	
Age (years)	53.17 ± 11.10	51.75 ± 10.01	56.25 ± 13.96	53.75 ± 11.34	48.67 ± 12.22	0.44
Height (cm)	165.30 ± 6.93	165.00 ± 3.56	169.75 ± 9.54	163.25 ± 6.03	168.00 ± 9.85	0.82
Weight (kg)	74.72 ± 14.34	83.75 ± 13.07	79.75 ± 15.15	70.25 ± 14.23	73.83 ± 14.63	0.53
Body mass index	27.30 ± 4.70	30.72 ± 4.24	27.60 ± 4.06	26.40 ± 5.32	25.93 ± 2.06	0.38
Neck (cm)	39.13 ± 4.10	40.75 ± 2.63	40.75 ± 4.92	37.67 ± 4.25	40.67 ± 3.51	0.36
Waistline (cm)	93.09 ± 12.94	101.75 ± 10.87	98.25 ± 9.50	88.17 ± 14.35	94.33 ± 6.66	0.12
AHI (1/hr)	34.37 ± 23.99	54.10 ± 13.13	41.43 ± 26.97	27.13 ± 24.33	27.60 ± 21.53	0.09
CPAP compliance*		> 70%	> 70%			

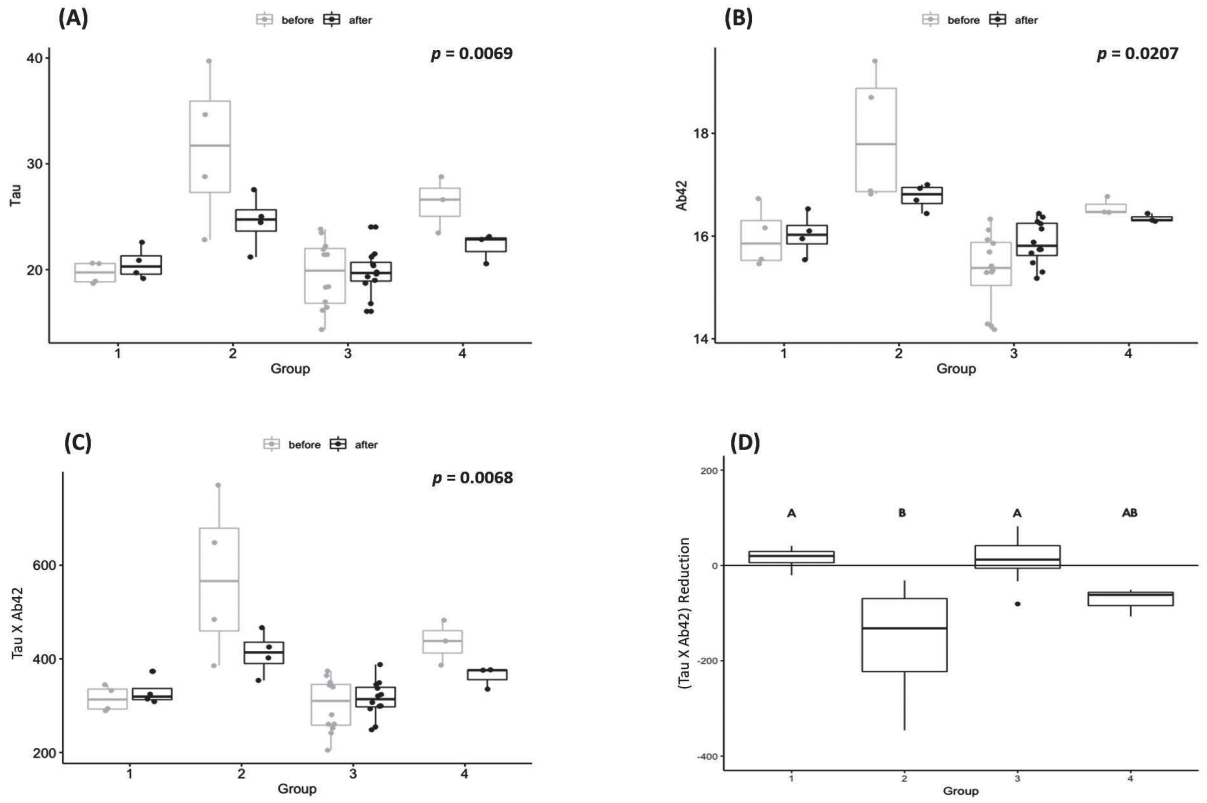

Fig. 1. Comparisons of AD-associated protein levels in serum before and after treatment. (A) Tau protein (pg/mL), (B) Aβ42 protein (pg/mL), and (C) the product of tau and Aβ42 (pg/mL)2 are shown with grouping based on AD risk (by initial level product of tau and Aβ42) and treatment chosen. Gray and black colors indicate values before and after treatment. (D) Comparison of the reduction of the product of tau and Aβ42 protein levels among the groups. Group 1: Low AD risk with CPAP treatment; Group 2: High AD risk with CPAP treatment; Group 3: Low AD risk with CPAP-free treatment; and Group 4: High AD risk with CPAP-free treatment.

* CPAP compliance was defined as percentage of CPAP use days (at least 4 hours) during the trial period, based on patient self-reporting.

patients with low AD risk were invariant, regardless of the treatment strategies. The results of the three protein indexes of the patients in the CPAP-free group who had high AD risk showed an ambiguous outcome, which did not differ from the outcome of patients in the CPAP treatment groups with high and low AD risk. However, a remarkable difference was observed between the high and low AD risk groups of patients receiving CPAP. More subjects are needed to diminish the deviation within groups and clarify the effects. The effectiveness of CPAP-free treatment in patients with high AD risk was confirmed through a statistical inspection of these 3 indexes (null hypothesis: reduction of protein level index was equal to zero; all 3 indexes: $p < 0.001$).

Discussion

This is the first investigation to show that CPAP therapy in patients with moderate/severe OSA reduces the serum level of AD-related proteins. Patients with high AD risk showed considerable reduction in tau and Aβ42 protein levels after CPAP therapy for 3–6 months,

which indicates that CPAP therapy decreases AD risk in this group of patients. Conversely, patients with low AD risk showed neither risk reduction nor side effects with CPAP therapy. Although the sample size was small, the outcome is significant. Furthermore, therapies other than CPAP therapy, such as weight loss, oral appliance use, and pharmacological and surgical treatment, caused a reduction in serum AD-related proteins in high-risk patients, but were less effective than CPAP therapy. This report reveals that commonly used clinical treatments may also reduce AD risk in OSA patients with a high AD risk.

OSA is characterized by recurrent episodes of breathing cessation during sleep due to upper airway collapse. In clinical practice, CPAP therapy is the first choice of treatment for OSA patients, and shows effectiveness in multiple respects. CPAP has been reported to completely prevent upper airway occlusion during sleep in all patients and to allow overnight uninterrupted sleep [13]. One study that used the Epworth Sleepiness Scale for sleep assessment found that with CPAP, sleep quality considerably improved, and the probability of sleep-related road traffic incidents considerably decreased [15]. In addition, CPAP treatment resulted in improvements in daytime activities, including work efficiency and the ability to drive safely [16]. Moreover, the odds of experiencing a response with CPAP treatment were almost triple when compared with conservative treatment [17]. However, the effect of CPAP varied among individuals and studies due to variations in patient compliance and differing experimental designs. In addition to opening the upper airway with continuous positive pressure, other strategies such as weight loss, oral appliance use, and pharmacological and surgical treatment, or even lifestyle changes, could improve sleep quality and quantity.

Although a lack of sleep is long known to impair brain function, the possible mechanism has been reported only recently. Sleep deprivation or poor sleep quality is associated with learning and cognitive performance impairment [18]. Sleep loss adversely affects pineal melatonin production, which disturbs the circadian physiology of cells, organs, neurochemicals, neuroprotective effects, and other metabolic functions [19]. Using the Drosophila model, Tabuchi et al. showed that chronic sleep deprivation increases Aβ accumulation through changes in intrinsic neuronal excitability [20]. They further suggested that neuronal hyperexcitability is an essential mediator of Aβ toxicity. To maintain a constant environment in the brain in the absence of the effect of the conventional lymphatic system, the mechanism of waste product clearance during neural metabolism may rely on CSF circulation. During sleep, the cortical interstitial space could increase by >60%, resulting in an obvious increase in the CSF convective exchange with interstitial fluid [21]. In other words, interstitial fluid convective fluxes increase the Aβ clearance rate during sleep.

The most well-known proteins associated with neurodegenerative disease are tau and Aβ, which are used as biomarkers for evaluating the risk and severity of AD [22]. Tau is a critical component in promoting the stabilization of microtubules. Once the dynamic equilibrium of tau binding to microtubules is disrupted, the abnormal increase in free (phosphorylated) tau enhances the probability of pathogenic conformational changes, which in turn result in aggregation and fibrillization, and finally contribute to synaptic dysfunction and neurodegeneration

[23]. Another pathological hallmark of AD is senile plaques, which primarily constitute the Aβ-peptide. The mechanisms leading to Aβ-mediated neurotoxicity are unclear, but a growing body of evidence indicates that oxidative stress plays a crucial role [24]. Aβ aggregation is neurotoxic both in vitro and in vivo, and free radicals peroxidize membrane lipids and oxidize proteins, causing severe cellular damage [25]. Antioxidants such as melatonin that are mainly secreted in the dark during sleep have had neuroprotective effects on Aβ-mediated cytotoxicity [26]. Thus, CPAP reduces AD risk through 2 possible mechanisms: first, providing steady pressure to prevent patients from arousal, which facilitates the clearance of tau and Aβ protein directly; and second, preventing apnea events, which reduces intermittent hypoxic pressure during sleep.

In addition to the observation bias due to the small sample size in our study, a limitation of our hypothesis may result from the methodology. Considering the safety, comfort, and convenience of the patient, AD markers in the plasma were assayed, and were assumed to be the same as or correspond to the levels in the CSF, using an extremely sensitive detection method. Although a study using an animal model showed that intermittent hypoxia did not alter blood–brain barrier (BBB) permeability [27], another study has suggested that BBB permeability to peptides may be altered through oxidative stress [28]. In addition, a human BBB model (in vitro) showed that the integrity decreased after incubation with sera from OSA patients [29]. A similar outcome was observed in pediatric patients [30]. Cyclic intermittent hypoxia diminished with CPAP therapy; thus, we could not exclude the possibility the BBB may be strengthened with CPAP therapy, thereby reducing the transport of tau and amyloid into the plasma. Another consideration is the uneven distribution of OSA severity in the 4 groups, in which, AHI tended to be higher in the CPAP groups. It is reasonable that patients with higher AHI would respond more favorably to CPAP treatment after conventional CPAP instruction or physician advice. As revealed in Figure 1(A) and 1(B), this might lead to higher initial AD-related protein levels in the group with high AD risk with CPAP treatment (group 2). In high AD risk patients, this might partially explain why CPAP therapy decreases AD risk more than other commonly used clinical treatments.

Conclusion

In this article, we reported that CPAP efficiently reduces AD risk in the high-risk group. Moreover, alternative treatments commonly suggested to OSA patients also may be helpful. However, more investigations are needed to examine the differences between treatments and to explore possible mechanisms. For low-risk groups, CPAP showed neither risk reduction nor side effects. Therefore, we highly recommend incorporating hematological biomarker examinations in routine tests for OSA patients and applying CPAP treatment for patients with a high AD risk.

Acknowledgements

This study has been partly funded by the Ministry of Science and Technology (MOST 109-2634-F-038-004) and a research grant from Taipei Medical University (108TMU-SHH-08). We are grateful to Yu-Fang Chiu, Shu-Fen Chiu, and Chiao-Yu Wang for helping with data

acquisition. We also thank Hsin-Chien Lee, MD, and technologist Shin-Mei Hsu for helpful discussions during the early stage of this study. This manuscript was initially edited by Wallace Academic Editing, and final editing was carried out by *Thoracic Medicine*.

References

1. Ott A, Breteler MM, van Harskamp F, *et al*. Prevalence of Alzheimer's disease and vascular dementia: association with education. The Rotterdam study. BMJ 1995; 310(6985): 970-973.
2. Evans DA, Funkenstein HH, Albert MS, *et al*. Prevalence of Alzheimer's disease in a community population of older persons. Higher than previously reported. JAMA 1989; 262(18): 2551-2556.
3. Duthey, B. Background Paper 6.11: Alzheimer Disease and other Dementias. In Priority Medicines for Europe and the World A Public Health Approach to Innovation 2013; 1-74.
4. Mangialasche F, Solomon A, Winblad B, *et al*. Alzheimer's disease: clinical trials and drug development. Lancet Neurol 2010; 9(7): 702-716.
5. Scheltens P, Blennow K, Breteler MM, *et al*. Alzheimer's disease. Lancet 2016; 388(10043): 505-517.
6. Georganopoulou DG, Chang L, Nam JM, *et al*. Nanoparticle-based detection in cerebral spinal fluid of a soluble pathogenic biomarker for Alzheimer's disease. Proc Natl Acad Sci USA 2005; 102(7): 2273-2276.
7. Yang CC, Chiu MJ, Yang SY, *et al*. Comprehensive study on plasma amyloid and tau protein related to neuropsychology and neuroimaging for diagnosing Alzheimer's disease. Alzheimer's Dement 2015; 11(17): 205-206.
8. Ooms S, Overeem S, Besse K, *et al*. Effect of 1 night of total sleep deprivation on cerebrospinal fluid β-amyloid 42 in healthy middle-aged men: a randomized clinical trial. JAMA Neurol 2014; 71(8): 971-977.
9. Spira AP, Gamaldo AA, An Y, *et al*. Self-reported sleep and β-amyloid deposition in community-dwelling older adults. JAMA Neurol 2013; 70(12): 1537-1543.
10. Punjabi NM. The epidemiology of adult obstructive sleep apnea. Proc Am Thorac Soc 2008; 5(2): 136-143.
11. Tufik S, Santos-Silva R, Taddei JA, *et al*. Obstructive sleep apnea syndrome in the Sao Paulo Epidemiologic Sleep Study. Sleep Med 2010; 11(5): 441-446.
12. Bu XL, Liu YH, Wang QH, *et al*. Serum amyloid-beta levels are increased in patients with obstructive sleep apnea syndrome. Sci Rep 2015; 5: 13917.
13. Sullivan CE, Issa FG, Berthon-Jones M, *et al*. Reversal of obstructive sleep apnoea by continuous positive airway pressure applied through the nares. Lancet 1981; 1(8225): 862-865.
14. Lue LF, Sabbagh MN, Chiu MJ, *et al*. Plasma levels of Aβ42 and tau identified probable Alzheimer's dementia: findings in two cohorts. Front Aging Neurosci 2017; 9: 226.
15. Engleman HM, Asgari-Jirhandeh N, McLeod AL, *et al*. Self-reported use of CPAP and benefits of CPAP therapy: a patient survey. Chest 1996; 109(6): 1470-1476.
16. Engleman HM, Martin SE, Deary IJ, *et al*. Effect of CPAP therapy on daytime function in patients with mild sleep apnoea/hypopnoea syndrome. Thorax 1997; 52: 114-119.
17. Redline S, Adams N, Strauss ME, *et al*. Improvement of mild sleep-disordered breathing with CPAP compared with conservative therapy. Am J Respir Crit Care Med 1998; 157: 858-865.
18. Stickgold R. Neuroscience: a memory boost while you sleep. Nature; 2006; 444(7119): 559-560.
19. Jan JE, Reiter RJ, Bax MC, *et al*. Long-term sleep disturbances in children: a cause of neuronal loss. Eur J Paediatr Neurol 2010; 14(5): 380-390.
20. Tabuchi M, Lone SR, Liu S, *et al*. Sleep interacts with aβ to modulate intrinsic neuronal excitability. Curr Biol 2015; 25(6): 702-712.
21. Xie L, Kang H, Xu Q, *et al*. Sleep drives metabolite clearance from the adult brain. Science 2013; 342(6156): 373-377.
22. Blennow K, Hampel H, Weiner M, *et al*. Cerebrospinal fluid and plasma biomarkers in Alzheimer disease. Nat Rev Neurol 2010; 6(3): 131-144.
23. Ballatore C, Lee VM, Trojanowski JQ. Tau-mediated neurodegeneration in Alzheimer's disease and related disorders. Nat Rev Neurosci 2007; 8(9): 663-672.
24. Barnham KJ, Masters CL, Bush AI. Neurodegenerative diseases and oxidative stress. Nat Rev Drug Discov 2004; 3(3): 205-214.

25. Miranda S, Opazo C, Larrondo LF, *et al*. The role of oxidative stress in the toxicity induced by amyloid beta-peptide in Alzheimer's disease. Prog Neurobiol 2000; 62(6): 633-648.
26. Wiesner CD, Davoli V, Schürger D, *et al*. Melatonin secretion during a short nap fosters subsequent feedback learning. Front Hum Neurosci 2018; 11: 648.
27. Kim LJ, Martinez D, Fiori CZ, *et al*. Hypomyelination, memory impairment, and blood-brain barrier permeability in a model of sleep apnea. Brain Res 2015; 1597: 28-36.
28. Bain AR, Ainslie PN, Hoiland RL, *et al*. Competitive apnea and its effect on the human brain: focus on the redox regulation of blood-brain barrier permeability and neuronal-parenchymal integrity. FASEB J 2018; 32(4): 2305-2314.
29. Voirin, AC, Celle, S, Perek, N, *et al*. Sera of elderly obstructive sleep apnea patients alter blood–brain barrier integrity in vitro: a pilot study. Sci Rep 2020; 10: 11309.
30. Khalyfa A, Gozal D, Kheirandish-Gozal L. Plasma exosomes disrupt the blood-brain barrier in children with obstructive sleep apnea and neurocognitive deficits. Am J Respir Crit Care Med 2018; 197(8): 1073-1076.

Prediction of Pulmonary Rehabilitation in Patients with Chronic Lung Disease Using 6-minute Walk Distance

Yu-Shan Li[1], Hui-Chuan Chen[1], Jung-Yien Chien[2], Huey-Dong Wu[1], Li-Ying Wang[3,4], Ping-Lun Hsieh[3,4]

Background: Pulmonary rehabilitation (PR) is an important part of the management and health maintenance of chronic lung disease (CLD) patients. This study aimed to identify the predictor of the percent predicted of the 6-minute walk distance (6MWD) in CLD patients.

Methods: Patients suffering from CLD, including both chronic obstructive pulmonary disease (COPD) (n=102) and non-COPD (n=39), who received an outpatient 8-week structured PR program between 2017 and 2019, were included, and their performance was analyzed.

Results: A total of 141 patients were included in the study. The patients were divided into 2 groups depending on whether the increase in the 6MWD reached the minimal clinically important difference (MCID) of 30 m after PR. A total of 78 and 63 patients were classified into the responders (> 30 m) and non-responders (≤ 30 m) group, respectively. All patients showed significant improvements in the 6MWD and modified Medical Research Council dyspnea scale. Multivariable logistic regression analysis showed that younger age (p= 0.005, OR = 0.89, 95% CI: 0.83 – 0.97) and < 60% predicted of the 6MWD value were independent factors predicting PR responders.

Conclusion: This study found that physical performance was improved after 8-week structured PR in patients with CLD. Younger age and 6MWD < 60% of the predicted value could predict a significant functional exercise capacity response to PR. ***(Thorac Med 2023; 38: 10-19)***

Key words: Pulmonary rehabilitation, chronic lung disease (CLD), 6-minute walk distance (6MWD)

[1]Department of Integrated Diagnostics & Therapeutics, National Taiwan University Hospital, Taipei 10002, Taiwan, [2]Department of Internal Medicine, National Taiwan University Hospital, National Taiwan University College of Medicine, Taipei, Taiwan, [3]Physical Therapy Center, National Taiwan University Hospital, Taipei, Taiwan, [4]School and Graduate Institute of Physical Therapy, National Taiwan University

Address reprint requests to: Dr. Hui-Chuan Chen, Department of Integrated Diagnostics & Therapeutics, National Taiwan University Hospital, Taipei 10002, Taiwan

Introduction

Patients with chronic lung disease (CLD) are markedly inactive in daily life and are often characterized by a downward spiral of symptom-induced inactivity, leading to deconditioning and muscle weakness [1], and consequently, reduced time being spent walking and standing compared with sedentary healthy elderly subjects.

There is convincing evidence of the positive effects of pulmonary rehabilitation (PR), as a comprehensive intervention that includes exercise training, education and behavioral change, on the progression of various pulmonary diseases, particularly for patients with chronic obstructive pulmonary disease (COPD) [2-3]. Even seriously ill lung patients without COPD can experience significant and clinically relevant improvements with PR [4].

In patients post-acute COPD exacerbation, PR significantly reduces the number of rehospitalizations and can possibly even lead to a reduced risk of mortality [5]. In CLD patients, the main adverse effects are ventilatory limitation and skeletal muscle dysfunction; in lung fibrosis patients, in addition to impaired gas exchange, cardiovascular dysfunction appears to be a limiting factor [6-9]. There is substantial evidence to support the importance of PR in the management of COPD. Daily symptoms, exercise performance and health status are generally improved following PR. However, this is not true for all patients [10]. There is some evidence that approximately 30% of patients who completed a PR course did not respond in aspects of quality of life and physical performance [11].

The 6-minute walk distance (6MWD) is a widely used, practical basic test for assessing exercise performance, and reflects the functional exercise level for daily physical activities [12-13]. The 6MWD and percent predicted 6MWD (% 6MWD) are important measures for assessing cardiopulmonary function [14-15]. Previous studies have proposed that % 6MWD was a better method for assessing subjects' clinical status [16]. Several reference equations already exist to calculate % 6MWD based on an individual's age, gender, height and weight, and can be used to assess functional exercise capacity [17-20]. However, studies on the % 6MWD predictor of PR program outcomes are lacking. In this study, we hypothesized that the % 6MWD may be a reliable predictor of PR responders among patients with CLD. We aimed to assess 8-month PR outcome predictions using the % 6MWD in patients with CLD.

Materials and Methods

Study Population

One hundred forty-one COPD patients were screened at the Outpatient Chest Clinic of National Taiwan University Hospital between 2017 and 2019. All subjects were > 20 years of age. Subjects with concomitant confounding diseases, such as malignant disorders, cardiovascular abnormalities or recent surgery, were excluded. All subjects underwent physical examinations, assessment of lung function and anthropometric measurements, including body mass index (BMI). BMI was calculated as body weight in kilograms divided by height in meters squared.

Pulmonary function and 6MWD

Patients were instructed to walk in a 15-m corridor for 6 minutes, receiving standard en-

couragement during the test. Spirometry was performed with a computerized spirometer (MST-PFT, Germany) by a trained technician, according to the American Thoracic Society (ATS) criteria. The tests were performed with the patient seated in an upright position, using a nose-clip and breathing through a non-compressible mouthpiece. All baseline spirometric measurements (forced expiratory volume in 1 second [FEV1], forced vital capacity [FVC], and FEV1/FVC) were obtained. COPD was diagnosed as stable airway obstruction with FEV1/FVC 70%, according to the Global Initiative for Chronic Obstructive Lung Disease (GOLD) criteria. Subjective scores of dyspnea included a modified version of the Borg visual analog scale (Borg scale) and the modified Medical Research Council dyspnea scale (mMRC). The Dyspnea Scale quantifies disability attributable to breathlessness and is useful for characterizing baseline dyspnea in patients with respiratory diseases.

The outpatient PR program

The PR program consisted of 1 supervised session per week over an 8-week period, for a total of 8~10 sessions. The PR program was conducted by a multidisciplinary team, including physicians, nurses, physiotherapists, respiratory therapists and a dietician. Participants received an individually tailored exercise program. The supervised exercise training in this study consisted of moderate-intensity aerobic exercises and strengthening exercises that focused on upper and lower extremities. The intensity of exercise training was targeted at 60-80% of the age-predicted maximal heart rate, 40-60% of the heart rate reserved, or the modified Borg Dyspnea Scale 4-6/10, depending on the participants' vital signs, medication use, and any condition that might influence their exercise responses [26-27]. Our PR program also included instructions in breathing techniques (pursed-lip breathing and diaphragmatic breathing), airway clearance techniques, energy-conservation techniques, and medication use. The exercise prescription included supervised dyspnea or fatigue-limited exercise training. Supplemental oxygen was used during training for patients with exercise-induced oxygen desaturation (and exercise SpO_2 less than 90%) and in patients who were already using home oxygen. Education included the importance of exercise and physical activity, proper use of medications, inhaler technique, diet, hypoxemia management, oxygen treatment, coping and relaxation strategies, bronchial hygiene techniques, and breathing retraining, as well as self-management plans for exacerbations. Supervised PR included at least 2 hours of exercise conditioning and education.

Data collection

Demographic data (current age, sex, BMI, and age at diagnosis) were obtained from the subject's medical records. A 6MWD was performed before and after completion of the PR program using published guidelines. % 6MWD prediction equations from a study are profiled below [17]:

Men: % 6MWD = (7.57 × height cm) – (1.76 × weight kg) – (5.02 × age) – 309 m

Women: % 6 MWD = (2.11 × height cm) – (2.29 × weight kg) – (5.78 × age) + 667 m

The patients were divided into 2 groups depending on the change in the 6MWD (responders > 30 m and non-responders ≤ 30 m) during PR. The "minimum clinically important difference" (MCID) of 30 m was reported by Polkey [21]. The total distance walked, and the

initial and final dyspnea scores were recorded. Dyspnea was scored with the mMRC Dyspnea Scale [22], and measured during exercise using a modified Borg scale [23-24].

Outcome measures

All subjects completed PR if they attended 100% of the PR sessions (minimum of 8 sessions). In the present study, the patients were divided into 2 groups depending on the change in 6MWD MCID (responders > 30m and non-responders ≤ 30m) before and after PR. All patients were assessed to determine whether there was a subjective and/or objective improvement following the structured PR program.

Data analysis

Data analyses and graphs were produced using SPSS V.21 (IBM, USA). Descriptive statistics (means, SD, counts, and frequencies in percent) were used to present patients' baseline characteristics. Differences between the responder and non-responder groups were calculated using unpaired t-tests. P-values were derived from an independent sample t-test for continuous variables and from the chi-square test for categorical variables. Multivariate regression analysis was used to identify patient variables associated with response to PR.

Ethical approval

The study was performed in accordance with current ethical guidelines (Declaration of Helsinki) and was approved by the Research Ethics Committee of National Taiwan

University Hospital (No. 201905059RINB).

Results

Subjects Baseline Characteristics:

During the study period, 141 patients who came to the outpatient clinic for PR and completed > 8 sessions between 2017 and 2019 were reviewed. Our study demographic characteristics revealed that more than 75% of the patient groups were males. This is similar to other studies that have shown a male predominance (78.9%) among combined COPD cohorts in Taiwan. The prevalence rates of COPD in Taiwan seem to have peaked in men. However, it is possible there was selection bias in our study population, since the outpatient chest clinic indicated that patients be referred to the PR department. The mean (± SD) age of the participants was 67.9±11.4 years, with 111 male subjects (78.7%). Subject demographics and characteristics included spirometry use, inclusion in the COPD group or non-COPD group, cardiovascular co-morbidity, and hospital utilization, such as emergency department (ED) visits and hospitalizations (Table 1).

The COPD and non-COPD groups were compared using the Dyspnea Severity Scale in response to PR. The COPD group results according to GOLD stage are shown in Table 2. Among the 141 patients, 102 (72.3%) were classified as having COPD. The non-COPD subjects were diagnosed as having bronchiectasis (13, 33.3%), pulmonary fibrosis (7, 17.9%), and other diseases (19, 48.7%), classified as interstitial lung disease or asthma associated with dyspnea. Seventy-eight participants (55%) had a responder outcome after PR. Patients in the responder group were significantly younger (P= 0.001), with a mean FEV1 of 51.3% ± 22.7% versus 61.4% ± 23.4% in the non-responder group (P= 0.012). The responder group had less cardiovascular co-morbidity (P= 0.015). The gender distribution, BMI, smoking history, ED visits, and hospitalizations were not significant-

Table 1. Baseline Characteristics Stratified According to Outcome

Variables	Total (N=141)	Response improved > 30 m (n = 78)	No response improved ≤ 30 m (n = 63)	*P*
Age (year)	67.9 ± 11.3	65.1 ± 11.3	71.4 ± 10.5	.001
Male	111 (78.7%)	63 (80.8%)	48 (76.3%)	.509
BMI (kg/m^2)	23.6 ± 10.1	22.9 ± 4.8	24.6 ± 14.0	.311
Smoking status				.772
Non-smoker	63 (44.7%)	34 (43.6%)	29 (46.0%)	
smoker	78 (55.3%)	44 (56.4%)	34 (54.0%)	0.09
COPD group	102 (72.3%)	59 (75.6%)	43 (68.3%)	.330
Non-COPD[a]				.404
Bronchiectasis	13 (33.3%)	6 (31.6%)	7 (35.0%)	
Lung fibrosis	7 (17.9%)	2 (10.5%)	5 (25.0%)	
Others	19 (48.7%)	11 (57.9%)	8 (40.0%)	
FEV1 % pred.	55.8 ± 23.5	51.4 ± 22.7	61.4 ± 23.4	.012
FEV1/FVC	55.7 ± 20.4	53.4 ± 19.9	58.6 ± 20.9	.137
Cardiovascular co-morbidity	69 (48.9%)	31 (39.7%)	38 (60.3%)	.015
ED visits	1.5 ± 2.43	1.7 ± 2.41	1.3 ± 2.5	.352
Hospitalizations	0.9 ± 1.4	0.9 ± 1.2	0.9 ± 1.6	.917

Data are presented as the mean ± SD for continuous variables and n (%) for categorical variables. BMI: body mass index; COPD: chronic obstructive pulmonary disease; FEV1: forced expiratory volume in the first second; FVC: forced vital capacity; ED: emergency department.

ly different between the 2 groups.

Six-minute walk distance, % 6MWD, and dyspnea score

COPD severity was staged by the degree of airflow limitation (i.e., GOLD stage). The responder group had significant improvement ($P< 0.001$) in both 6MWD (absolute values and percent of predicted) and mMRC, with equal effectiveness in different stages of COPD. After our comprehensive PR program, the % 6MWD was greatly improved in the responder group (65.05% vs 82.42%). The 6MWD mean change of 113 m in the non-COPD group post-PR was much more than the 90 m in the COPD group (Table 2). The non-responder group with COPD GOLD stages 1 and 2 had significant decreases in 6MWD (absolute values) post-8 weeks of PR (mean 338.20 ± 86.03 m versus 325.10 ± 93.19 m; P=0.014), as did the non-responder group with COPD (349.49 ± 90.91 m versus 337.05 ± 95.70 m; P=0.013). In contrast, the non-responder groups with COPD and with non-COPD showed no significant change in % 6MWD after 8 weeks of PR.

The mMRC was significantly decreased between the responder group and the total group. However, the Borg score after PR was not significantly decreased in either the responder or non-responder group.

Predictors of response in CLD post-pulmonary rehabilitation

Univariate logistic regression was used to determine the associations between patient characteristics and response outcome variables, and showed a univariate association with response post-PR (at P< 0.10). This was included

Table 2. Six-minute Walk Distance and % 6MWD after Pulmonary Rehabilitation (PR)

Response group / Outcome	pre-PR M ± SD	post-PR M ± SD	*P*
Responder (n = 78)			
% 6MWD, %	63.27 ± 20.55	81.64 ± 18.05	<.001
6MWD, m	309.28 ± 101.95	405.28 ± 90.94	<.001
COPD GOLD 1,2 % 6MWD, % (n = 18)	71.77 ± 21.08	90.59 ± 17.95	<.001
COPD GOLD 1,2 6MWD, m (n = 18)	326.96 ± 105.27	428.42 ± 86.32	<.001
COPD GOLD 3,4 % 6MWD, % (n = 41)	59.02 ± 19.09	77.16 ± 16.51	<.001
COPD GOLD 3,4 6MWD, m (n = 41)	65.05 ± 20.67	82.42 ± 18.14	<.001
COPD group % 6MWD, % (n = 59)	71.77 ± 21.08	90.59 ± 17.95	<.001
COPD group 6MWD, m (n = 59)	310.08 ± 99.60	400.69 ± 87.92	<.001
Non-COPD group % 6MWD, % (n = 19)	57.73 ± 19.65	79.21 ± 18.02	<.001
Non-COPD group 6MWD, m (n = 19)	306.79 ± 111.77	419.53 ± 100.93	<.001
Borg scale	3.97 ± 1.37	4.05 ± 1.86	.726
mMRC	2.10 ± 0.95	1.63 ± 0.86	<.001
Non-responder (n = 63)			
% 6MWD, %	72.87 ± 16.44	71.65 ± 16.93	.092
6MWD, m	342.37 ± 86.73	328.41 ± 100.18	.015
COPD GOLD 1,2 % 6MWD, % (n = 20)	76.23 ± 15.93	74.16± 16.95	.128
COPD GOLD 1,2 6MWD, m (n = 20)	338.20 ± 86.03	325.10 ± 93.19	.014
COPD GOLD 3,4 % 6MWD, % (n = 23	74.94 ± 17.85	74.28 ± 18.11	.583
COPD GOLD 3,4 6MWD, m (n = 23)	359.30± 95.77	347.43± 98.70	.151
COPD group % 6MWD, % (n = 43)	75.54 ± 16.80	74.22 ± 17.37	.139
COPD group 6MWD, m (n = 43)	349.49 ± 90.91	337.05 ± 95.70	.013
Non-COPD group % 6MWD, % (n = 20)	66.84 ± 14.22	65.83 ± 14.68	.435
Non-COPD group 6MWD, m (n = 20)	327.05 ± 76.88	309.85 ± 109.42	.250
Borg scale	3.79 ± 1.69	3.71 ± 1.34	.738
mMRC	2.14 ± 0.94	1.95 ± 1.07	.154
Total (n = 141)			
% 6MWD, %	67.52 ± 19.37	77.21 ± 18.19	<.001
6MWD, m	324.06 ± 96.54	370.94 ± 102.30	<.001
COPD GOLD 1,2 % 6MWD, % (n = 38)	77.29 ± 17.73	83.64 ± 20.04	<.001
COPD GOLD 1,2 6MWD, m (n = 38)	345.08 ± 94.63	383.00 ± 105.98	.008
COPD GOLD 3,4 % 6MWD, % (n = 64)	64.83 ± 19.53	76.19 ± 16.55	<.001
COPD GOLD 3,4 6MWD, m (n = 64)	315.78 ± 98.34	368.44 ± 90.25	<.001
COPD group % 6MWD, % (n = 102)	69.47 ± 19.74	78.96 ± 18.19	<.001
COPD group 6MWD, m (n = 102)	326.70 ± 97.55	373.86 ± 96.15	<.001
Non-COPD group % 6MWD, % (n = 39)	62.28 ± 17.53	72.52 ± 17.57	<.001
Non-COPD group 6MWD, m (n = 39)	317.18 ± 94.76	363.28 ± 117.89	.003
Borg scale [§]	3.89 ± 1.52	3.90 ± 1.64	.965
mMRC	2.11 ± 0.94	1.77 ± 0.97	<.001

Data are presented as mean ± standard deviation

6MWD: 6-minute walk distance; % 6MWD: percent predicted for 6-minute walk distance; GOLD stage: Global Initiative for Chronic Obstructive Lung Disease stage; mMRC: modified Medical Research Council.

[§]This visual is designed for rehabilitation therapists to assess and document perceived exertion throughout a therapy task. Based on the Borg scale and numbered 1-10

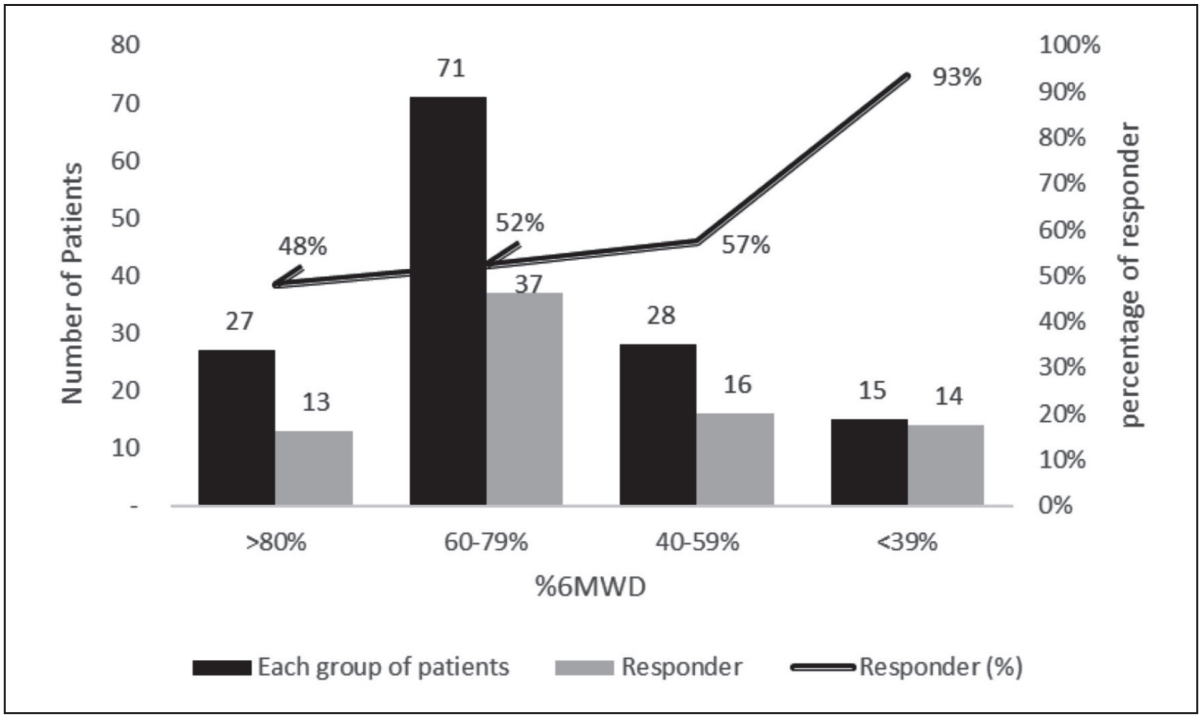

Fig. 1. Distribution of responses and non-responses stratified by > 80%, 60-79%, 40-59%, < 39% predicted 6MWD (% 6MWD) before pulmonary rehabilitation.

in stepwise backward multivariate logistic models to adjust for confounders. This study addressed an important clinical issue regarding the role of % 6MWD in the predictors of response in CLD post-PR. The thresholds of % 6MWD on response between groups had obviously changed to 57% (Figure 1). The univariate analysis shows that < 60% 6MWD may be a stronger predictor of response.

After adjustment for possible confounding factors, including age, pre-PR % 6MWD < 60%, FEV_1, and cardiovascular co-morbidity, multivariate analysis showed that age (OR = 0.89, P = 0.005) and % 6MWD < 60 % (OR = 8.11, P = 0.032) were independently confirmed as predictors of response in CLD after PR (Table 3).

Table 3. Multivariate Analysis for Identifying Predictors of Response Post-PR

Factors	Univariate		Multivariate	
	OR (95%CI)	*P*	OR (95%CI)	*P*
Age (years)	0.95 (0.92 - 0.98)	.002	0.89 (0.83–0.97)	.005
Pre-PR % 6MWD < 60%	2.40 (1.12–5.15)	.024	8.11 (1.20 – 54.8)	.032
FEV1%	0.98 (0.97 - 1.00)	.016	0.94 (0.87 - 1.01)	.094
CV co-morbidity	1.88 (0.22 - 0.86)	.011	0.41 (0.55–10.7)	.239

Factors included in the multivariate analysis in order to identify independent predictors of response. CV: cardiovascular; OR: odds ratio; CI: confidence interval.

Discussion

The present study sought to identify factors that could predict clinical outcomes after PR in CLD patients. The results showed that age and % 6MWD < 60 were independent predictors associated with response to PR. In current clinical practice, the 6MWD is the only critical factor for physicians when making clinical decisions, but the significant value of % 6MWD is unknown in CLD patients. In a past study, the % 6MWD was better correlated with respiratory function than the actual 6MWD [17]. However, no recent study has explored the correlations between the percentage values of % 6MWD and response to PR. In the present study, it was necessary to standardize the use of % 6MWD, and we suggested that < 60% predicted 6MWD would be a higher predicted response post-PR.

Our study reinforced the existing scientific evidence regarding the benefit of PR in improving exercise capacity and decreasing mMRC in all patients. Fifty-five percent of patients in the study had a response post-PR. The response rates were comparable to those of previous studies that reported improvements of 50%–68% [18-19] and 50%–75% [20-21] in 6MWD, respectively. These previous studies showed that reference equations, actual 6MWD and % 6MWD are important for assessing cardiopulmonary function. Gender was an important bias factor for actual 6MWD, and %6MWD was better related to pulmonary function than 6MWD. In the present study, we used reference equations for 6MWD in CLD patients after outpatient PR, and assessed their value in reflecting exercise capacity. We endeavored to demonstrate whether the percentage predicted value is a better predictor for the response post-PR.

Hence, knowledge of the factors predicting response is crucial for ensuring better PR efficacy. The role of baseline lung functions in predicting benefit after PR for COPD patients has been investigated previously. However, the results have been discordant, with a few studies showing a negligible value, while others demonstrated a positive association between a worse baseline lung function and improvement in exercise capacity [21-24]. In the present study, patients with FEV1 demonstrated that the exercise capacity of a responder was significantly lower than that of a non-responder, compared to those with a preserved lung function, and in the present population, FEV1 percent of predicted was a weak predictor for outcome of PR. Nevertheless, this study demonstrated the positive outcomes of a comprehensive PR program in COPD patients at all stages of the disease.

This study did not reveal an association between BMI, smoking and the COPD group after a PR response. Other variables such as dyspnea score and cardiovascular co-morbidity have also been evaluated previously, but these factors did not yield a predictive response in this study. Certain cardiovascular co-morbidities, such as coronary artery disease, heart attack, arrhythmia, peripheral artery disease and heart failure, have also been evaluated as predictors of response to PR. But, in our population, the incidence of cardiovascular co-morbidities was significantly lower in the responder group. Despite the fact that impairment is different in patients with CLD or cardiovascular co-morbidity, the underlying symptoms reported by these patients during exercise are common, and are related predominantly to leg discomfort and shortness of breath. A PR program significantly increases functional capacity in patients with CLD or

congestive heart failure after completion of the program. Cardiovascular risk assessment and management is an important component of the initial evaluation at the start of a PR program. This is a part of the integrated approach to PR, and provides optimal management and safety. [25] In patients with CLD, the ability of the lungs to maintain arterial oxygen content is often impaired, oxygen delivery is compromised, and exercise ability is typically reduced. During PR training, patients may experience worsened hypoxemia with exercise. In our study, administration of oxygen in patients with SpO2 below 88% to adjust oxygen supplementation with exercise during PR can maintain and/or further improve physical capacity.

In conclusion, the present study, comprising patients with CLD after an outpatient PR program, revealed that younger age and < 60% predicted 6MWD were associated with a high probability of predicting the response to PR. In addition, a significant < 60% predicted 6MWD was an important predictor. This information may help clinicians in their advanced management and increase the effectiveness of PR, even if the physical performance of the patient is less than 60% predicted 6MWD.

References

1. Rennard S, Decramer M, Calverley PM, *et al*. Impact of COPD in North America and Europe in 2000: subjects' perspective of Confronting COPD International Survey. Eur Respir J 2002; 20(4): 799-805.
2. Spruit MA, Singh SJ, Garvey C, *et al*. An official American Thoracic Society/European Respiratory Society statement: key concepts and advances in pulmonary rehabilitation. Am J Respir Crit Care Med 2013; 188(8): e13-64.
3. McCarthy B, Casey D, Devane D, *et al*. Pulmonary rehabilitation for chronic obstructive pulmonary disease. Cochrane Database Syst Rev 2015(2): Cd003793.
4. Ariel R, Nissim A, Romem A, *et al*. The effect of pulmonary rehabilitation on non-COPD patients. Eur Respir J 2014; 44: P3049.
5. Puhan MA, Gimeno-Santos E, Scharplatz M, *et al*. Pulmonary rehabilitation following exacerbations of chronic obstructive pulmonary disease. Cochrane Database Syst Rev 2011(10): CD005305.
6. Kozu R, Senjyu H, Jenkins SC, *et al*. Differences in response to pulmonary rehabilitation in idiopathic pulmonary fibrosis and chronic obstructive pulmonary disease. Respiration 2011; 81(3): 196-205.
7. Nishiyama O, Taniguchi H, Kondoh Y, *et al*. Quadriceps weakness is related to exercise capacity in idiopathic pulmonary fibrosis. Chest 2005; 127(6): 2028-33.
8. Spruit MA, Thomeer MJ, Gosselink R, *et al*. Skeletal muscle weakness in patients with sarcoidosis and its relationship with exercise intolerance and reduced health status. Thorax 2005; 60(1): 32-8.
9. Mendes P, Wickerson L, Helm D, *et al*. Skeletal muscle atrophy in advanced interstitial lung disease. Respirology 2015; 20(6): 953-9.
10. Troosters T, Gosselink R, Janssens W, *et al*. Exercise training and pulmonary rehabilitation: new insights and remaining challenges. Eur Respir Rev 2010; 19(115): 24-9.
11. Garrod R, Ford K, Daly C, et al. Pulmonary rehabilitation: analysis of a clinical service. Physiother Res Int 2004; 9(3): 111-20.
12. ATS Committee on Proficiency Standards for Clinical Pulmonary Function Laboratories. ATS statement: guidelines for the six-minute walk test. Am J Respir Crit Care Med 2002; 166(1): 111-7.
13. Solway S, Brooks D, Lacasse Y, *et al*. A qualitative systematic overview of the measurement properties of functional walk tests used in the cardiorespiratory domain. Chest 2001; 119(1): 256-70.
14. Bittner V, Weiner DH, Yusuf S, *et al*. Prediction of mortality and morbidity with a 6-minute walk test in patients with left ventricular dysfunction. SOLVD Investigators. JAMA 1993; 270(14): 1702-7.
15. Ingle L, Rigby AS, Carroll S, *et al*. Prognostic value of the 6 min walk test and self-perceived symptom severity in older patients with chronic heart failure. Eur Heart J 2007; 28(5): 560-8.

16. Güngör G, Karakurt Z, Adigüzel N, *et al*. The 6-minute walk test in chronic respiratory failure: does observed or predicted walk distance better reflect patient functional status? Respir Care 2013; 58(5): 850-7.
17. Enright PL, Sherrill DL. Reference equations for the six-minute walk in healthy adults. Am J Respir Crit Care Med 1998; 158(5 Pt 1): 1384-7.
18. Boutou AK, Tanner RJ, Lord VM, *et al*. An evaluation of factors associated with completion and benefit from pulmonary rehabilitation in COPD. BMJ Open Respir Res 2014; 1(1): e000051.
19. Zanini A, Chetta A, Gumiero F, *et al*. Six-minute walking distance improvement after pulmonary rehabilitation is associated with baseline lung function in complex COPD patients: a retrospective study. Biomed Res Int. 2013; 2013: 483162.
20. Vagaggini B, Costa F, Antonelli S, *et al*. Clinical predictors of the efficacy of a pulmonary rehabilitation programme in patients with COPD. Respir Med 2009; 103(8): 1224-30.
21. van Ranst D, Otten H, Meijer JW, *et al*. Outcome of pulmonary rehabilitation in COPD patients with severely impaired health status. Int J Chron Obstruct Pulmon Dis. 2011; 6: 647-57.
22. Garrod R, Marshall J, Barley E, *et al*. Predictors of success and failure in pulmonary rehabilitation. Eur Respir J 2006; 27(4): 788-94.
23. Selzler AM, Simmonds L, Rodgers WM, *et al*. Pulmonary rehabilitation in chronic obstructive pulmonary disease: predictors of program completion and success. COPD 2012; 9(5): 538-45.
24. Altenburg WA, de Greef MH, ten Hacken NH, *et al*. A better response in exercise capacity after pulmonary rehabilitation in more severe COPD patients. Respir Med 2012; 106(5): 694-700.
25. Chen W, Thomas J, Sadatsafavi M, *et al*. Risk of cardiovascular comorbidity in patients with chronic obstructive pulmonary disease: a systematic review and meta-analysis. Lancet Respir Med 2015; 3(8): 631-9.
26. American College of Sports M. ACSM's Resource Manual for Guidelines for Exercise Testing and Prescription. Philadelphia: Lippincott Williams & Wilkins, 2012.
27. Garvey C, Bayles MP, Hamm LF, *et al*. Pulmonary Rehabilitation Exercise Prescription in Chronic Obstructive Pulmonary Disease: Review of Selected Guidelines: An Official Statement from The American Association of Cardiovascular and Pulmonary Rehabilitation. J Cardiopulm Rehabil Prev 2016; 36(2): 75-83. doi: 10.1097/HCR.0000000000000171. PMID: 26906147.

Three-Dimensional Reconstruction for Mediastinal Surgery in a Patient with Left-Sided Superior Vena Cava

Pei-Hsing Chen[1], Chien-Lun Chen[2], Jin-Shing Chen[3]

Persistent left-sided superior vena cava, the most common congenital malformation of the thoracic venous return, occurs most frequently in patients with congenital heart disease. We reported the case of a 64-year-old man with a mediastinal tumor complicated with left-sided superior vena cava, which was incidentally found on a computed tomography scan. The patient underwent tumor excision via median sternotomy. His postoperative course was uncomplicated, and he continued to be well during his regular follow-ups. Three-dimensional reconstruction for left-sided superior vena cava before thoracic surgery could easily facilitate a safer surgery. ***(Thorac Med 2023; 38: 20-24)***

Key words: persistent left-sided superior vena cava, mediastinal tumor, 3-dimensional reconstruction

Introduction

Persistent left-sided superior vena cava (SVC) (PLSVC) is the most common congenital malformation of the thoracic venous return. If an individual has congenital heart disease, the probability of a PLSVC increases to 4.5% [1]. The PLSVC passes lateral to the aortic arch, anterior to the left hilum, and crosses posterior to the posterior wall of the left atrium [2], then drains into the right atrium, where there is no heart abnormality or hemodynamic consequences [3]. In early fetal life, the left anterior cardinal and left common cardinal veins regress, persisting only in some small parts, and result in the left-sided superior intercostal vein and coronary sinus, respectively [1].

Case description

A 64-year-old man with underlying hypertension, but a stable health status, was accidentally found to have mediastinal widening after undergoing chest radiography at a local clinic (Figure 1). He denied any discomfort. The mediastinal widening was suspected to be caused by a thymic mass. As a result, he was admitted to the hospital. The laboratory tests showed normal alpha-fetoprotein, beta-human chorionic gonadotropin, and carcinoembryonic antigen

[1]Division of Thoracic Surgery, Department of Surgery, National Taiwan University Hospital Yun-Lin Branch; No.579, Sec. 2, Yunlin Rd., Douliu City, Yunlin County 640, Taiwan, [2]National Taiwan University College of Medicine; No.1 Jen Ai Road, Section 1, Taipei 100 Taiwan, [3]Department of Surgical Oncology, National Taiwan University Cancer Center; No. 57, Lane. 155, Sec. 3, Keelung Rd., Da'an Dist., Taipei City 106, Taiwan
Address reprint requests to: Dr. Jin-Shing Chen, No. 57, Lane. 155, Sec. 3, Keelung Rd., Da'an Dist., Taipei City 106, Taiwan Vice Superintendent, National Taiwan University Cancer Center

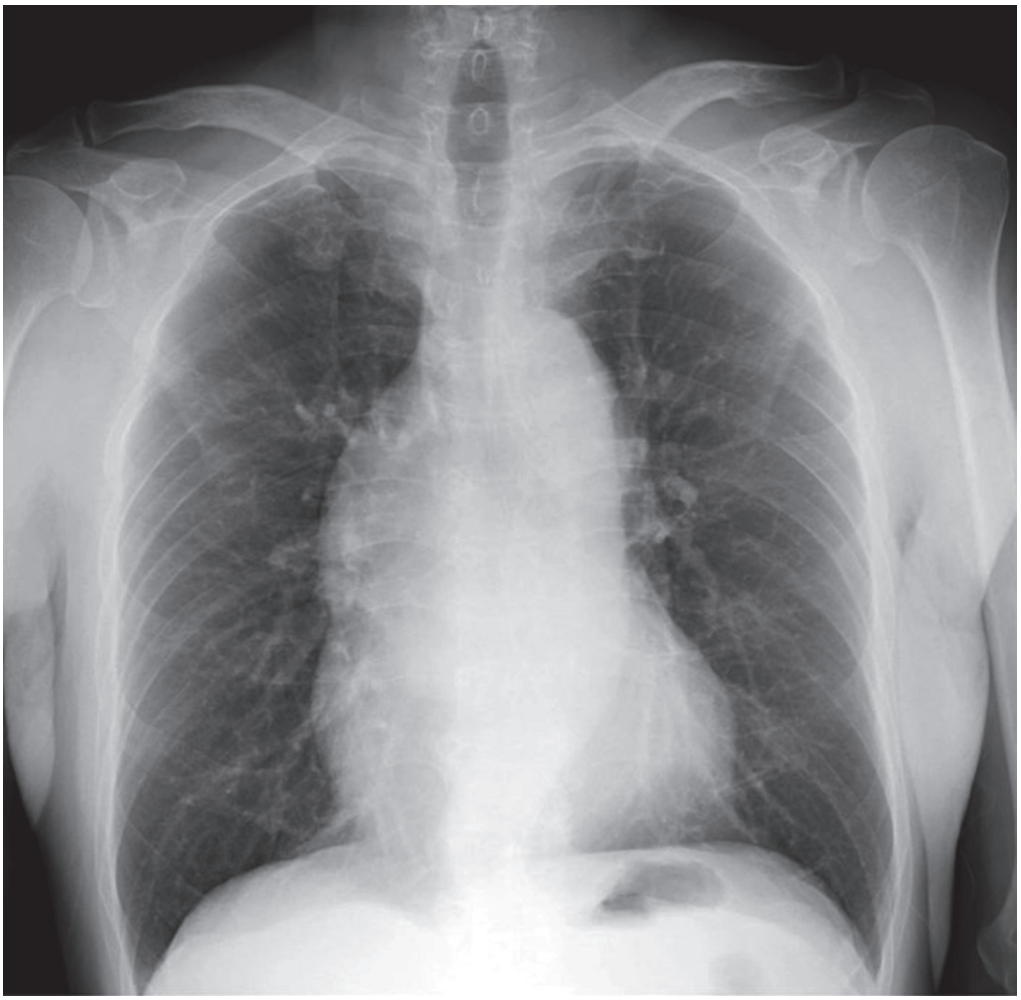

Fig. 1. a. Chest radiograph showing a widened mediastinum. b. Contrast-enhanced CT revealing an anterior mediastinal tumor with great vessels entrapment, as well as an incidentally left-sided superior vena cava. A solid anterior mediastinal tumor, with trace enhancement and without cystic change, was found between the aortic arch and the left-sided superior vena cava.

values. The anti-acetylcholine receptor antibody screening test showed negative results. No myasthenia gravis-related symptoms or abnormal laboratory results were noted.

Chest computed tomography (CT) scan revealed a solid anterior mediastinal tumor located between the aortic arch and an incidentally found left-sided SVC. Chest CT also revealed that the right brachiocephalic vein passing through the left common carotid artery flowed into the left brachiocephalic vein and formed the left-sided SVC. Then, the left-sided SVC passed laterally to the aortic arch and the anterior mediastinal tumor and anteriorly to the left pulmonary vein, flowing into the coronary sinus (Figures 2, 3). Formal echocardiography revealed the left and right ventricles had normal sizes and functions. Moderate aortic regurgitation, mild pulmonary hypertension, and an enlarged coronary sinus were noted.

Due to the complicated vessel structure, a high-speed, high-quality 3-dimensional (3D) image analysis system (Synapse Vincent, Fuji Film Co., Ltd., Tokyo, Japan) was used to ob-

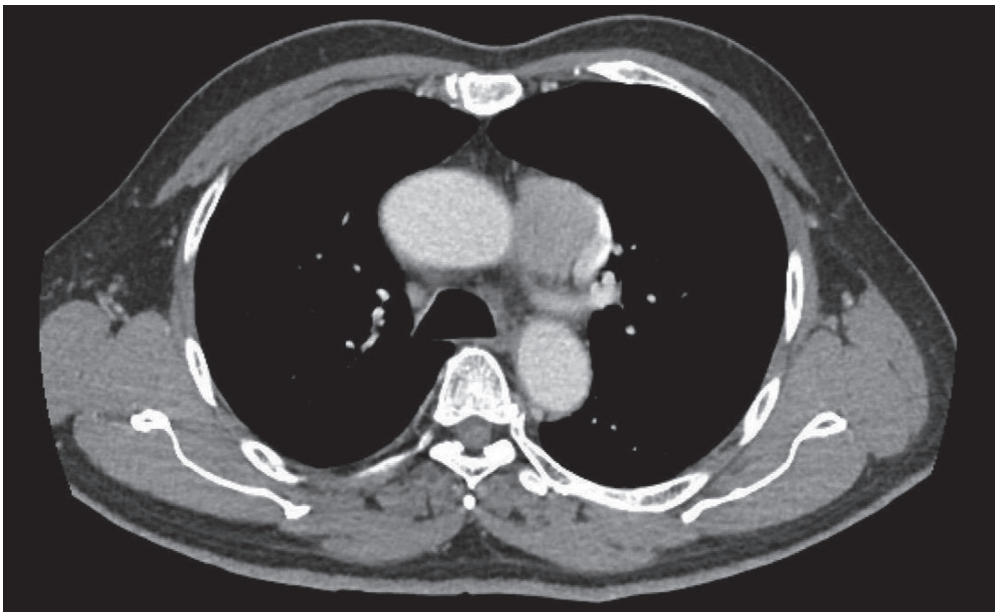

Fig. 2. Contrast-enhanced CT revealing an anterior mediastinal tumor with great vessels entrapment, as well as an incidentally left-sided superior vena cava. A solid anterior mediastinal tumor, with trace enhancement and without cystic change, was found between the aortic arch and the left-sided superior vena cava.

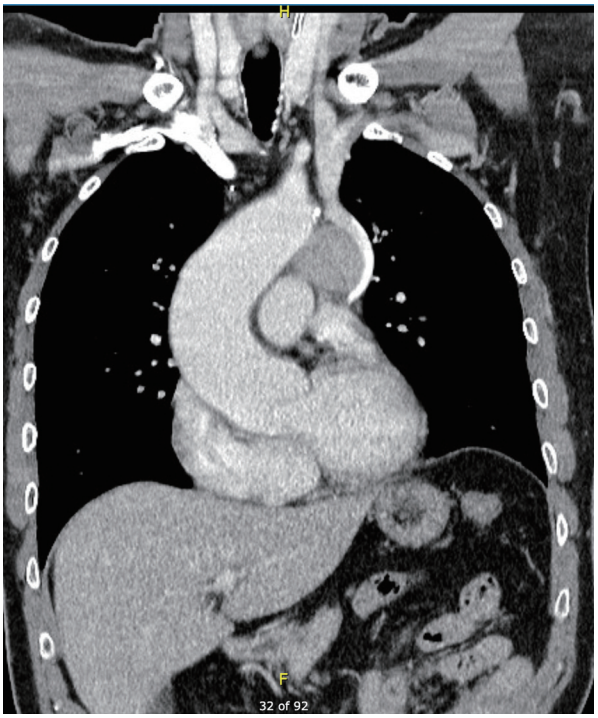

Fig. 3. Contrast-enhanced CT coronary view.

tain 3D images of the pulmonary vessels and the tracheobronchial tree. The system automatically extracts information on the structures and displays 3D images. The simulations then were used for pre-surgical planning (Figure 4a, b).

Later, the patient underwent a median sternotomy with dissection of the thymus gland and the fibro-fatty tissues anterior to the pericardium. The left-sided SVC, left phrenic nerve, and left recurrent laryngeal nerve were identified and preserved. During dissection of the mediastinal tumor, severe adhesion between the tumor and pericardium was noted. After dissection, the tumor was removed with part of the pericardium. The resected mass was 5.3 × 4.0 × 0.8 cm in size. Histopathological examination revealed type AB thymoma with capsular invasion but without regional lymph node metastasis or lymphovascular invasion. The modified Masaoka stage for the thymoma was stage II, represent-

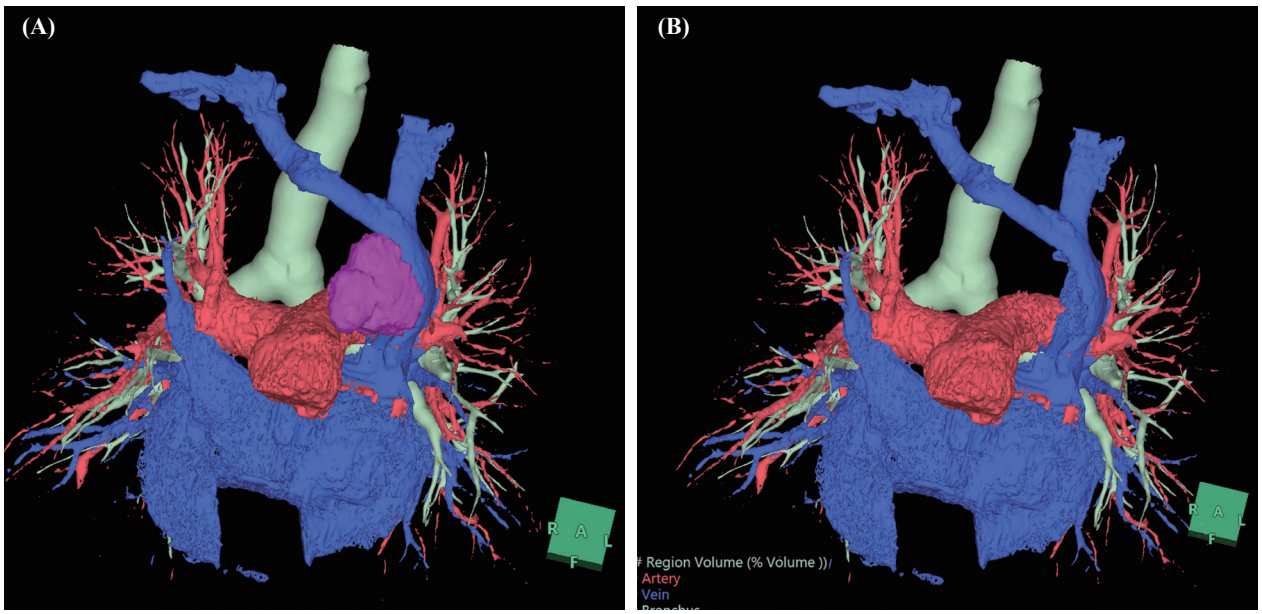

Fig. 4. (A). Three-dimensional reconstruction showing that the left brachiocephalic vein ran on the left side of the aortic arch to the caudal side and outside of the left upper pulmonary vein on the caudal side. Tumor and vessels together. (B). Three-dimensional reconstruction with vessels only.

ing both gross and microscopic encapsulation. The patient was discharged on postoperative day 6 and the postoperative course was unremarkable.

Discussion

A diagnosis of PLSVC is usually reached during cardiovascular imaging or surgery. Transthoracic echocardiography is also a useful way to diagnose PLSVC, by revealing the presence of a dilated coronary sinus on 2-dimensional echocardiography without evidence of elevated right-sided filling pressure. Multi-slice CT or magnetic resonance imaging can also be used to confirm the diagnosis and rule out other variations [4].

We confirmed the diagnosis of PLSVC using a CT scan. However, CT could not realize the detailed structure of the large vessels near the PLSVC. As a result, 3D CT reconstruction was performed. The simulation showed detailed information of the vascular variations and regional structure information.

In some cases, PLSVC may be misidentified as lymph node metastasis or lymphadenopathy during preoperative cancer staging using horizontal CT slices [3]. Multidetector-row CT can help differentiate between PLSVC and mediastinal lymph nodes [2].

In cases of mediastinal tumor surgery with PLSVC, surgeons should pay close attention to the blood flow in large vessels, including the PLSVC near the tumor. Proper tumor excision and identification of the great vessels and nerves require a firm grasp of anatomic details and more precise imaging. Pagini et al. reported a wedge resection of the left upper lobe of the lung through thoracotomy in a patient with PLSVC. Yoshida *et al*. reported that left lower pulmonary vein excision can be performed without difficulty in PLSVC patients after iden-

tifying the PLSVC [2].

In our case, we successfully identified the nearby vessels preoperatively, including the innominate vein (Figures 2, 3), which is absent in 65% of PLSVC cases [5], thus preventing possible surgical errors. Some research has demonstrated the possibility of using video-assisted thoracoscopic surgery (VATS) thymectomy with partial SVC resection for advanced thymic tumors. But patient selection is very important [6]. For our patient, we decided to perform a median sternotomy due to suspected local adhesion and an unusual anatomy. However, with 3D CT reconstruction, VATS could be considered for patients with a less advanced tumor.

To the best of our knowledge, this is the first reported case of PLSVC treated with 3D CT reconstruction in mediastinal surgery. In the future, we hope that the 3D CT reconstruction method we employed will be more extensively applied for various anatomic anomalies. 3D reconstruction for left-sided SVC preoperatively could facilitate safer thoracic surgery, and be routinely used in future surgeries for these patients.

Acknowledgment

We would like to thank the radiology department for the technical support provided during the 3D reconstruction.

References

1. Oliveira JD, Martins I. Congenital systemic venous return anomalies to the right atrium review. Insights Imaging 2019; 10:115.
2. Yoshida M, Hino H, Machida H, *et al*. Cancer of the left lung with persistent left superior vena cava. Ann Thorac Surg 2012; 94: 1326-1328.
3. Pagini A, Bassi M, Diso D, *et al*. Vena cava anomalies in thoracic surgery. J Cardiothorac Surg 2018; 13: 19.
4. Goyal SK, Punnam SR, Verma G, *et al*. Persistent left superior vena cava: a case report and review of literature. Cardiovasc Ultrasound 2008; 6: 50.
5. Webb WR, Gamsu G, Speckman JM, *et al*. Computed tomographic demonstration of mediastinal venous anomalies. Am J Roentgenol 1982; 139: 157-161.
6. Xu N, Gu Z, Ji C, *et al*. Thoracoscopic thymectomy with partial superior vena cava resection for locally advanced thymomas. J Thorac Dis 2019; 11: 438-444.

Accidentally Found Lung Cancer in Teenager Donor Lung

Hao-Yun Liu[1], Yen-Lin Huang[2], Pei-Hsing Chen[3], Hsao-Hsun Hsu[1,4]

For most post-transplantation patients, the meantime from transplantation to the diagnosis of lung cancer was 76 months (range, 9-192 months). In previous, the cases were considered as induced lung cancer. Advances in immunosuppression management have led to prolonged survival in many transplant recipients. A by-product of this improvement, however, has been the identification of several complications of chronic immunosuppression. Among the most important of these is the substantially increased incidence of malignancies in transplant recipients. But in our recipient, a left upper lung adenocarcinoma was accidentally found, which is 0.001 cubic centimeter in size, and resected randomly due to the oversize of the lung during the sternum closure. In past, most post-transplantation lung cancer is considered immunosuppression related. But our case showed the incidence might be underestimated, especially in the high lung cancer prevalence area like Taiwan. The combination of the donor's family history and the routine pre-transplantation donor's chest CT might be help for early detection of donor's lung malignancy. The frozen pathology could be applied after the pre-donation lung computed tomography scan if suspected lesion was identified. In this way, we believe the pre-donation evaluation could be more adequate. ***(Thorac Med 2023; 38: 25-28)***

Key words: lung cancer, adenocarcinoma, teenager donor lung, teenager recipient, lung transplantation

Introduction

Lung transplantation is a procedure for end-stage lung disease (ESLD). The first human lung transplantation was operated in 1963 [1]. Up to now, lung transplantation has become a viable treatment option for patients with a variety of ESLD. With the knowledge improvement of post-operative care, the primary and the long-term outcome focus on the pre-lung transplantation evaluation of recipient, even donor.

The same as donor liver, computer tomography (CT) can give much information when a primary survey of the donor lungs. We could

[1]Division of Thoracic Surgery, Department of Surgery, National Taiwan University Hospital, Taipei, Taiwan. [2]Department of Pathology, National Taiwan University Cancer Center, Taipei, Taiwan. [3]Division of Thoracic Surgery, Department of Surgery, National Taiwan University Hospital Yun-Lin Branch, Yun-Lin, Taiwan. [4]National Taiwan University College of Medicine, Taipei, Taiwan
Address reprint requests to: Dr. Pei-Hsing Chen, Division of Thoracic Surgery, Department of Surgery, National Taiwan University Hospital Yun-Lin Branch, No. 579, Sec. 2, Yunlin Rd., Douliu City, Yunlin County 640, Taiwan

find lung nodules in donor lungs by CT scan. Unfortunately, unlike donor liver, the donor lung CT scan is not popular for fear of less organ harvest. The donor lung evaluation is mostly based on the short time palpation and grossly view by the donor team. Some nodules would be missed.

Case report

This report describes a case of a 23-year-old female with history of acute myeloblastic leukemia. Then she received 3 times of stem cell transplantation between 2013 and 2014, and with complete remission. However, 2 years after, severe chronic graft versus host disease (GVHD) developed in the lung, which caused bronchiolitis obliterans, and with recurrent pneumothorax from 2016 to 2019. During this period, the pulmonary function test (PFT) showed decreasing forced vital capacity (FVC) and forced expiratory volume in one second (FEV_1). The latest PFT showed FVC 24.4% and FEV_1 14.7%, under the impression of severe mixed ventilatory defect, obstructive predominant. Then, she received a lung transplantation evaluation in 2020. Later, she received lung transplantation with the donor lungs in the same year.

The donor is a 17-year-old male non-smoker and did not have any underlying disease. There was no family history about lung cancer. A traffic accident occurred and caused an intracranial hemorrhage. After 3 days of treatment, brain death was declared and he became a potential donor. The pre-donation survey was done. Fortunately, unlike previous lung transplantation, the CT with contrast was arranged from the lower neck to the upper abdomen was arranged. Besides contusion hemorrhage and pneumonia in bilateral lungs, no other abnormality was found by the radiologist (figure 1). The NTUH donor team went to the donor's hospital. After no abnormal finding under palpation and grossly view, the donor lung was harvested and sent back to NTUH.

The evaluation before the operation, the donor height is 170 cm, the weight is 85 kg and the chest circumference is 99 cm. However, the recipient height is 160 cm, the weight is 41 kg, and the chest circumference is only 69 cm. During the operative period of lung transplantation, to make the size of the donor lung to fit the recipient's chest cavity for the obviously size discrepancy, a part of lung was resected and was sent for pathology. After some days of lung transplantation, the pathology report showed 0.2cm, mix type (Acinar: 40%, papillary: 20%, lepidic: 40%) adenocarcinoma (Figure 2). During the period of hospital stay, she received immunosuppression drugs as the protocol. No obvious structure abnormal was found during the following chest image. After postoperative day 60, she was discharged healthily.

The following chest CT at 2020/06 and 2020/12 showed no change, comparing to the CT after 1 week of the operation, under the radiologist visit. The patient is still healthily in following in outpatient clinic of NTUH up to now.

Comment

For most post-transplantation patients, the meantime from transplantation to the diagnosis of lung cancer was 76 months (range, 9-192 months) [2]. In previous, the cases were considered as induced lung cancer. We could be hard to know the existence of malignant cell in donor's lung in the short time of survey if no assist of image study.

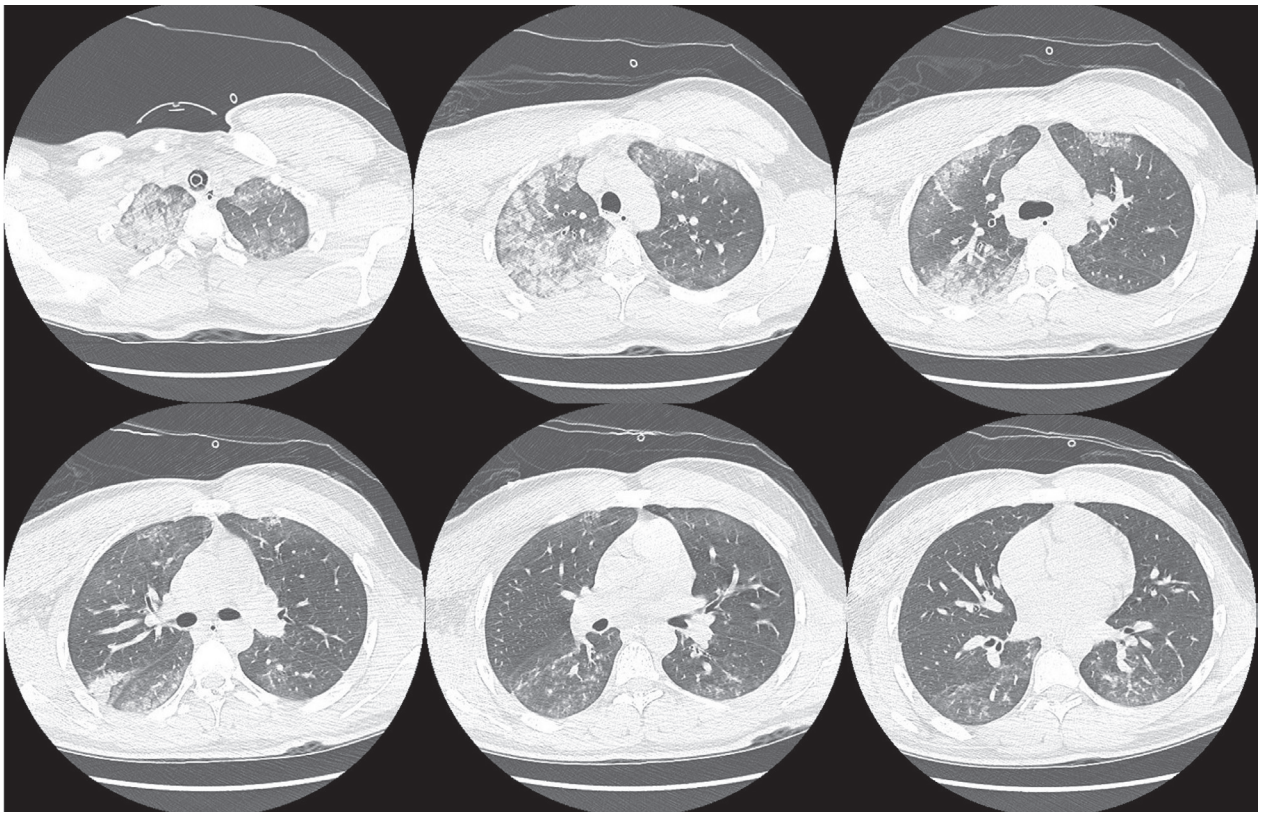

Fig. 1. The chest CT image of the donor before the lung transplantation. The multiple lesions of contusion in bilateral lungs.

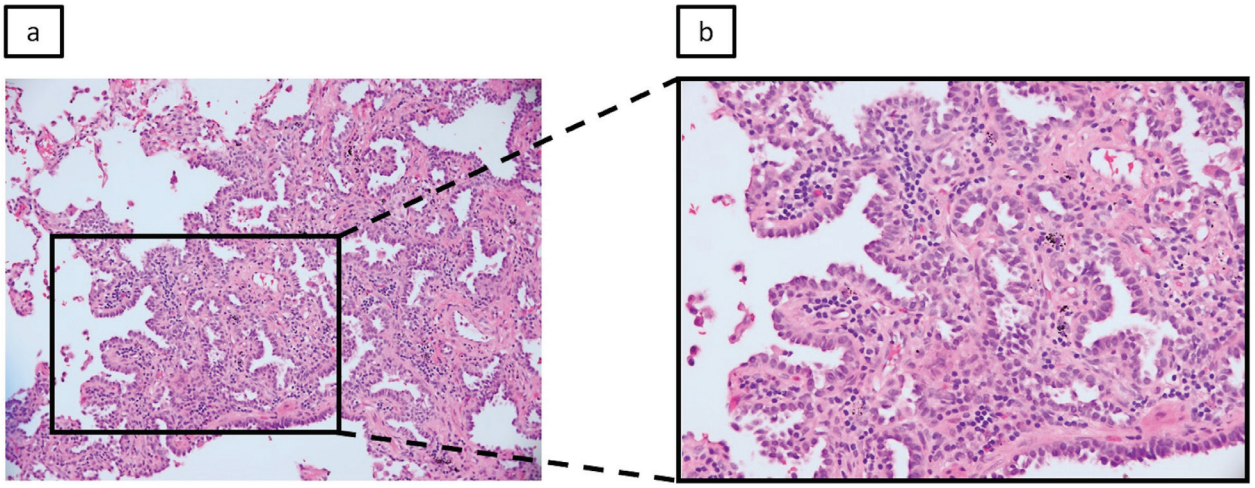

Fig. 2. (a). One small focus of adenocarcinoma arranged predominant in acinar and papillary patterns (100x). (b). On higher magnification, acinar arrangement with crowded and hyperchromatic nuclei are seen (200x).

In the real world, there was less young donor lung harvested. According to the United Network for Organ Sharing (UNOS) database, there was less than 10% of donor lung belonging to < 18 years [3]. So, the young donor lung less than 18 years is very rare. This is the same

in Taiwan.

Turn back to our case, we accidentally find lung adenocarcinoma in the 17-year-old donor. This event showed some hints. First, even young age, there was also the possibility of having lung cancer. This fact lets us think outside the box. In normal thinking, there would be less possibility of lung cancer in so young teenagers. When we survey the young age donor, there might ignore the existence of cancer. Second, there might be some cases of immunosuppression induced lung cancer, in reality, caused by the existed cancer in donor organs, and the routine survey protocol could be hard to find out. The previous studies showed the prevalence of lung cancer after lung transplantation was 1.9% to 3.6% [4,5]. Some of them might suffer lung cancer from the undetected malignancy donor lung. Third, with the limited of donor organ survey, a chest CT scan could be helpful to identify small nodule which may be ignored during the palpation. Although the routine CT scan for the donor lungs was currently not suggested by the guideline, we believed it could decreased the risk of undetected malignancy in donor lungs. Moreover, if the suspected lesion was noticed at the pre-donation lung CT scan, the resection could be made at the initial evaluation period and send the specimen for the frozen pathology to determine the etiology. In this way, we believe the pre-donation evaluation could be more adequate.

In conclusion, in past, most post-transplantation lung cancers are considered immunosuppression-related. But our case showed lung cancer from the donor's undetected malignancy incidentally. We suggested that combination of the donor's family history and the routine pre-transplantation donor's chest CT might be help for early detection of donor's lung malignancy if the size of malignancy were large enough and could be distinguished from the changes of trauma and infection. If needed, the frozen pathology could be applied during the pre-donation evaluation. Active surveillance by annual post-transplantation chest CT might be a more practical option to find the lung abnormalities early.

Acknowledgment

The authors give sincerely thank to the transplant coordinators at the National Taiwan University Hospital, and the Taiwan Organ Registry and Sharing Center for their continuous efforts in increasing the safety, availability, and quality of donors for organ transplantation. This work was supported by grants from the National Taiwan University Hospital (MS441).

References

1. Hardy JD, Webb WR, Dalton ML, *et al*. Lung homotransplantation in man. JAMA 1963 Dec 21;186: 1065-74.
2. Zahoor Ahmed, M Blair Marshall, John C Kucharczuk, *et al*. Lung cancer in transplant recipients: a single-institution experience. Arch Surg 2004 Aug;139(8): 902-6. doi: 10.1001/archsurg.139.8.902.
3. David J Hall, Eric I Jeng, Jon A Gregg, *et al*. The Impact of Donor and Recipient Age: Older Lung Transplant Recipients Do Not Require Younger Lungs. Ann Thorac Surg 2019 Mar;107(3): 868-876. doi: 10.1016/j.athoracsur.2018.09.0669.
4. Amardeep S Grewal, Robert F Padera, Steve Boukedes, *et al*. Prevalence and outcome of lung cancer in lung transplant recipients. Respir Med 2015 Mar; 109(3): 427-33.
5. David Pérez-Callejo, María Torrente, Consuelo Parejo, *et al*. Lung cancer in lung transplantation: incidence and outcome. Postgrad Med J 2018 Jan;94(1107):15-19.

Localized Pleural Amyloidosis

Pei-yi Chu[1], Kuan-Hsun Lin[1], Tsai-Wang Huang[1], Shih-Chun Lee[1]

Amyloidosis, defined as the deposition of fibrous protein amyloid, usually involves systemic organs and produces symptoms. Localized asymptomatic amyloidosis is rare. We describe the case of an asymptomatic 67-year-old woman who was admitted for investigation of multiple abnormal pleural tumors that were detected on chest radiography. Localized pleural amyloidosis was diagnosed after video-assisted thoracoscopic resection. We discuss this case and review the relevant literature. ***(Thorac Med 2023; 38: 29-33)***

Key words: Chalk powder, Pleural amyloidosis, Surgery

Introduction

Amyloidosis is characterized by the extracellular deposition in various organs of a fibrous protein termed amyloid (1); it is classified into systemic and localized types. In systemic disease, amyloid accumulates in several organs, such as the kidneys, heart, and liver, and in the peripheral nervous system; fatigue and weight loss are the most common presenting symptoms. Localized disease is usually asymptomatic, because the amyloid deposits affect only 1 target organ. Although the lung parenchyma is sometimes a target organ, amyloidosis in the pleura is extremely rare. We herein report a rare case of multiple asymptomatic amyloid deposits in the visceral and parietal pleura without systemic disease.

Case report

Our patient was a 67-year-old woman who was an elementary school teacher and had been exposed to chalk dust for more than 40 years. Approximately 7 years prior, a regular chest radiograph had shown a round pleural tumor in the left lung field, but she did not pay attention to it. About 2 months before she was admitted, she had undergone a health check-up, wherein a radiograph and computed tomography (CT)

[1]Division of Thoracic Surgery, Department of Surgery, Tri-Service General Hospital, National Defense Medical Center, Taipei, Taiwan, Republic of China
Address reprint requests to: Dr. Shih-Chun Lee, Division of Thoracic Surgery, Department of Surgery, Tri-Service General Hospital 325 Cheng-Kung Road, Section 2, Taipei 114, Taiwan, Republic of China.

scan of the chest both found multiple bilateral pleural tumors without involvement of any other organs. Mediastinal lymphadenopathy, hilar lymphadenopathy, and distant metastasis were absent. There was no abnormal fluid accumulation. Laboratory data and physical examination were unremarkable.

The patient underwent video-assisted thoracoscopy (VATS) with excisional biopsy of the pleural tumor. Intraoperative findings revealed multiple visceral and parietal pleural tumors at the left lower lung, pericardium, diaphragm, and para-sternum (Figures 1A and 1B). Resection of the visceral and parietal pleural tumor was performed. The pathological examinations of all the resected specimens yielded amyloid deposition. Histochemical staining with thioflavin-S and Congo red yielded a positive result (Figures 2A, 2B, Figures 3A, 3B, 3C, 3D). The tumors were pathologically confirmed to be amyloidosis.

Recovery was uneventful, without any nosocomial infection or other complication, and the patient was discharged on postoperative day 10. As of 4 months after surgery, no systemic symptoms of amyloidosis related to other or-

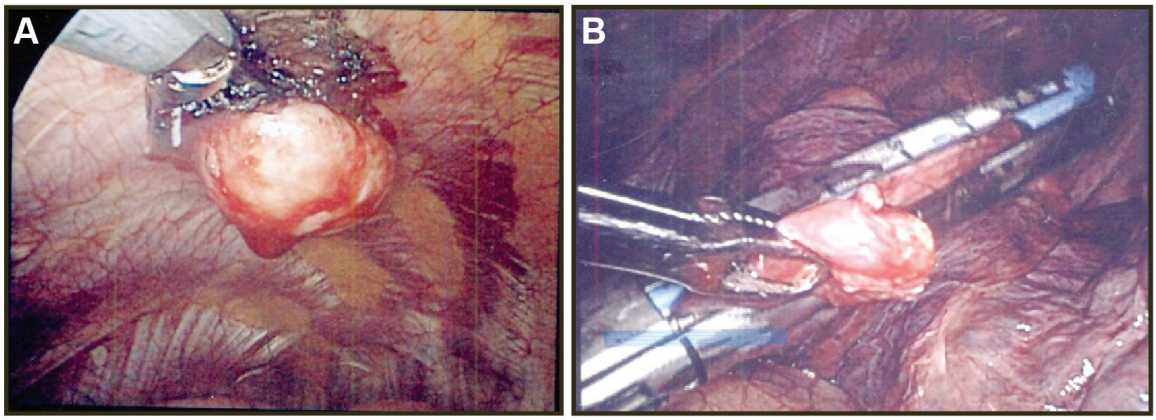

Fig. 1. (A). Pleural tumor at the left chest wall. (B). Intraoperative finding of a nodule at the lingular segment.

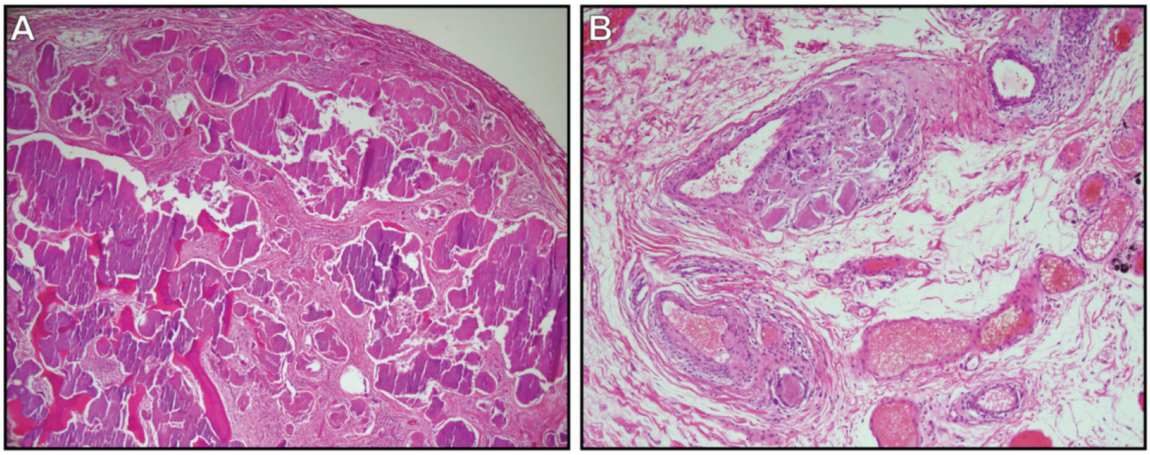

Fig. 2. (A). HE stain 100×: Pale and pink amorphous material around the pleura. (B). HE stain 100×: Pale and pink amorphous material around the pulmonary tissue.

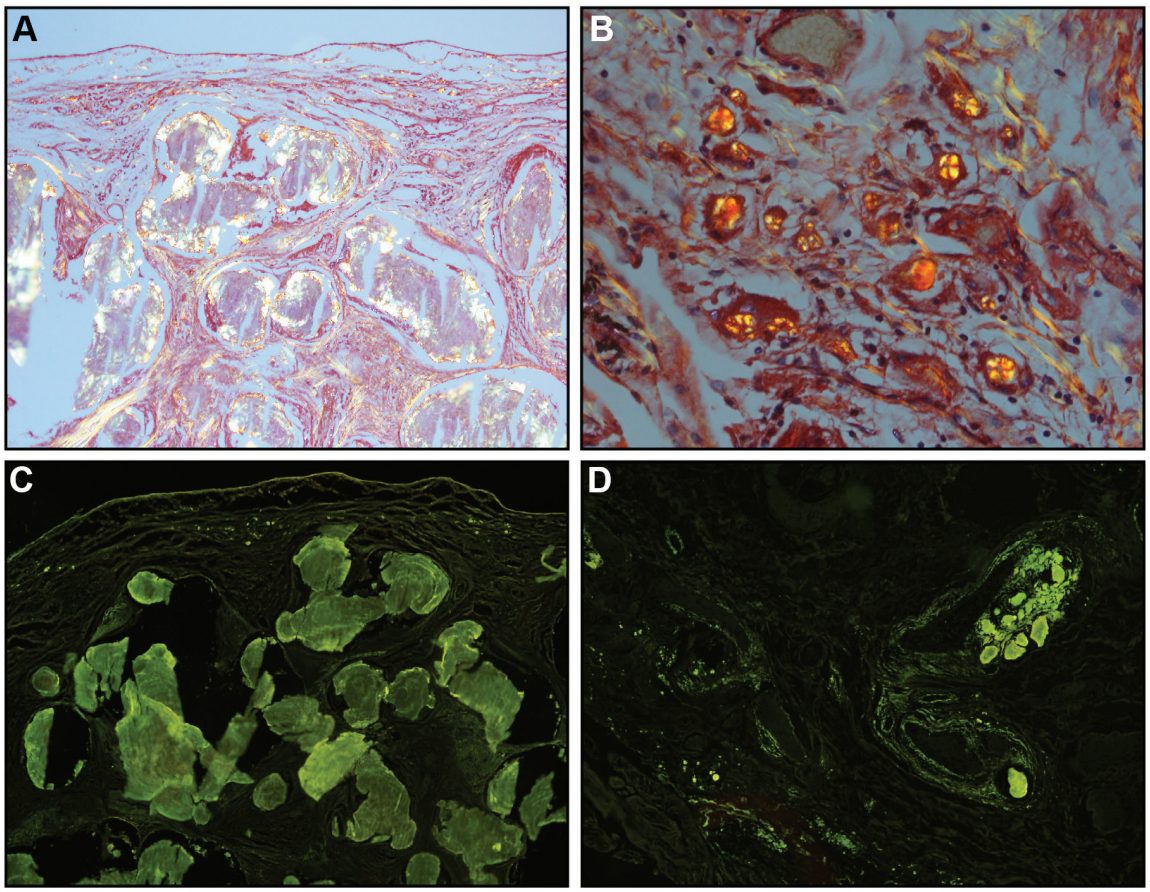

Fig. 3. (A). Congo red stain 100×: amorphous material around the pleura. (B). Congo red stain 100×: amorphous material around the pulmonary tissue. (C). Thioflavin S stain 100×: apple-green material around the pleura. (D). Thioflavin S stain 100×: apple-green material around the pulmonary tissue.

gans such as the heart, kidneys, liver, spleen, or adrenals have been detected. The patient's treatment was approved by the ethics committee and carried out in accordance with the principles outlined in the Declaration of Helsinki.

Discussion

Amyloidosis is a heterogeneous group of disorders characterized by deposition of autologous protein fibrils in the extracellular space. Histological findings are characterized by amorphous, eosinophilic, extracellular material that shows an apple-green birefringence when stained with Congo red. The pathological examinations of our patient revealed the presence of multiple pleural amyloidosis. The patient had no relevant medical history, including any connective tissue disease (especially rheumatoid arthritis or Sjogren's syndrome), chronic infection (especially tuberculosis), bronchiectasis, or neoplasms. The patient did not have a family history of amyloidosis and had never undergone dialysis. Amyloidosis either affects multiple organs, ultimately leading to organ failure, or can be localized to a single organ. Nevertheless, amyloidosis with overlapping features is common (2).

In systemic disease, the symptoms and signs may be nonspecific; fatigue, weakness, and weight loss are common symptoms, but the diagnosis is usually reached once the condition affects a particular organ. Amyloid material particularly affects the kidneys, heart, liver, spleen, and peripheral nervous system. Symptoms and signs in such cases depend on the type of organ involvement: arrhythmias on ECG, dilated atrium, ventricular hypertrophy, and pleural effusion are found in cases of cardiac involvement-related congestive heart failure; dyspnea, cough, and occasionally hemoptysis in cases of pulmonary amyloidosis; and proteinuria in cases of amyloid deposits in the kidney. Reducing the supply of precursor proteins for amyloid fibril is considered in the treatment of systemic amyloidosis. Chemotherapy and immunomodulatory agents are used in certain types of amyloidosis. In addition, supportive care is crucial to control symptoms and maintain organ function (3).

In localized disease, amyloid deposition usually occurs in a single organ. In many cases of localized amyloidosis, there are no specific symptoms. The most common sites of local amyloid deposition include the skin, urethra, bladder, larynx, eyes, thyroid, pancreas, atrium, heart, joints, cerebral area, tracheobronchial area, lung parenchyma, and lymph nodes. Abdominal CT, echocardiography, electrocardiography, and urine biochemistry examinations should be carried out to distinguish between localized and systemic amyloidosis. Other investigations such as abdominal fat aspiration, bone marrow aspiration, rectal biopsy, and biopsy of the suspected organ can also enable diagnosis. Diagnosis may be difficult with a small biopsy specimen (4). The final diagnosis depends on the pathological findings. In localized amyloidosis, surgical resection is considered curative.

Localized amyloid deposition in the pleura is extremely rare. To the best of our knowledge, incidental detection of pleural amyloid deposits is rare in a patient without pleural effusions. Very few cases of pleural amyloidosis are reported (5). Amyloid accumulation in the pleura might be an accidental finding (6). In spite of the unusual distribution of amyloid along the pleural surface, it is difficult to make a precise diagnosis without pleural tumor biopsy. The differential diagnosis of pleural tumors includes pleural amyloid, mesothelioma, sarcomatoid, metastatic lesions, and solitary fibrous tumor of the pleura. Most cases with systemic amyloidosis with pleural involvement causing pleural effusion are commonly due to heart failure or nephrotic syndrome.

Blackboard chalk is usually composed of calcium carbonate, and long-term exposure can affect health to a great extent. Chalk powder can cause respiratory discomfort, asthma, emphysema, or chronic bronchitis. Long-term exposure to calcium carbonate powder may cause difficulty in breathing and related systemic problems, such as substance accumulation (7). However, the relationship between powder and amyloidosis is still uncertain.

In our case, the patient had a history of chalk inhalation for more than 40 years. The pleural lesion was found via chest radiography, and systemic disease was absent. The patient was asymptomatic and various examinations revealed no abnormalities. However, the pathological examination revealed multiple amyloid deposits in the visceral and parietal pleura, left lower lung, pericardium, diaphragm, and parasternal region. Therefore, we diagnosed the tumor as multiple localized pleural amyloidosis without systemic disease.

Conclusion

The differential diagnosis of pleural tumors is a major challenge. Long-term exposure to carbonate powder can cause systemic problems such as substance accumulation. A detailed history including the patient's occupation and systemic disease history, as well as pre-operative examinations are important to determine the final diagnosis. Excision biopsy enables a precise diagnosis.

Disclosure statement

The authors declare no conflicts of interest.

References

1. Gillmore JD, Hawkins PN. Amyloidosis and the respiratory tract. Thorax 1999; 54: 444-51.
2. Kyle RA, Greipp PR. Amyloidosis (AL). Clinical and laboratory features in 229 cases. Mayo Clin Proc 1983; 58: 665-83.
3. Wechalekar AD, Gillmore JD, Hawkins PN. Systemic amyloidosis. Lancet 2016 Jun 25; 387(10038): 2641-2654.
4. Knapp MJ, Roggli VL, Kim J, *et al*. Pleural amyloidosis. Arch Pathol Lab Med 1988; 112: 57-60.
5. Kavuru MS, Adamo JP, Ahmad M, *et al*. Amyloidosis and pleural disease. Chest 1990; 98: 20-3.
6. Maeno T, Sando Y, Tsukagoshi M, *et al*. Pleural amyloidosis in a patient with intractable pleural effusion and multiple myeloma. Respirology 2000; 5: 79-80.
7. Nikam KD, Hirkani MA. Effects of chalk dust on peak expiratory flow rate in school teachers. Int J Med Health Sci 2013; 2: 407-9.

A case of Primary Pleural Epithelioid Angiosarcoma Mimicking Malignant Pleural Effusion of Advanced Prostate Cancer

Cheng-Kang Lu[1], Chun-Liang Tung[2], Hung-I Kuo[1]

Angiosarcomas are rare cancers and are often aggressive. A pleural origin is extremely rare, and seen only in some case reports. We reported the case of a patient with advanced prostate cancer presenting with pleural effusion that was initially assumed to be pleural metastasis. This 84-year-old smoker presented with bilateral chest pain. The chest X-ray and chest computed tomography revealed bilateral pleural effusion. Evaluation of the pleural fluid obtained from a thoracentesis revealed an exudative effusion with no evidence of malignant cells. Diagnostic pleuroscopy was performed, and the pleural biopsy revealed primary pleural epithelioid angiosarcoma. The patient died 1 month after the diagnosis. Pleural epithelioid angiosarcoma often leads to a poor prognosis, with the majority of patients dying within months of diagnosis. This unusual case that was diagnosed as primary epithelioid angiosarcoma mimicking malignant pleural effusion of prostate cancer is a reminder that clinical physicians should make a differential diagnosis for emerging clinical signs and symptoms less common in the patient's underlying disease. ***(Thorac Med 2023; 38: 34-39)***

Key words: angiosarcoma, pleural effusion, chest pain, pleuroscopy

Introduction

Angiosarcoma is a rare and highly aggressive endothelial cell malignancy that is seen most commonly in the deep soft tissues, although various solid organ primary sites are also reported [1]. Primary pleural angiosarcoma is extremely rare, with fewer than 30 cases reported in the English literature [2]. Herein, we report a case of primary pleural epithelioid angiosarcoma mimicking malignant pleural effusion of prostate cancer, diagnosed by proactive examination with diagnostic pleuroscopy.

Case Presentation

This 84-year-old smoker was retired from construction work, and had underlying disease

[1]Division of Chest Medicine, Department of Internal Medicine, Ditmanson Medical Foundation Chia-Yi Christian Hospital, [2]Department of Pathology, Ditmanson Medical Foundation Chia-Yi Christian Hospital
Address reprint requests to: Dr. Hung-I Kuo, Division of Chest Medicine, Department of Internal Medicine, Ditmanson Medical Foundation Chia-Yi Christian Hospital, No. 539, Zhongxiao Road, East Dist., Chiayi City, Taiwan

with hypertension and coronary artery disease status post-coronary artery bypass graft 20 years ago. Dysuria with elevated prostate-specific antigen (PSA) was noted in 2018, followed by a diagnosis of prostate cancer with liver metastasis after biopsy and a series of image examinations. He received hormone therapy and regular outpatient department follow-up at Chiayi Chang Gung Memorial Hospital. Chemotherapy was suggested by the urologist, under the impression that the prostate cancer was progressing along with the pleural effusion, based on the family's description. However, the patient was lost to follow-up at the urology outpatient department because of the panic among the public regarding hospital visits during the coronavirus disease-2019 outbreak period in 2020.

The patient had experienced bilateral chest pain for 2 weeks, so he visited the emergency room at Chia-Yi Christian Hospital in November, 2020. The chest X-ray (CXR) and computed tomography (CT) showed bilateral pleural effusion (Figure 1). He was then admitted to the chest ward under the impression of bilateral pleural effusion with pleuritic pain. Thoracentesis showed bloody pleural effusion, and the laboratory examination revealed exudative pleural effusion with non-hematopoietic cells predominant (Table 1). The pleural effusion cell block revealed some atypical cells with enlarged nuclei and prominent nucleoli, rather than malignant cells. Immunohistochemistry (IHC) staining was positive for calretinin (+) and Wilms' tumor 1 (WT1) (+), and negative for thyroid transcription factor-1 (TTF1) and

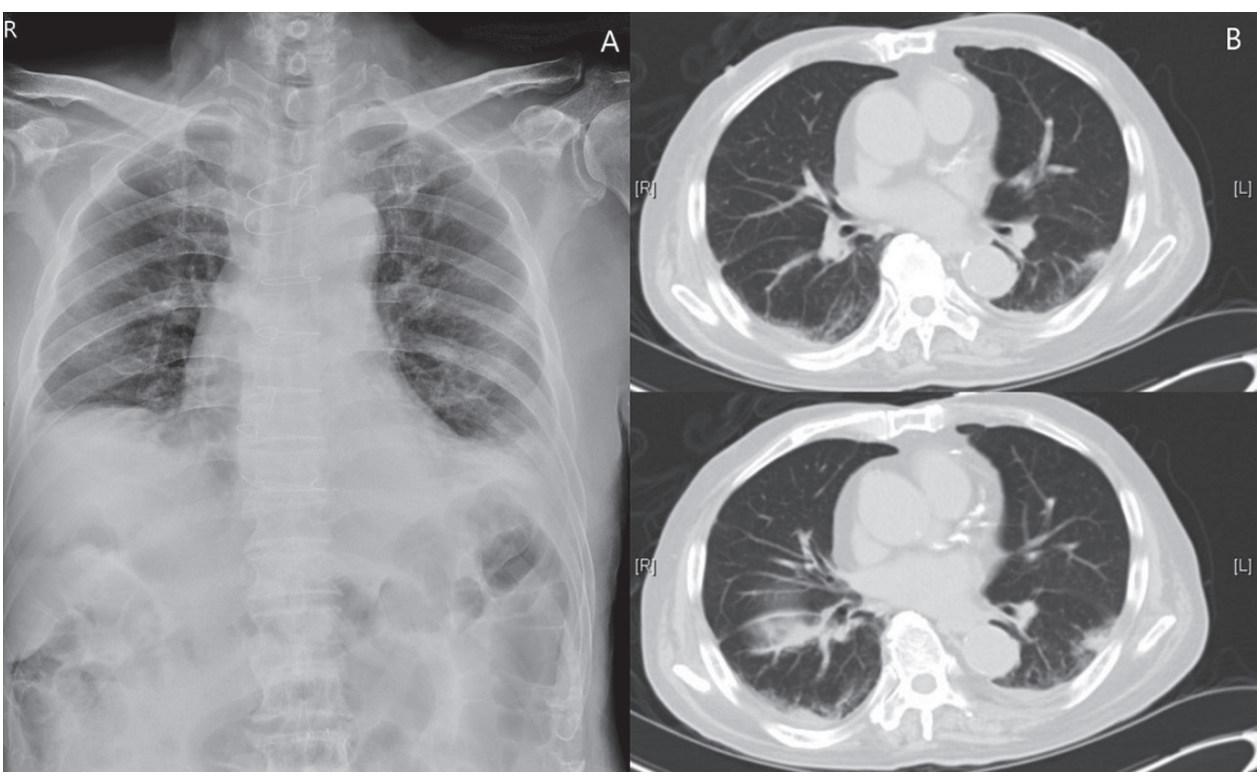

Fig. 1. (A). Chest radiograph showing bilateral pleural effusion and surgical wires from the previous coronary artery bypass graft surgery. (B). Chest CT showing mild bilateral pleural effusion with mild infiltration in the bilateral lower lobes.

Table 1. Laboratory and Pathology Parameters of Pleural Effusion

Pleural effusion		**Normal range**
Color/clarity	Reddish/Bloody	NA
pH	7.69	NA
RBC count (/μL)	63200	NA
Nucleated cell count (/μL)	3132	NA
WBC count (/μL)	1848	NA
Neutrophil (%)	39	NA
Lymphocytes (%)	11	NA
Monocyte (%)	9	NA
Eosinophil (%)	0	NA
Basophil (%)	0	NA
Non-hematopoietic (%)	41	NA
TP (g/dL)	3.5	NA
LDH (U/L)	165	NA
TP (blood) (g/dL)	5.5	6~8.3
LDH (blood) (U/L)	194	106~211
Cell block	Calretinin (+), WT1(+)	NA

RBC, red blood cell; WBC, white blood cell; TP, total protein; LDH, lactate dehydrogenase; NA, not available.

carcinoembryonic antigen (CEA).

Diagnostic pleuroscopy performed for the uncertain pleural effusion etiology showed some fleshy nodules with an irregular surface covered with bloody secretions, scattered on the parietal pleura with some whitish fibrinous material (Figure 2). The pathological examination of the pleuroscopy biopsy of the pleural tissue revealed poorly differentiated hyperchromatic pleomorphic neoplastic cells with prominent nucleoli and pale-to-eosinophilic cytoplasm in loose clusters with occasional slit spaces under the microscope. The IHC results were positive for cytokeratin (CK), ERG and CD31 (Figure 3), but negative for CK20, TTF-1, napsin A, p63, Hepa-1, arginase, glypican 3, synaptophysin, CD34, NKX 3.1, alpha-methylacyl-CoA racemase (AMACR), and PSA. CK7 showed weak positive staining, but prostate-specific membrane antigen (PSMA) revealed equivocal positive staining. The pathological examination indicated primary pleural epithelioid angiosarcoma, rather than pleural metastasis of prostate cancer. The patient decided to receive palliative treatment only and died 1 month later.

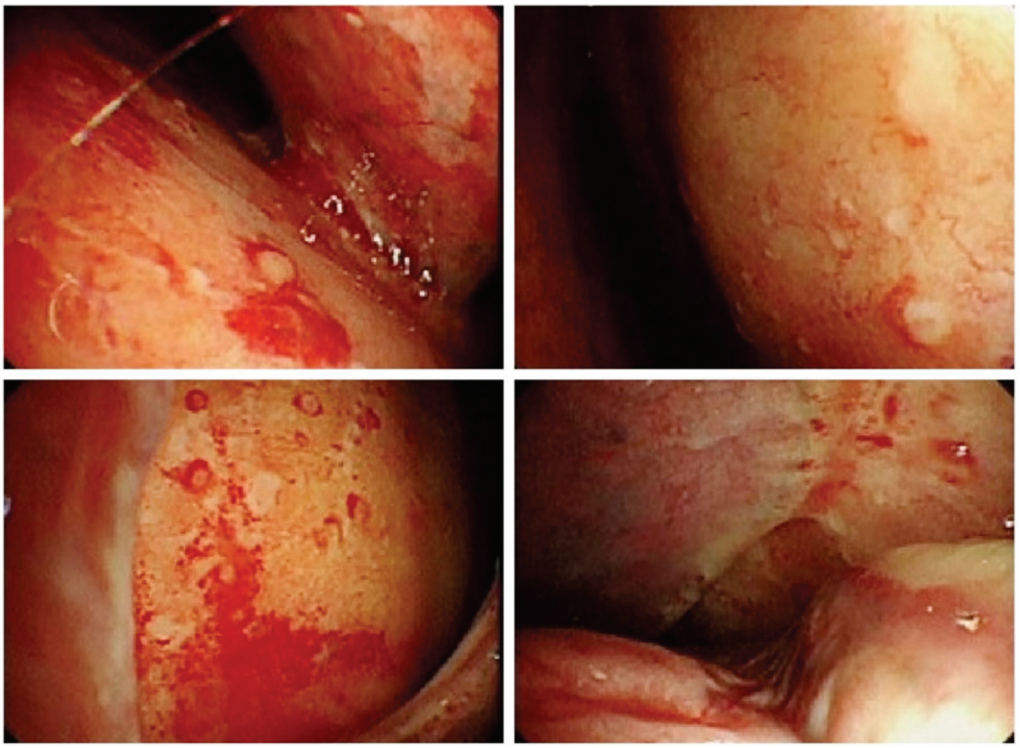

Fig. 2. Diagnostic pleuroscopy revealed small fleshy nodules with an irregular surface, covered with bloody secretions and some whitish fibrinous material scattered on the parietal pleura.

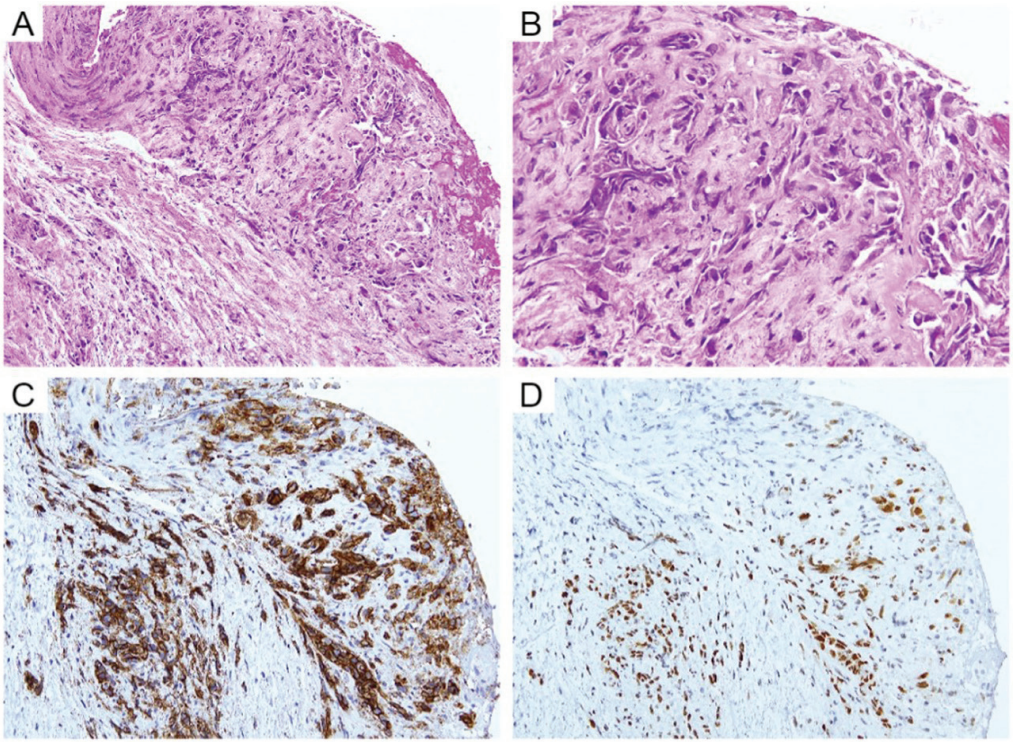

Fig. 3. The sections show pleural tissue infiltrated by poorly differentiated hyperchromatic pleomorphic neoplastic cells with prominent nucleoli and pale-to-eosinophilic cytoplasm in loose clusters with occasional slit spaces (A, hematoxylin and eosin stain (H&E stain) 200X; B, H&E stain 400X). IHC results revealed positivity for CK, CD31 (C, CD31 stain, 200X) and ERG (D, ERG stain, 200X).

Discussion

Epithelioid angiosarcoma is a rare and aggressive malignancy. Primary epithelioid angiosarcoma originating from the pleura or chest wall is extremely rare [1]. Although the pathogenesis and etiology are still unclear, pleural vascular sarcomas and occupational exposure to asbestos are reported as risk factors [3]. The most commonly reported clinical signs and symptoms of primary epithelioid angiosarcoma include chest pain, pleuritic chest pain, dyspnea, cough, hemoptysis, recurrent hemothorax and anemia [4]. Most terminal prostate cancers show progression with bone, lymphoid node and lung metastases, but less commonly with pleural metastasis [5].

CXR and CT initially revealed bilateral pleuritic chest pain with bilateral pleural effusion in our patient (Figure 1). Further survey was arranged due to the unusual pleuritic pain in the progressing prostate cancer. Diagnostic pleuroscopy showed fleshy nodules scattered on the parietal pleura (Figure 2), similar to the finding of Durani, *et al* [2].

IHC plays an important role in identifying this rare cancer, and in confirming the endothelial origin of the neoplasm. Previous case reports in the English literature have described positive findings for CD31, CD34, CK, WT1 and ERG [3, 6-8]. CD31, CD34, factor VIII and FLI-1 are specific markers of angiosarcoma, and at least 1 of them must be positive to make the diagnosis [9]. CD31 is the most specific and sensitive endothelial marker, reacting rarely and only weakly with non-vascular tumors [6, 9]. WT1 protein expression is maintained during the angiogenesis and malignant transformation of endothelial cells, and is considered a specific endothelial marker [7]. ERG, another marker for endothelial cell neoplasms, is expressed in vascular tumors, such as angiosarcomas, and helps to distinguish cutaneous and non-cutaneous angiosarcomas from other histologic mimics [8]. IHC is the most important factor in diagnosing certain rare cancers, such as angiosarcoma, and CD31and ERG findings can corroborate this diagnosis [6, 8].

The positive IHC findings for CD31 and ERG (Figure 3) in the pleural tissue and for WT1 in the pleural effusion cell block in our case indicated that the cancer was an angiosarcoma. CK7 positivity is characteristic of an epithelioid angiosarcoma [9]. Negative staining of CK20, TTF-1, synaptophysin and napsin A signify that the cancer did not originate from the lung [10-11]. In addition, negativity for p63, Hepa-1, arginase, glypican 3 and synaptophysin imply that the cancer was not related to the liver mass [12]. Otherwise, specific markers for diagnosing prostate cancer, such as PSA, NKX 3.1 and AMACR, were negative, and only PSMA showed equivocal positive staining, which would indicate that it is metastasis of advanced prostate cancer [13-14]. As stated above, primary pleural epithelioid angiosarcoma, rather than pleural metastasis of prostate or lung or liver cancer, was the most likely diagnosis.

This patient died 1 month after diagnosis under palliative care. Previous studies have also shown that epithelioid angiosarcomas are very aggressive and often incurable, with most patients dying within months of diagnosis, even while undergoing treatment [9, 15].

Conclusion

Primary pleural angiosarcoma is an extremely rare and aggressive malignant disease. Its unspecific clinical sign and symptom of

chest discomfort might distract clinical physicians from the underlying malignant disease progressing with pleural metastasis. This case is a reminder that clinical physicians should make a differential diagnosis of emerging clinical signs and symptoms that are less common in the patient's underlying disease.

Declaration of interest

The authors have no conflicts of interest to declare.

Disclosure Statement

Appropriate written informed consent was obtained for publication of this case report and accompanying images.

Acknowledgment

We are thankful to the patient and his legal representatives for their kind permission to report the clinical presentation and data relating to his illness.

References

1. Alexiou C, Clelland CA, Robinson D, *et al*. Primary angiosarcomas of the chest wall and pleura. Eur J Cardiothorac Surg 1998; 14(5): 523-526.
2. Durani U, Gallo de Moraes A, Beachey J, *et al*. Epithelioid angiosarcoma: a rare cause of pericarditis and pleural effusion. Respir Med Case Rep 2018; 24: 77-80.
3. Dainese E, Pozzi B, Milani M, *et al*. Primary pleural epithelioid angiosarcoma. A case report and review of the literature. Pathol Res Pract 2010; 206(6): 415-419.
4. Bocklage T, Leslie K, Yousem S, *et al*. Extracutaneous angiosarcomas metastatic to the lungs: clinical and pathologic features of twenty-one cases. Mod Pathol 2001; 14(12): 1216-1225.
5. Renshaw AA, Nappi D, Cibas ES. Cytology of metastatic adenocarcinoma of the prostate in pleural effusions. Diagn Cytopathol 1996; 15(2): 103-107.
6. Sullivan HC, Edgar MA, Cohen C, *et al*. The utility of ERG, CD31 and CD34 in the cytological diagnosis of angiosarcoma: an analysis of 25 cases. J Clin Pathol 2015; 68(1): 44-50.
7. Timar J, Meszaros L, Orosz Z, *et al*. WT1 expression in angiogenic tumours of the skin. Histopathology 2005; 47(1): 67-73.
8. Stockman DL, Hornick JL, Deavers MT, *et al*. ERG and FLI1 protein expression in epithelioid sarcoma. Mod Pathol 2014; 27(4): 496-501.
9. Sedhai YR, Basnyat S, Golamari R, *et al*. Primary pleural angiosarcoma: case report and literature review. SAGE Open Med Case Rep 2020; 8: 2050313x20904595.
10. Selves J, Long-Mira E, Mathieu MC, *et al*. Immunohistochemistry for diagnosis of metastatic carcinomas of unknown primary site. Cancers (Basel) 2018; 10(4): 108.
11. Inamura K. Update on immunohistochemistry for the diagnosis of lung cancer. Cancers (Basel) 2018; 10(3): 72.
12. Takahashi Y, Dungubat E, Kusano H, *et al*. Application of immunohistochemistry in the pathological diagnosis of liver tumors. Int J Mol Sci 2021; 22(11): 5780.
13. Gurel B, Ali TZ, Montgomery EA, *et al*. NKX3.1 as a marker of prostatic origin in metastatic tumors. Am J Surg Pathol 2010; 34(8): 1097-1105.
14. Rubin MA, Zhou M, Dhanasekaran SM, *et al*. α-Methylacyl coenzyme A racemase as a tissue biomarker for prostate cancer. JAMA 2002; 287(13): 1662-1670.
15. Patel AM, Ryu JH. Angiosarcoma in the lung. Chest 1993; 103(5): 1531-35.

Multiple Ground-Glass Nodules Treated with Surgery and Radiofrequency Ablation–A Case Report

Pei-Chin Su[1], Frank Cheau-Feng Lin[1,2*]

A feasible therapeutic plan for ground-glass nodules is surgical resection. Operation plays an important role in both diagnosis and treatment. But, for a patient with multiple ground-glass nodules, adequate preservation of lung volume is an important issue. We present the case of a female with multiple ground-glass nodules who was treated using minimally invasive lobectomy, pre-operative localization followed with wedge resections, and radiofrequency ablation. The outcome was satisfactory. The combined treatment was effective, but further application and discussion are needed. ***(Thorac Med 2023; 38: 40-45)***

Key words: Ground glass nodule, lobectomy, wedge resection, RFA

Introduction

With its increasing incidence, lung cancer is the leading cause of cancer-related death in Taiwan. Low-dose computed tomography (CT) of the chest is commonly used for cancer screening. Early diagnosis and treatment can lead to excellent cancer survival and a better quality of life.

Malignant pulmonary nodules can be detected incidentally in a CT scan [1]. Lung nodules are defined as small (≤ 30 mm) lesions in the lung parenchyma. The malignant etiologies of pulmonary nodules can include primary lung cancer, metastatic cancer, carcinoid tumors, and benign lesions such as infection, harmatoma, and arteriovenous malformations. In addition, the features of nodules can be described in terms of size, attenuation, growth or stable size, calcification, and location. To attain a definite diagnosis, management options include non-surgical biopsy (bronchoscopic techniques, CT-guided percutaneous biopsy) and surgical excision, which is the gold standard for diagnosis of a lung nodule.

Percutaneous radiofrequency ablation (RFA) of pulmonary malignancies, a less invasive procedure, has a promising survival benefit [2]. Surgical resection is the standard treatment for early lung cancer. However, for the patient who cannot undergo surgery because of certain clinical conditions, such as poor lung function, previous lung surgery, or COPD, lung ablation approaches are alternative choices [3]. In addi-

[1]Division of Thoracic Surgery, Department of Surgery, Chung Shan Medical University Hospital, Taichung, Taiwan, R.O.C, [2]College of Medicine, Chung Shan Medical University, Taichung, Taiwan, R.O.C
Address reprint requests to: Dr. Frank Cheau-Feng Lin, No.110, Sec.1, Jianguo N. Rd., Taichung City 40201, Taiwan

tion, for early-stage lung cancer patients with resected stage IA disease, adjuvant systemic therapy such as chemotherapy and targeted therapy is not indicated [4]. For these patients, RFA would be a method of choice.

With the advent of the era of low-dose CT screening, the incidence of multiple primary lung cancer has increased [3]. For these patients, lung volume preservation is emphasized. We report the case of a patient with bilateral multiple ground-glass nodules (GGN). The treatment plan included a combination of surgical resection of the most affected region, preoperative localization for targeted resection, and percutaneous RFA to treat the patient and preserve as much lung function as possible. Follow-up studies yielded satisfactory results.

Case Report

A 50-year-old female treated for diabetes mellitus for more than 20 years was referred to our thoracic surgery clinic because of incidental abnormal findings on low-dose chest CT in a health examination. The CT images revealed bilateral GGN. Eleven GGNs were located on the right side, and 5 GGNs were found on the left-side lung (Figure 1). The most affected lobe was the right upper lobe, within which were 9 GGNs (nodules 1-9 (N1-N9)). The other nodules were in the right middle lobe (nodule 10, N10), right lower lobe (nodule 11, N11), left upper lobe (nodules 12-15, N12-N15) and left lower lobe (nodule 16, N16). The patient denied any specific respiratory symptoms and signs.

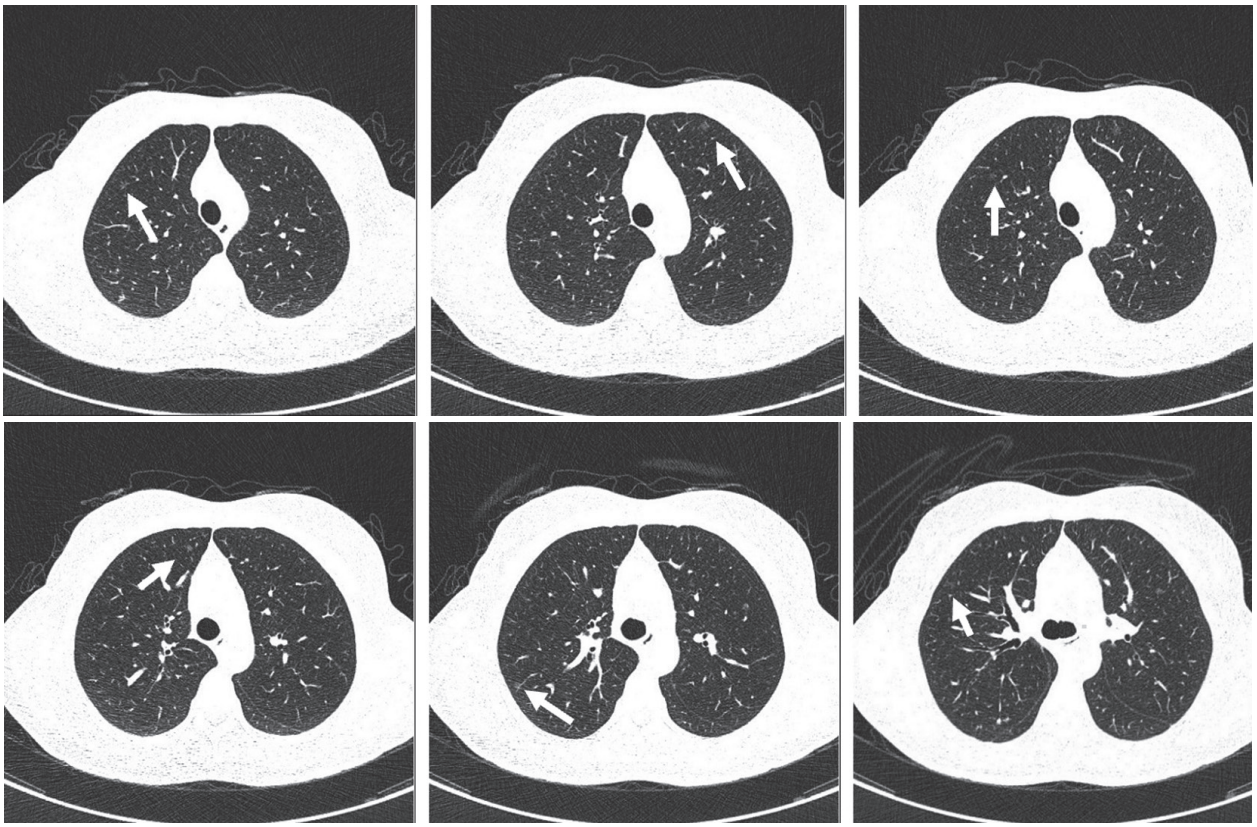

Fig. 1. Multiple bilateral ground-glass nodules in an axial view.

Since the affected regions included both lungs, the treatment plan combined surgical intervention for the most affected part and RFA for the remaining tumors. The pre-operative lung function test of forced expiratory volume in 1 second (FEV_1) was 2.38 liters, forced vital capacity (FVC) was 2.91 liters, and diffusing capacity of the lung for carbon monoxide (DLCO) was 17.83 ml/min/mmHg.

First, lobectomy of the right upper lobe and wedge resection of the right middle lobe and right lower lobe were arranged. To discriminate the location of the nodules with limited targeted resection, pre-operative CT guidance using Laser Angle Guide Assembly® (LAGA) assistance and injection of patent blue dye was performed (Figure 2) [8]. Under general anesthesia with the patient in a left decubitus position, right upper lobe lobectomy for N1-N9 resection was performed using a 2 minimal-incisions approach. Then, 2 gray-yellowish nodules with pleural dimpling at the right middle and lower lobes, which were marked by a tattoo, were resected (N10, N11). The pathological report was minimally invasive adenocarcinoma and atypical adenoid hyperplasia for N1-N9, atypical ductal hyperplasia for N11, and atelectasis with anthracosis for N10.

One and a half months after the operation, and before RFA, the follow-up pulmonary function was FEV_1: 1.97 liters, FVC: 2.08 liters, and DLCO: 14.38 ml/min/mmHg. There were no changes in pulmonary function after the RFA interventions. We were able to preserve adequate lung function without influencing the patient's daily life.

Two months post-operation, 3 percutaneous CT-guided RFA procedures under LAGA assistance were scheduled to eliminate the residual tumors (N12-16) of the left upper and lower lobe. The intervals for RFA were 18 days and 28 days. Using RF electrode needle probe punctures, the actual RFA mean time was 6 minutes. The patient experienced no pneumothorax, hemothorax, hemoptysis, or shortness of breath. The clinical course was smooth and no complications occurred.

Follow-up CT every 3 months disclosed no obvious tumor enlargement, but the scar formation of the GGN region which had been treated by RFA could be seen (Figure 3). We used 3D imaging to clarify the lesions (Figure 4a,b). The outcome showed good local control of the disease, with no recurrence or residual tumor.

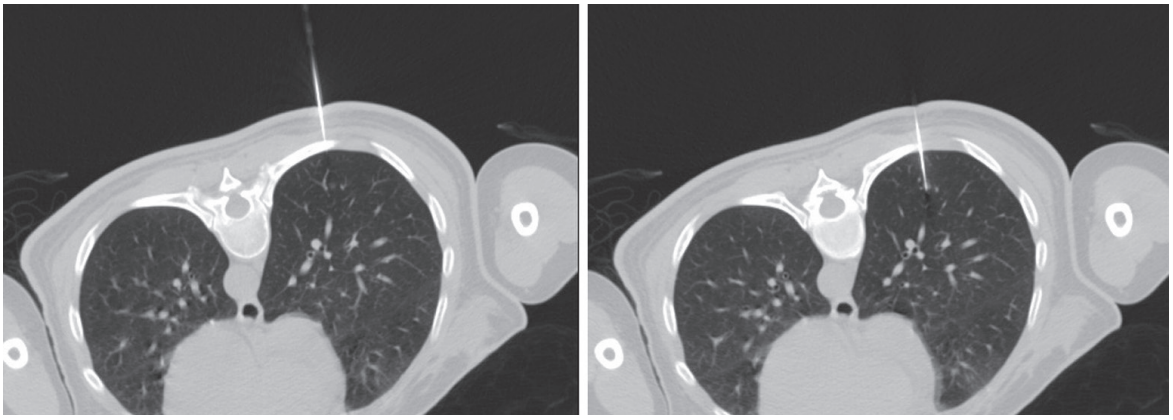

Fig. 2. Pre-operative CT-guided localization with patent blue dye.

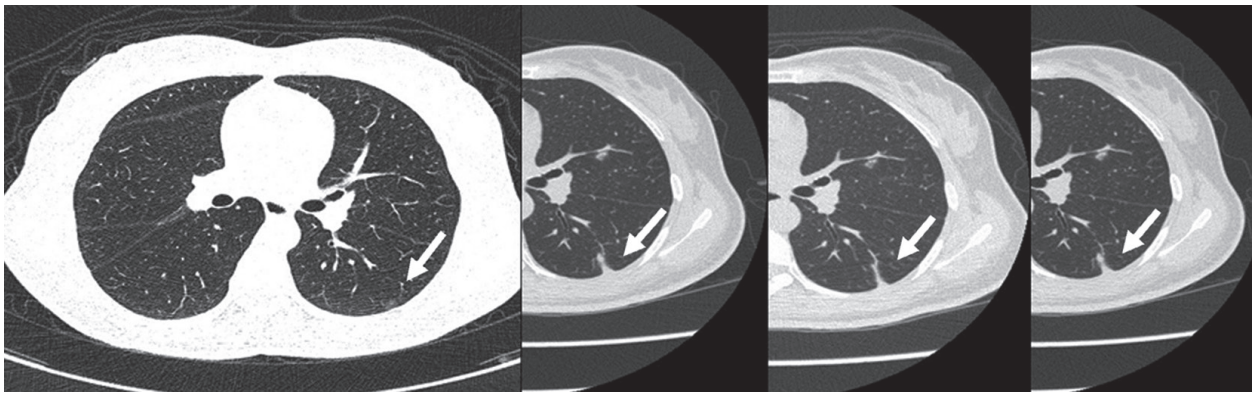

Fig. 3. Follow-up imaging every 3 months showed scarring after RFA.

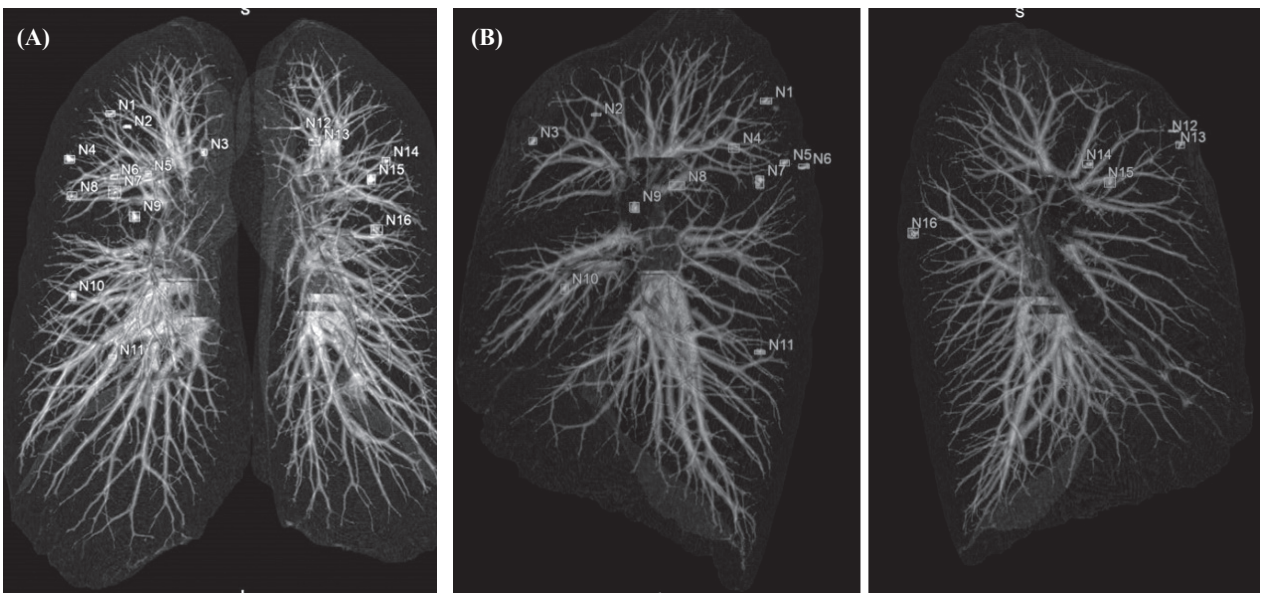

Fig. 4. (A).3D images of the lung. (B).3D images of the lung (lateral view).
N1-N9 GGO (right upper lobe) were resected by lobectomy.
N10 (right middle lobe) and N11 (right lower lobe) underwent wedge resection with pre-operative CT-guided localization.
N12-N14 (left upper lobe) ablated in the 1st RFA.
N15 (left upper lobe) ablated in the 2nd RFA.
N16 (left lower lobe) ablated in the 3rd RFA.

Discussion

Pulmonary GGN is defined as an opacity that does not obscure the underlying structures or vessels in the CT scan. In clinical practice, pulmonary GGN has become an important issue, as its diagnosis rate has increased with the increased use of low-dose CT screening. The incidence of malignancy in resected GGN was 63% and 83% in previous studies [5, 6]. But, GGN-dominant tumors were also characterized by a lower incidence of pathologic invasion, and rare pleural invasion and lymph node or vascular metastasis. GGN can be successfully treated with surgical intervention, and has an extremely favorable prognosis [7].

The high incidence of malignancy in GGN and lung cancer is the main cause of cancer-related death in the world. There is now much more evidence revealing the benefits of low-dose CT screening of lung cancer, and detecting early-stage lung cancer via low-dose CT scan may reduce the mortality rate [8]. In Western countries, most studies have focused on patients with a smoking history. However, the diversity of clinical, epidemiological, and demographic features should be taken into account.

Depending on the affected region or numbers of nodules, anatomic resection such as lobectomy and segmentectomy, or non-anatomic wedge resection can be chosen as a definite treatment. Lobectomy and segmentectomy ligate the contributing pulmonary arteries, veins and bronchi. The 2 procedures may ensure a safe margin of the disease, but are accompanied with a certain extent of lung volume loss. By contrast, wedge resection preserves much more lung tissue and is often chosen for pathological diagnosis and lesion removal. To evaluate where the nodule is located, pre-operative localization can be used. A variety of methods, such as CT-guided needle localization, dye marking, and use of a hybrid operating room, are effective. These are all effective techniques to ensure a successful wedge resection [9].

Furthermore, pre-operative CT-guided localization plays an important role in allowing the operation to be performed precisely with limited resection. To arrive at the target nodule in this case, the use of LAGA and CT imaging can provide a 3D space, including longitudinal position, depth of distance and direction of angle. The result is reliable because of the precise angle provided through laser guidance, and the procedure can be finished in minutes. Due to the accuracy of 1-shot localization, complications with this procedure are rare [10].

After adequate resection of the nodules, calculating postoperative lung function using predicted postoperative values for FEV1 (ppo FEV1) and predicted postoperative values for DLCO (ppo DLCO) is important. There may be an increased incidence of postoperative morbidity in patients with ppo FEV1 or ppo DLCO < 40% [11]. In our case, ppo FEV1 and ppo DLCO decreased after right-side lung surgery with lobectomy and 2 wedge resections. Post-surgery management of the left lung nodules should be continued.

RFA is an alternative, effective treatment. It is the most widely used ablative technique for lung tumors. Lung RFA yields satisfactory outcomes and a promising long-term survival [12]. In a systematic review, complete tumor necrosis rates of 38-97% (median, 90%) were reported [13]. In addition, the technique is safe. It has acceptable risks, including pneumothorax, and is not associated with increased mortality [14]. With regard to preservation of lung function, in most cases, there was no significant worsening of FEV1, FEV1% predicted, FVC, or FVC% predicted at 6 months after RFA [15].

In patients with multiple nodules, known as synchronous lesions, hybrid approaches combining both surgical and nonsurgical interventions have been considered. A comprehensive pre-operative evaluation is conducive to further management.

There is some discussion comparing the clinical outcome of surgical resection and that of CT-guided percutaneous ablation. For resection of early-stage lung cancer, surgery remains the recommended choice; for those patients not suitable for operation, RFA still has promising results, including overall survival.

Few reports have mentioned the use of RFA

for GGN lesions after surgical resection. The use of minimally invasive procedures and percutaneous intervention as a strategy for dealing with multiple GGNs would be beneficial. Even for the definite diagnosis and management of lesions, a combined multiple therapeutic plan could be individualized. Further cases studies and discussions are warranted.

Conclusion

The use of a combination of minimally invasive lobectomy, pre-operative localization wedge resection and RFA for multiple GGNs is curative and safe, and preserves pulmonary function.

References

1. MacMahon H. Using computer analysis to predict likelihood of cancer in lung nodules. Radiology 2018; 286(1): 296-297.
2. Lguchi T, Hiraki T, Gobara H, *et al*. Percutaneous radiofrequency ablation of lung cancer presenting as ground-glass opacity. Cardiovasc Intervent Radiol 2015; 38(2): 409-15.
3. Teng J, Xu J, Jiao J, *et al*. Radiofrequency ablation of synchronous multiple primary lung cancer assisted by a magnetic navigation system: a case report. Ann Palliat Med 2020; 9(2): 478-482.
4. Pignon JP, Tribodet H, Scagliotti GV, *et al*. Lung adjuvant cisplatin evaluation: a pooled analysis by the LACE Collaborative Group. J Clin Oncol 2008; 26(21): 3552-9.
5. Migliore M, Fornito M, Palazzolo M, et al. Ground glass opacities management in the lung cancer screening era. Ann Transl Med 2018; 6(5): 90.
6. Mei X, Wang R, Yang W, *et al*. Predicting malignancy of pulmonary ground-glass nodules and their invasiveness by random forest. J Thorac Dis 2018; 10(1): 458-463.
7. Tsutani Y, Miyata Y, Nakayama H, *et al*. Appropriate sublobar resection choice for ground glass opacity-dominant clinical stage IA lung adenocarcinoma: wedge resection or segmentectomy. Chest 2014; 145(1): 66-71.
8. Duffy SW, Field JK. Mortality reduction with low-dose CT screening for lung cancer. N Engl J Med 2020; 382(6): 572-573.
9. Sun SH, Gao J, Zeng XM, *et al*. Computed tomography-guided localization for lung nodules: methylene-blue versus coil localization. Minim Invasive Ther Allied Technol; 2020: 1-6.
10. Lin FC, Tsai SC, Tu HT, *et al*. Computed tomography-guided localization with laser angle guide for thoracic procedures. J Thorac Dis 2018; 10(6): 3824-3828.
11. Colice GL, Shafazand S, Griffin JP, *et al*. Physiologic evaluation of the patient with lung cancer being considered for resectional surgery: ACCP evidenced-based clinical practice guidelines (2nd edition). Chest 2007; 132(3 Suppl): 161S-77S.
12. Simon CJ, Dupuy DE, DiPetrillo TA, *et al*. Pulmonary radiofrequency ablation: long-term safety and efficacy in 153 patients. Radiology 2007; 243(1): 268-75.
13. Zhu JC, Yan TD, Morris DL, *et al*. A systematic review of radiofrequency ablation for lung tumors. Ann Surg Oncol 2008; 15(6): 1765-74.
14. Welch BT, Brinjikji W, Schmit GD, *et al*. A national analysis of the complications, cost, and mortality of percutaneous lung ablation. J Vasc Interv Radiol 2015; 26(6): 787-91.
15. Ambrogi MC, Fanucchi O, Cioni R, *et al*. Long-term results of radiofrequency ablation treatment of stage I non-small cell lung cancer: a prospective intention-to-treat study. J Thorac Oncol 2011; 6(12): 2044-51.

Pulmonary Cavitary Lesion as A Rare Radiologic Finding of Organizing Pneumonia: A Case Report

Yu-Chi Tsai[1], Fan-Min Lin[1,2]

Organizing pneumonia, a type of interstitial lung disease, has a unique pathologic and radiologic presentation. Manifestations of cryptogenic organizing pneumonia on plain film are typically quite distinctive, with features similar to extensive pneumonia, including bilateral, patchy or diffuse, consolidative or ground glass opacities. A cavitary lesion is a rare radiologic presentation of organizing pneumonia. We present a case of organizing pneumonia with a cavitary lesion on chest films. Timely diagnosis and corticosteroid use are the cornerstones of treatment for organizing pneumonia. ***(Thorac Med 2023; 38: 46-53)***

Key words: Organizing pneumonia, cryptogenic organizing pneumonia, cavitation

Introduction

Organizing pneumonia (OP) is a type of interstitial lung disease with characteristic pathologic features, such as intraluminal fibroblastic plugs, also called Masson bodies, seen in respiratory bronchioles, alveolar ducts, and alveoli, surrounded with mild interstitial inflammation in the adjacent lung. The disease reflects a reparative process for alveolar epithelial injury. The pathologic presentation consists of inflammatory exudates, foamy cells recruitment in alveolar spaces, and alveolar epithelial cells hyperplasia within the small airways [1].

Successful diagnosis of OP should be based on an adequate clinical history, imaging, laboratory data, and pathological clues. OP can result from various causes, such as an infectious disease, including pathogens of human immunodeficiency virus, influenza virus, bacteria, and even fungus. Drugs, connective tissue disorder, hematologic malignancy, organ transplantation, and radiation are also found in association with OP. In most cases, the cause remains unknown [2].

Most patients respond well to systemic corticosteroids and have an excellent prognosis [1-6]. Patients with OP have a subacute process, and imaging typically reveals findings of ground glass or consolidative opacities. However, pleural effusion, mediastinal adenopathy, and even cavitary lesions have been documented as

[1]Department of Internal Medicine, Kaohsiung Armed Forces General Hospital, Kaohsiung, Taiwan, [2]Department of Thoracic Medicine, Kaohsiung Armed Forces General Hospital, Kaohsiung, Taiwan
Address reprint requests to: Dr. Fan-Min Lin, Kaohsiung Armed Forces General Hospital, No.2, Zhongzheng 1st Rd., Lingya Dist., Kaohsiung City, 80284 Taiwan (R.O.C.)

rare presentations in previous case reports. We report a case of excavated cryptogenic organizing pneumonia (COP), after excluding other possible contributive etiologies. Biopsy is mandatory to exclude other common etiologies of cavitary lesions.

Case Report

A 61-year-old man presented to our chest medicine clinic with a 5-day history of worsening cough with much gray turbid sputum production, and a 1-month history of left upper back pain. The illness occurred off and on and was associated with drenching night sweats. His tenderness was relieved after taking pain killers, and was not related to a changing of position. The patient had smoked cigarettes since he was 24 years old, and infrequently drank alcohol. He was a bus driver and had been in his usual state before this visit. The patient denied any use of medication and claimed no history of significant disease.

On physical examination, he was noted to have dull percussion in his left upper back and rhonchi breathing sounds in the same area. The patient looked well and was without respiratory distress. His temperature was 36.7°C; blood pressure, 121/95 mm Hg; heart rate, 105 beats per minute; and respiratory rate,18 breaths per minute. Chest radiograph revealed a patchy consolidation with multiple cavitation and an air-fluid level content at the left upper lobe (Figure 1a).

The hemogram disclosed leukocytosis with neutrophils predominant and normocytic anemia. Blood levels of electrolytes and glucose, and hepatic and renal function were normal. The other laboratory test results are shown in Table 1. The patient was admitted to our ward for left upper lung lesion management. The differential diagnosis included lung abscess, pulmonary tuberculosis, neoplasm, and chronic fungal infection.

Initially, the patient received treatment with amoxicillin/clavulanate after blood and sputum cultures were obtained. On day 4, because of his persistent fever and worsening fatigue, we

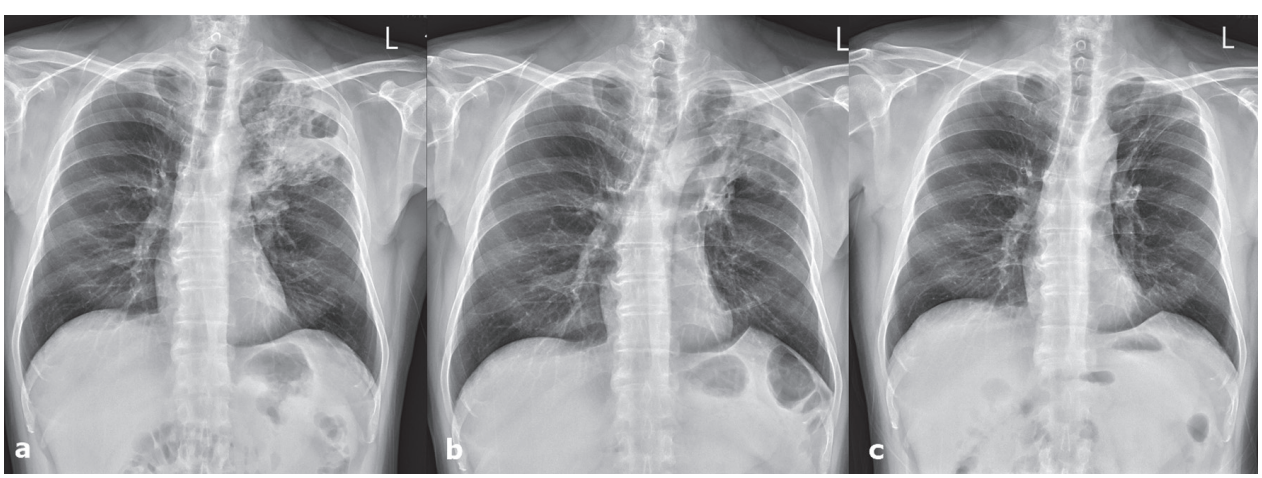

Fig. 1. (a).Chest radiograph revealed a left upper lobe cavitary lesion with an air-fluid level presentation. (b).The same patient's chest film after a 1-month treatment with corticosteroid, showing improvement. (c).Remission of the left upper lobe lesion with only some fibrotic band retention, after a half year of corticosteroid treatment.

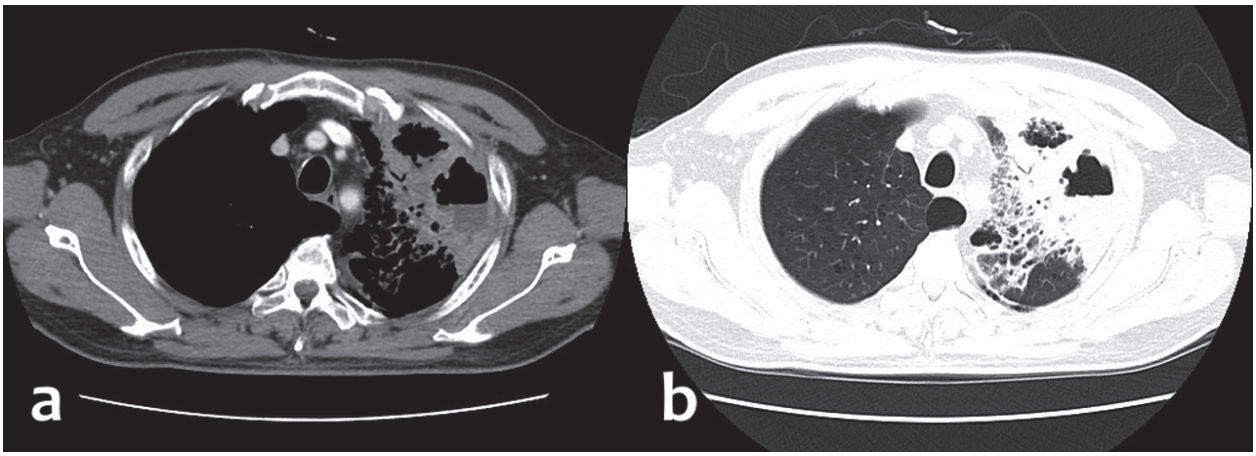

Fig. 2. (a).Computed tomography of the chest disclosed left upper lobe ground glass opacity with cavitary lesion and low attenuation content. (b). Lung window of computed tomography at the same area revealed multifocal ill-defined patchy consolidation in a perilobular pattern.

escalated the empiric antibiotics to piperacillin/tazobactam and amikacin for broad spectrum coverage. Testing for a lung lesion was arranged. Computed tomography of the chest revealed multifocal ill-defined ground glass opacities with consolidation, and cavitary change at the left upper and left lower lung without pleural effusion (Figure 2).

Given the lack of an initial adequate microbiological clue and the deterioration of this patient, bronchoscopy was performed to assist the diagnosis. However, there was no evidence of an endobronchial lesion. Repeated sputum culture samples and rapid serology tests, including pneumococcus urine antigen and a cryptococcus antigen serum test, were negative. Four acid-fast stain sputum smear sets and the final tuberculosis culture results were negative. The sputum fungus culture yielded a negative result as well.

After a 10-day empiric antibiotics treatment course without an evident response, percutaneous transthoracic ultrasound-guided lung biopsy and pleural biopsy were done. The histologic examination of the specimen from the left upper lobe disclosed an organizing pulmonary area, composed of plugs of young fibrous tissue distributed within alveolar ducts and spaces (Figure 3a, 3b). Many inflammatory cells, including mainly lymphocytes and a small portion of polymorphonuclear granulocytes and macrophages, and proteinaceous exudate without evidence of malignancy, were noted. OP was suspected based on the pathologic evidence.

Systemic corticosteroid with oral prednisolone 0.5 mg/kg/day was prescribed, based on the patient's body weight (67 kg, so an estimated 30 mg of oral prednisolone daily divided into 2 doses), beginning late in the second week of admission. Concurrent antibiotics were continued until the third week of admission, when the patient reported his fever and chest pain had resolved. After 1 month of oral corticosteroid treatment, the left upper lobe lesion was significantly improved (Figure 1b). We maintained corticosteroid treatment for 6 months, with doses of oral prednisolone 15 mg twice daily (0.5 mg/kg/day) for the first 2 months, 10 mg twice daily for the following 2 months, and finally 10 mg daily, followed by 5 mg daily for the last 2

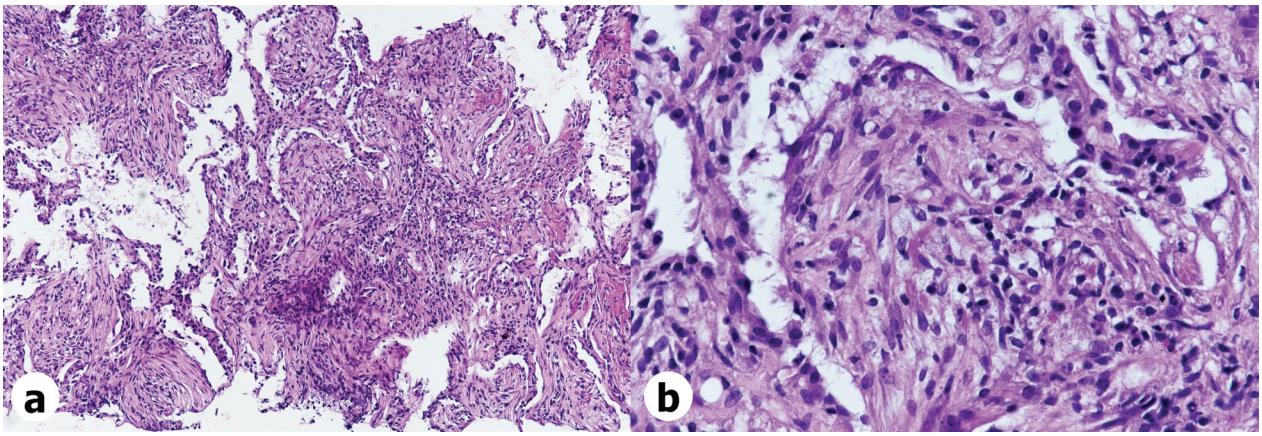

Fig. 3. (a).(Low power field, 100x). Photomicrograph of the specimen from transthoracic biopsy. Intraluminal plugs consisted of fibroblasts distributed within alveolar sacs. (b).(High power field, 400x). High power photomicrograph of picture 3a revealed spindled fibroblasts constituting an intraluminal plug with numerous inflammatory cell infiltrations, mainly lymphocytes, and some polymorphonuclear granulocytes and macrophages.

months. Sequential chest films revealed consolidation resolution with some residual fibrotic bands (Figure 1c).

Discussion

Organizing pneumonia (OP), a type of interstitial lung disease, can be involved from the alveolar walls to the distal bronchioles [1-6]. A variety of factors, including drugs, connective tissue disorders, hematologic malignancy, infections, organ transplantation, other interstitial lung diseases, radiation, and environmental exposure, are recognized as causes of the pathologic features of secondary OP.

In the early 1900s, bacterial pneumonia was mentioned as a cause of secondary OP [7]. Today, a variety of infectious pathogens, such as bacteria (Chlamydia pneumoniae, Legionella pneumophila, Mycoplasma pneumoniae, Norcardia asteroides) [6,8,9], viruses (human immunodeficiency virus, influenza virus) [8,10], fungi (Aspergillus, Cryptococcus neoformans) [6], and even parasites [6], are found to be the leading causes of secondary OP. The use of some drugs, for example, amiodarone and bleomycin, can result in secondary OP [11]. Distinguishing between OP caused by a drug or by the patient's preexisting comorbidities is challenging. Resolution of OP after discontinuing the drug may be a feasible diagnostic method for drug-induced OP [5,11].

Migratory OP after radiation therapy for breast cancer may share pathologic features similar to OP [12]. Rheumatoid arthritis [13], Sjögren's syndrome [14], and other rheumatoid diseases can be associated with a secondary etiology of OP [13]. Hematologic malignancy such as leukemia [15], and chemical irritants such as gastric contents aspiration [6], can be conditions linked to secondary OP.

However, most cases of OP are idiopathic, or so-called cryptogenic organizing pneumonia (COP) [1,2,5,6]. The previous name used – bronchiolitis obliterans organizing pneumonia (BOOP), is confusing and overlaps with the category of obliterative bronchiolitis (OB), which is composed of bronchiole obstruction, but exists with minimal or no evidence of pulmonary inflammatory cells infiltration [3,4].

The American Thoracic Society and European Respiratory Society ended this confusion in 2002 by suggesting the use of the terms OP and COP to avoid further misinterpretation [16,17].

COP is a rare disease with an estimated incidence of less than 10 cases per 100,000 persons/year [18]. It occurs approximately within the fifth to sixth decade of life, without a sex predominance [4,19]. Approximately 56-68% of OP cases cannot be clearly linked to a known possible cause, so they are then reclassified as COP [20].

OP may reflect an inflammatory or healing process due to lung injury. When damage occurs at the involved alveolar epithelial cells and capillary endothelial cells, intra-alveolar space leakage of plasma proteins and coagulation factors lead to fibroblasts migrating into the damaged area and generating fibrin clotting on alveolar surfaces. Small polyps composed of loose fibrous tissue may develop. Intraluminal plugs of granulation tissue proliferate and may coat and fill adjacent alveolar sacs and bronchioles [2,5].

Subacute symptoms such as dry cough, dyspnea, fever, fatigue, and weight loss are reported as clinical presentations of OP. Patients who are suspected of having community pneumonia at first, but do not respond well to empirical antibiotics, or who have delayed resolution on chest film, may be exhibiting the initial features of OP [7].

Both OP and COP share similar radiographic presentations [19]. Three categories of specific imaging findings have been reported [2]. The first characteristic radiologic finding of OP is multiple alveolar opacities, which commonly have a peripheral, subpleural, bilateral, and usually migratory distribution. The lesion size varies from a few centimeters to a whole lobe [2,5]. Air bronchogram with bronchial wall thickening and dilatation are also common [1]. A peripheral, peribronchial distribution and recurrent migratory lesion are thought of as distinctive features of OP. Computed tomography may display a greater extent of bilateral multifocal airspace opacities than chest films, and a distribution that is mainly peripheral or in the lower lung zone [5].

Solitary focal opacity is another image presentation of OP. Since its radiologic manifestation can be confused with that of pulmonary malignancy, the diagnosis usually depends on surgical biopsy [22]. Most of the patient's lesions are located in the upper lobes. Cavitation may be an associated manifestation [2,5]. The third pattern is OP as an infiltrative type, in which bilateral and diffuse interstitial infiltration is demonstrated [5]. The severity of interstitial inflammation is consistent with the degree of image infiltration. Nonspecific interstitial pneumonia and idiopathic pulmonary fibrosis are possible radiologic differential diagnoses [2]. The reverse halo sign is described as a central ground glass opacity surrounded by a crescentic ring-like air space. Although highly specific, it presents in about 20% of patients with OP [21]. Other rare manifestations, including pleural effusion [2] and mediastinal lymphadenopathy [23], have been described in some case reports.

Cavitation is seldom mentioned in textbooks, but it has existed in some case series since 1985 [3,24-33]. Multiple or single pulmonary cavitary nodules, massive alveolar infiltrates with multiple cavities, and diffuse opacities with cavitations have been described. The range of influence is from diffuse bilateral to focal unilateral lesions [24-30]. Upper lobes are frequent sites of cavitary OP involvement [2,5,27-29]. Unresolved pneumonia [6] or

pneumatocele [31] may be present at the adjacent pulmonary area. Honey-combing has been documented in very few patients with late advanced progressive disease [6]. Cavitary OP has been found sporadically among patients with cryoglobulinemia [32], and rarely among those with primary non-Hodgkin's lymphoma [33].

With regard to subacute cavitary pulmonary disease, the most important differential diagnoses include: chronic infection (such as fungus, mycobacterium), neoplasms (squamous cell), and a vascular etiology (granulomatosis with polyangiitis) [2,5,18,19].

Diagnosis of COP relies on pathology, imaging, clinical manifestations, and excluding all identifiable secondary factors. In this way, a final diagnosis can be established [16]. Invasive biopsy procedures including transbronchial or open lung biopsy are usually required, due to inadequate information gained from the clinical disease process and radiologic findings.

Treatment for OP and COP depends on the severity of the disease, the degree of pulmonary function impairment, and the rapidity of progression [6,34]. Systemic corticosteroids are the cornerstone of therapy for COP [4,19]. Although there is a lack of large clinical trials regarding optimal dosage and duration, starting treatment at 0.75 mg/kg/day and gradually tapering the dosage based on clinical response and drug side effects during 6-12 months of therapy is generally suggested [16,35]. The overall prognosis is very good. Only 20% of patients experienced relapse [4,36], and about 80% of patients have complete remission [4,5.16]. Improvement is radiologically documented during the first 4 weeks after treatment add-on [3,18].

Conclusion

OP is a type of interstitial lung disease. COP is varied, and the etiology seems idiopathic. COP usual occurs in patients in the fifth to sixth decade of life, without a sex predominance. Most patients have a subacute disease process, and migratory recurrent multiple ground-glass or consolidative opacities are the majority of radiologic findings. Cavitary lesion as a radiologic presentation is rare, but has been reported in case series since the late 1900s. Clarifying the potential differential diagnosis is important to this unusual finding. Histopathology discloses granulation plugs that extend excessively into the small airway and alveoli, with infiltration of chronic inflammatory cells. A definite diagnosis of COP requires clinical, radiological, and pathological proof, and the exclusion of other secondary factors. Corticosteroid is the standard treatment for COP. Most patients respond well and have a good prognosis.

List of abbreviations:

BOOP: bronchiolitis obliterans organizing pneumonia

COP: cryptogenic organizing pneumonia

OB: obliterative bronchiolitis

OP: organizing pneumonia

References

1. Graney BA, Lee JS, King TE. Nonspecific interstitial pneumonitis and other idiopathic interstitial pneumonias. In: Broaddus VC, *et al*. ed. Murray & Nadel's Textbook of Respiratory Medicine, 7th ed., Philadelphia; Saunders, Elsevier, 2021: 1235-1247.
2. Cordier JF. Cryptogenic organising pneumonia. Eur Respir J 2006; 28: 422-446.
3. Davison AG, Heard BE, McAllister WA, *et al*. Cryptogenic organizing pneumonitis. Q J Med 1983; 52: 382-394.

4. Epler GR, Colby TV, McLoud TC, *et al*. Bronchiolitis obliterans organizing pneumonia. N Eng J Med 1985; 312:152-158.
5. Cordier JF. Organising pneumonia. Thorax 2000; 55: 318-328.
6. King TE. Organizing pneumonia. In: King TE, Schwarz MI, ed. Interstitial lung disease, 5th ed., New Haven; People's Medical Publishing House, Shelton, 2011: 981-994.
7. Floyd R. Organization of pneumonitic exudates. Am J Med Sci 1922; 163: 527-548.
8. Colby TV, Myers JL. Clinical and histologic spectrum of bronchiolitis obliterans, including bronchiolitis obliterans organizing pneumonia. Semin Respir Med 1992; 13: 119-133.
9. Camp M, Mehta JB, Whitson M. Bronchiolitis obliterans and Nocardia asteroides infection of the lung. Chest 1987; 92: 1107-1108.
10. Khater FJ, Moorman JP, Myers JW, *et al*. Bronchiolitis obliterans organizing pneumonia as a manifestation of AIDS: case report and literature review. J Infect 2004; 49: 159-164.
11. Epler GR. Drug-induced bronchiolitis obliterans organizing pneumonia. Clin Chest Med 2004; 25: 89-94.
12. Kaufman J, Komorowski R. Bronchiolitis obliterans. A new clinical-pathologic complication of irradiation pneumonitis. Chest 1990; 97: 1243-1244.
13. Lohr RH, Boland BJ, Douglas WW, *et al*. Organizing pneumonia. Features and prognosis of cryptogenic, secondary, and focal variants. Arch Intern Med 1997; 157: 1323-1329.
14. Matteson EL, Ike RW. Bronchiolitis obliterans organizing pneumonia and Sjogren's syndrome. J Rheumatol 1990; 17: 676-679.
15. Daniels CE, Myers JL, Utz JP, *et al*. Organizing pneumonia in patients with hematologic malignancies: a steroid-responsive lesion. Respir Med 2007; 101: 162-168.
16. American Thoracic Society; European Respiratory Society. American Thoracic Society/European Respiratory Society International Multidisciplinary Consensus Classification of the Idiopathic Interstitial Pneumonias. This joint statement of the American Thoracic Society (ATS), and the European Respiratory Society (ERS) was adopted by the ATS board of directors, June 2001, and by the ERS Executive Committee, June 2001. Am J Respir Crit Care Med 2002; 165: 277-304.
17. Travis WD, Costabel U, Hansell DM, *et al*. An official American Thoracic Society/European Respiratory Society statement: Update of the international multidisciplinary classification of the idiopathic interstitial pneumonias. Am J Respir Crit Care Med 2013; 188: 733-748.
18. Alasaly K, Muller N, Ostrow DN, *et al*. Cryptogenic organizing pneumonia. A report of 25 cases and a review of the literature. Medicine (Baltimore) 1995; 74: 201-211.
19. Drakopanagiotakis F, Paschalaki K, Abu-Hijleh M, *et al*. Cryptogenic and secondary organizing pneumonia: clinical presentation, radiographic findings, treatment response, and prognosis. Chest 2011; 139: 893-900.
20. Gudmundsson G, Sveinsson O, Isaksson HJ, *et al*. Epidemiology of organising pneumonia in Iceland. Thorax 2006; 61: 805.
21. Kim SJ, Lee KS, Ryu YH, *et al*. Reversed halo sign on high-resolution CT of cryptogenic organizing pneumonia: diagnostic implications. AJR Am J Roentgenol 2003; 180: 1251-1254.
22. Maldonado F, Daniels CE, Hoffman EA, *et al*. Focal organizing pneumonia on surgical lung biopsy: causes, clinico-radiologic features, and outcomes. Chest 2007; 132: 1579-1583.
23. Souza CA, Müller NL, Lee KS, *et al*. Idiopathic interstitial pneumonias: prevalence of mediastinal lymph node enlargement in 206 patients. AJR Am J Roentgenol 2006; 186: 995-999.
24. Flowers JR, Clunie G, Burke M, *et al*. Bronchiolitis obliterans organizing pneumonia: the clinical and radiologic features of seven cases and a review of the literature. Clin Radiol 1992; 45: 371-377.
25. Froudarakis M, Bouros D, Loire R, *et al*. BOOP presenting with hemoptysis and multiple cavitary nodules. Eur Respir J 1995; 8: 1972-1974.
26. Haro M, Vizcaya M, Texido A, *et al*. Idiopathic bronchiolitis obliterans organizing pneumonia with multiple cavitary lung nodules. Eur Respir J 1995; 8: 1975-1977.
27. Heller I, Biner S, Isakov A, *et al*. TB or not TB: cavitary bronchiolitis obliterans organizing pneumonia mimicking pulmonary tuberculosis. Chest 2001; 120: 674-678.
28. Ackerman LV, Elliott GV, Alanis M. Localized organizing pneumonia: its resemblance to carcinoma; a review of its

clinical, roentgenographic and pathologic features. Am J Roentgenol Radium Ther Nucl Med 1954; 71: 988-996.
29. Cordier JF, Loire R, Brune J. Idiopathic bronchiolitis obliterans organizing pneumonia. Definition of characteristic clinical profiles in a series of 16 patients. Chest 1989; 96: 999-1004.
30. Yang PS, Lee KS, Han J, *et al*. Focal organizing pneumonia: CT and pathologic findings. J Korean Med Sci 2001; 16: 573-578.
31. Linsen VM, van Noord JA. A large air-filled cyst in a patient with migratory infiltrates. Chest 1994; 105: 253-254.
32. Zackrison LH, Katz P. Bronchiolitis obliterans organizing pneumonia associated with essential mixed cryoglobulinemia. Arthritis Rheum 1993; 36: 1627-1630.
33. Safadi R, Berkman N, Haviv YS, *et al*. Primary non-Hodgkin's lymphoma of the lung presenting as bronchiolitis obliterans organizing pneumonia. Leuk Lymphoma 1997; 28: 209-213.
34. Bradley B, Branley HM, Egan JJ, *et al*. Interstitial lung disease guideline: the British Thoracic Society in collaboration with the Thoracic Society of Australia and New Zealand and the Irish Thoracic Society. Thorax 2008; 63 Suppl 5: v1.
35. Wright L, King TE. Cryptogenic organizing pneumonia (idiopathic bronchiolitis obliterans organizing pneumonia): an update. Clin Pulm Med 1997; 4: 152-158.
36. Lazor R, Vandevenne A, Pelletier A, *et al*. Cryptogenic organizing pneumonia: characteristics of relapses in a series of 48 patients. Am J Respir Crit Care Med 2000; 162: 571-577.

A Rare Case of Endobronchial Pulmonary Metastasis of Hepatocellular Carcinoma: Case Report and Literature Review

Juei-Yang Ma[1], Pei-Chien Tsai[2], Chia-You Kuo[1], Chia-Min Chen[1], Wei-An Chang[1,3]

Hepatocellular carcinoma (HCC) is the fourth leading cause of cancer-related deaths worldwide (1), and in Taiwan. According to previous reviews, the lung is the most frequently involved organ in extrahepatic metastases (55%). The typical presentation of pulmonary metastasis of HCC is noncalcified soft-tissue nodules with a lower lobe predominance. Another frequently reported radiologic finding of lung metastasis of HCC is pulmonary tumor emboli. Here, we reported the case of a 62-year-old man who suffered from frequent intermittent hemoptysis, progressive dyspnea, and productive cough for 2-3 weeks. He was diagnosed with endobronchial pulmonary metastasis of HCC, and the symptoms improved significantly after bronchoscopic intervention. During the procedure, we encountered massive hemoptysis after removing the easily detached tumor. The hemoptysis was treated using several methods of hemostasis along with fiberoptic bronchoscopy. A similar episode recurred 7 months later. After 2 interventions, the patient had an uneventful recovery without further fatal hemoptysis or respiratory failure. Our case reveals a unique characteristic of HCC lung metastasis and highlights the usefulness of fiberoptic bronchoscopy in containing hemostasis.
(Thorac Med 2023; 38: 54-61)

Key words: pulmonary metastasis of hepatocellular carcinoma, endobronchial type

Introduction

The lung is the most common metastatic site of hepatocellular carcinoma (HCC), and the 1-year overall survival (OS) rate of HCC with lung metastasis is approximately 10% [2]. Pulmonary HCC metastasis commonly presents as parenchymal soft-tissue nodules and pulmonary vascular emboli [3]. Based on the pathophysiology, extrahepatic HCC can occur in 3 distinct ways: direct extension, hematogenous spread, or lymphatic invasion. Pulmonary HCC metas-

[1]Division of Pulmonary and Critical Care Medicine, Department of Internal Medicine, Kaohsiung Medical University Hospital, Kaohsiung, Taiwan, [2]Respiratory Therapy Team, Division of Pulmonary and Critical Care Medicine, Department of Internal Medicine, Kaohsiung Medical University Hospital, [3]School of Medicine, College of Medicine, Kaohsiung Medical University, Kaohsiung, Taiwan
Address reprint requests to: Dr. Wei-An Chang, Division of Pulmonary and Critical Care Medicine, Department of Internal Medicine, Kaohsiung Medical University Hospital, Kaohsiung Medical University, No.100, Tzyou 1st Road, Kaohsiung 807, Taiwan

tases occur via hematogenous dissemination to the pulmonary capillary network, leading to the common presentation of parenchymal soft-tissue nodules and pulmonary vascular emboli [3]. Therefore, the lower lobes of the lung are more often involved with metastases than the upper lobes. The common sources of endobronchial metastases are breast, colorectal and kidney cancers, rather than hepatomas [4].

Bronchoscopic treatment strategies for massive bleeding include cold saline, topical vasoconstriction agents, balloon tamponade, endobronchial stent or spigot, oxidized regenerated cellulose, N-butyl cyanoacrylate glue, gel and thrombin slurry fibrinogen-thrombin, tranexamic acid, laser photocoagulation, argon plasma coagulation, electrocautery, cryotherapy, and brachytherapy [5, 6]. Among these methods, tranexamic acid, laser photocoagulation, argon plasma coagulation, electrocautery, and cryotherapy have been reported to be effective for malignant bleeding [7-12]. Here, we present our experience managing endobronchial pulmonary metastasis of HCC with massive bleeding using bronchoscopic balloon tamponade.

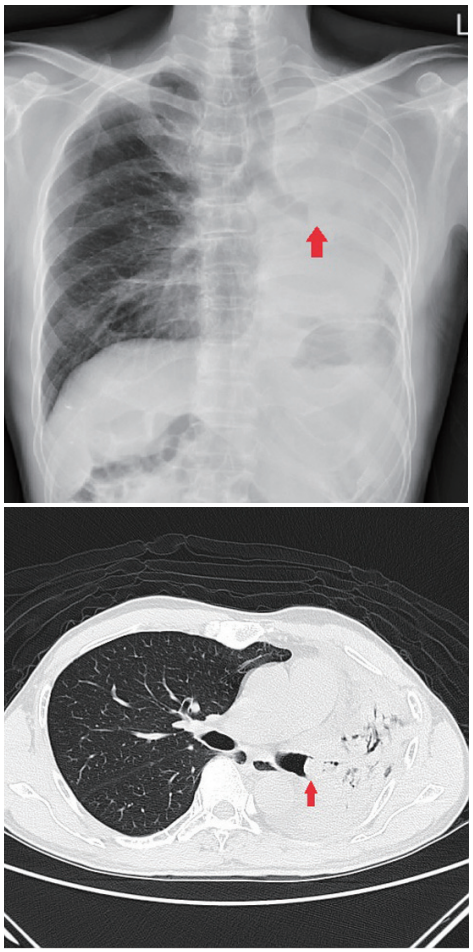

Fig. 1. Chest radiography and CT scan showing endobronchial pulmonary metastasis in the left main bronchus causing left lower lung collapse. The red arrows indicate the endobronchial mass.

Case Presentation

A 62-year-old man with HCC presented with lung metastasis (T3aN0M1, stage IVB), liver cirrhosis (Child-Pugh score A), and chronic hepatitis C. The patient had suffered from productive cough for 2-3 weeks. He had intermittent hemoptysis of approximately 30-50 ml each time for about 1 day, accompanied by progressive dyspnea (respiratory rate: 30 cycles per minute; pulse oximeter oxygen saturation under ambient air: 84%). He denied fever, chills, or other symptoms related to infection. Chest radiography and computed tomography (CT) in our hospital showed lung metastasis in the left lower lobe of the lung with progressive left main bronchus invasion, leading to left lung collapse and consolidation. Bronchoscopy revealed a solid tumor in the left main bronchus, which caused obstruction of the bronchus. During the procedure, a well-encapsulated, easily detached tumor (3.0 x 1.5 x 1.5 cm) was excreted while the patient coughed, followed by massive hemoptysis. Urgent bronchoscope-guided endotracheal tube intubation was performed for single-lung ventilation. Topical epinephrine and cold saline lavage were used for hemostasis.

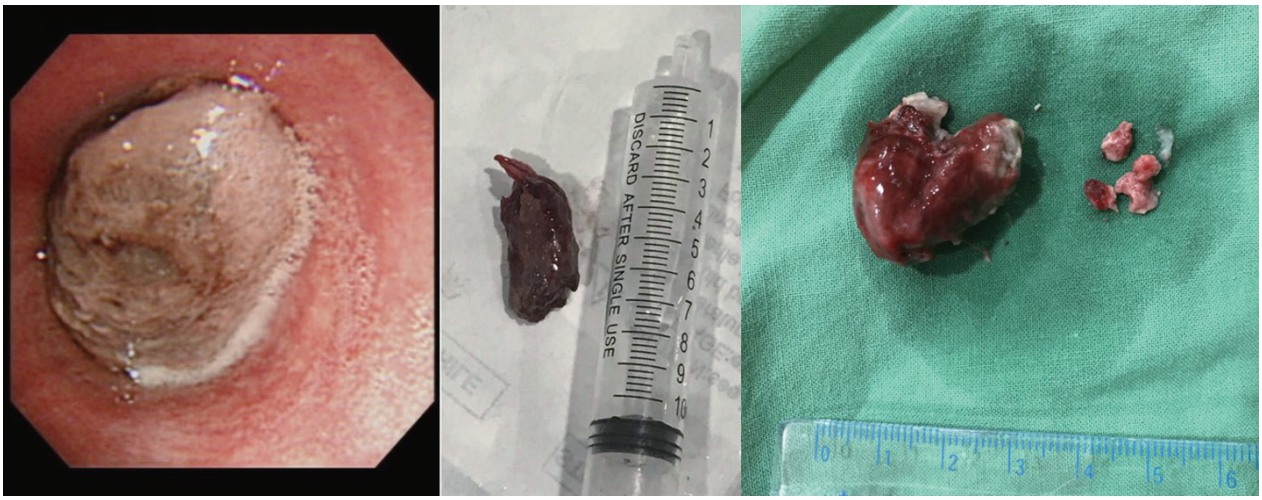

Fig. 2. Bronchoscopic finding of a huge endobronchial pulmonary HCC metastasis with a totally occluding and easily detachable, well-margined tumor mass (Middle: first time; Right: second time)

The bleeding finally was stopped using a Fogarty balloon tamponade in the left main bronchus. Even though there was a residual tumor in his left lower bronchus, the patient was extubated smoothly 2 days after successful hemostasis.

The pathologic findings of the tumor, including thick trabeculae, organoid structures, and a solid pattern of polygonal cells exhibiting hyperchromatic nuclei with distinct nucleoli and decreased pale or granular cytoplasm, were consistent with metastatic HCC. Seven months later, we performed bronchoscopy for the progressive endobronchial tumor in the left lower bronchus, which led to obstruction of the left main bronchus. We also used bronchoscopic cryotherapy for tumor removal. After removing the well-encapsulated, easily detached, large (2.7 x 2.3 x 1.5 cm) tumor, massive hemoptysis occurred. The pathologic findings of the tumor were consistent with metastatic HCC. The patient then received endotracheal intubation for airway protection. After critical care, he was extubated and fully recovered, and was able to live his daily life independently.

Discussion

Hepatocellular carcinoma (HCC) is the fourth leading cause of cancer-related deaths worldwide [1], and in Taiwan, as well. According to published reviews, the lung is the most frequently involved organ in extrahepatic metastases (36.2-55%), and the most frequent site of the first detectable metastasis [2, 13, 14]. The 1-year OS and cancer-specific survival (CSS) of HCC with lung metastasis were 10% and 12.6%, respectively; lung metastasis was identified as a risk factor for mortality in HCC (OS, HR 2.63; 95% CI: 2.40-2.88; CSS, HR 2.72; 95% CI: 2.48-2.99; both $p < 0.001$) [2].

Even though symptoms due to HCC metastases are observed more frequently in patients with bone and brain metastases, lung metastases can lead to death due to respiratory failure caused by the growth of metastatic tumors. Owing to the evolution of fiberoptic bronchoscopy, it is easier to approach the intra-bronchial tumor causing respiratory stress and airway obstruction.

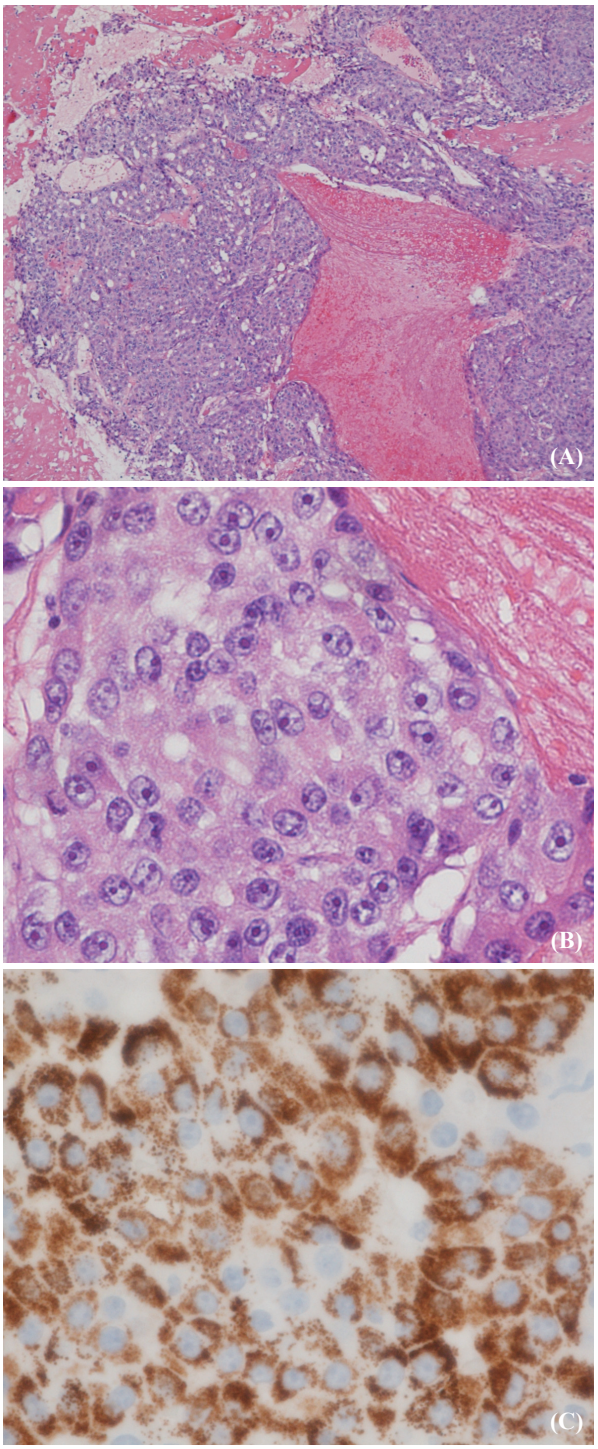

Fig. 3. Microscopic findings of the specimen with hematoxylin and eosin stain ((A) magnification × 40; (B) magnification × 400 (C) magnification × 400 revealed: (A) and (B) metastatic hepatocellular carcinoma composed of thick trabeculae or a solid pattern of polygonal neoplastic cells exhibiting hyperchromatic nuclei with distinct nucleoli and pale cytoplasm. (C) The tumor cells were immunoreactive for Hep par-1.

In a search of the Medline and Embase databases (from 1980 to 2021) using the following keywords: "endobronchial metastases" and "hepatocellular carcinoma," case reports of 13 patients were found (Table 1) [15-27]. The most common symptoms were hemoptysis, dyspnea, and cough. The time from primary diagnosis varied from a synchronous presentation to more than 15 years. Even though endobronchial metastases rarely occur and are difficult to distinguish from primary lung cancer using radiographic findings and clinical symptoms, prompt diagnosis and management are crucial for most clinical scenarios and sequelae. Nowadays, improvements in survival seem to be due to the evolution of advanced bronchoscopic techniques, radiotherapy, and new medications for HCC. Kiryu et al. described 4 types of endobronchial metastasis modes: type I, direct metastasis to the bronchus; type II, bronchial invasion by a parenchymal lesion; type III, bronchial invasion by mediastinal or lymph node metastasis; and type IV, peripheral lesions extending along the bronchus [28]. Due to the difficulty in differentiating between type II and type IV lesions, Akoglu et al. proposed a similar classification in 2005 with a modification of type IV, defined as endobronchial invasion with lymphangitis carcinomatosa [29]. In both classifications, type I lesions result from hematogenous or lymphatic metastatic spread, and types II to IV lesions occur by secondary invasion of the tracheobronchial tree, providing a sound developmental model of classification. The present case likely corresponds to a type II metastatic lesion, based on the image findings.

In this case, easily detached intra-bronchial pulmonary metastasis of HCC was removed by bronchoscopy twice, followed by massive hemoptysis. The patient's survival relied not only

Table 1. Case reports of Eendobronchial Metastasis from Hepatocellular Carcinoma

Author	Year	Age (years)/Sex	Symptoms	Duration of Symptoms	Time from primary diagnosis	Bronchus location	Developmental mode	Treatment	Follow up
Camps (15)	1988	66/F	Pneumonia	*	Synchronous presentation	Right upper lobe	*	Chemotherapy	Died, 7 months
Murayama (16)	1992	61/M	Hemoptysis, cough	*	9 years	Right main	IV	*	Died, 3 days
Salud (17)	1996	*	*	*	9 months	*	*	*	*
Lee (18)	2003	61/F	Hemoptysis, cough	1 month	16 months	Right upper lobe	I	Lobectomy	Alive, 18 months
Kido (19)	2005	80/M	Hemoptysis	*	2 years	Left lower lobe	I	Radiotherapy	Alive, 25 months
Purandare (20)	2009	65/M	Hemoptysis	*	8 years	Right truncus intermedius	I	Pneumonectomy	Alive, 6 months
Uchida (21)	2010	71/F	Dyspnea, respiratory failure	3 months	7 years	Bilateral	IV	Bronchial stent	Died, 20 days
Szumera-Cieckiewicz (22)	2013	20/F	Dyspnea, chest pain	2 months	3 years	Right upper lobe	III	Chemotherapy	Alive, 6 months
Dong (23)	2014	51/M	Cough	2 months	6 years	Left lower lobe	*	*	*
Onofrei (24)	2016	58/M	Hemoptysis	*	*	Right truncus intermedius	III	Bronchoscopy + Targeted therapy + Radiotherapy	*
Cheung (25)	2019	62/M	Hemoptysis, cough, dyspnea	3 months	12 months	Left main	I	Bronchoscopy + Immunotherapy	Alive, 16 months
Cai (26)	2020	72/M	Hemoptysis	4 days	15 years	Right upper lobe	*	*	*
Dumortier (27)	2021	60/M	Hemoptysis	*	8 years	Left lower lobe	I	*	*
Current report	2021	62/M	Hemoptysis, cough, dyspnea, respiratory failure	3 weeks	9 years	Left lower lobe and left main bronchus	II	Bronchoscopy + Targeted therapy + Radiotherapy	Alive, 12 months

on tumor debulking but also on prompt airway protection and bronchoscopic hemostasis for massive hemoptysis.

Massive hemoptysis usually originates from high-pressure bronchial circulation (90%), mostly due to the etiology of bronchiectasis, tuberculosis, mycetomas, necrotizing pneumonia, bronchogenic carcinomas, trauma, vasculitis, and pulmonary arteriovenous malformation [6]. In recent studies, the mortality rates for massive hemoptysis decreased from >75% to 13%-17.8% owing to early operative intervention and advances in medical imaging, fiberoptic technology, and interventional radiology [5]. However, the mortality rate was still positively correlated with the proportion of patients diagnosed with advanced carcinoma, and non-tumor-related hemoptysis was associated with better survival compared to tumor-related bleeding following endovascular management [8, 30]. Aspergilloma and bronchiectasis also carry a higher hemoptysis-related mortality due to increased risks of recurrent hemoptysis [31].

Initial management of massive hemoptysis included protection of the airways, volume resuscitation, and correction of any bleeding disorder [32]. To detect the site of bleeding, we usually perform chest radiography, chest CT, and bronchoscopy. However, chest radiography is known to have limited sensitivity [33, 34]. In a study of 80 patients with large or massive hemoptysis, chest radiography revealed the location of hemorrhage in only 46% of cases, and suggested a specific cause of bleeding in only 35% [33]. If the bleeding side is known, the patient should be placed laterally decubitus with the bleeding side down to prevent aspiration into the unaffected lung. Hemostasis can be performed using a bronchoscope, endovascular therapy, or surgery. Below, we discuss the current bronchoscopic interventions for hemoptysis and our practice in this case.

To choose the most effective bronchoscopic methods of hemostasis, we need to consider certain aspects of the patient's condition, whether it is a visible endoluminal lesion, a malignancy, the bleeding amount, and the availability of bronchial artery embolization [6]. For visible endoluminal lesions, cold saline, epinephrine, antidiuretic hormone analogs, endobronchial stent tamponade, Nd-YAG laser, argon plasma coagulation, electrocautery, and cryotherapy are recommended [5, 6, 32]. If the bleeding origin is not a visible endoluminal lesion, cold saline, epinephrine, antidiuretic hormone analogs, balloon tamponade, endobronchial spigot, oxidized regenerated cellulose mesh, biocompatible glue, endobronchial stent tamponade, fibrinogen-thrombin, and tranexamic acid can be considered [5, 6, 32]. In this case, the bleeding occurred at the left main bronchus after the endobronchial tumor was detached. Airway protection by placing the patient in the decubitus position, cold saline with epinephrine spray, Fogarty embolectomy catheter balloon tamponade, and single-lung endobronchial intubation were performed for the first occurrence. During the second occurrence, when some visible endoluminal bleeding sources were noted, we also performed cryotherapy, but in vain. Massive hemoptysis was limited mainly by Fogarty embolectomy catheter balloon tamponade and single-lung endobronchial intubation. Successful extubation with improved clinical manifestations was achieved at the end of both episodes.

In summary, we reported a rare case of endobronchial pulmonary metastasis of hepatocellular carcinoma that improved after bronchoscopic intervention. Further study may be needed to determine whether the bronchial

microenvironment or special bronchial tissue cells are related to peripheral necrosis of HCC and the difficulty of trans-bronchial invasion. In this case, we validated the use of bronchoscopic intervention for accurate diagnosis and prompt management.

References

1. Villanueva A. Hepatocellular carcinoma. N Engl J Med 2019; 380(15): 1450-62.
2. Wu W, He X, Andayani D, *et al*. Pattern of distant extrahepatic metastases in primary liver cancer: a SEER-based study. J Cancer 2017; 8(12): 2312-8.
3. Becker AK, Tso DK, Harris AC, *et al*. Extrahepatic metastases of hepatocellular carcinoma: a spectrum of imaging findings. Can Assoc Radiol J 2014; 65(1): 60-6.
4. Seo JB, Im JG, Goo JM, *et al*. Atypical pulmonary metastases: spectrum of radiologic findings. Radiographics 2001; 21(2): 403-17.
5. Davidson K, Shojaee S. Managing massive hemoptysis. Chest 2020; 157(1): 77-88.
6. Sakr L, Dutau H. Massive hemoptysis: an update on the role of bronchoscopy in diagnosis and management. Respiration 2010; 80(1): 38-58.
7. Solomonov A, Fruchter O, Zuckerman T, *et al*. Pulmonary hemorrhage: a novel mode of therapy. Respir Med 2009; 103(8): 1196-200.
8. Coban S, Yuksel O, Koklu S, *et al*. Atypical presentation of hepatocellular carcinoma: a mass on the left thoracic wall. BMC Cancer 2004; 4: 89.
9. Hetzel MR, Smith SG. Endoscopic palliation of tracheobronchial malignancies. Thorax 1991; 46(5): 325-33.
10. Morice RC, Ece T, Ece F, *et al*. Endobronchial argon plasma coagulation for treatment of hemoptysis and neoplastic airway obstruction. Chest 2001; 119(3): 781-7.
11. Simoff MJ. Endobronchial management of advanced lung cancer. Cancer Control 2001; 8(4): 337-43.
12. Sheski FD, Mathur PN. Cryotherapy, electrocautery, and brachytherapy. Clin Chest Med 1999; 20(1): 123-38.
13. Katyal S, Oliver JH, 3rd, Peterson MS, *et al*. Extrahepatic metastases of hepatocellular carcinoma. Radiology 2000; 216(3): 698-703.
14. Natsuizaka M, Omura T, Akaike T, *et al*. Clinical features of hepatocellular carcinoma with extrahepatic metastases. J Gastroenterol Hepatol 2005; 20(11): 1781-7.
15. Camps C, Soler JJ, Juan G, *et al*. An unusual form of metastasis of hepatocarcinoma: endobronchial metastasis. Rev Esp Enferm Apar Dig 1988; 74: 155-157.
16. Murayama J, Naitoh T, Doi M, *et al*. A case of small liver cancer presenting as a huge mediastinal mass. Nihon Kyobu Shikkan Gakkai Zasshi 1992; 30: 708-713.
17. Salud A, Porcel JM, Rovirosa A, *et al*. Endobronchial metastatic disease: analysis of 32 cases. J Surg Oncol 1996; 62: 249-252.
18. Lee KY, Ryu SJ, Joo M. Endobronchial metastasis of hepatocellular carcinoma. Yonsei Med J 2003; 44: 544-547.
19. Kido T, Iwanaga T, Takata S, *et al*. A case of solitary endobronchial metastasis of hepatocellular carcinoma. Nihon Kokyuki Gakkai Zasshi 2005; 43:422–426.
20. Purandare NC, Pramesh CS, Rangarajan V, et al. Hepatocellular carcinoma recurring as isolated endobronchial metastasis 8 years after primary surgery. J Thorac Imaging 2009; 24: 147-149.
21. Uchida R, Masugi Y, Nishizawa T, *et al*. Extensive endobronchial growth of metastatic hepatocellular carcinoma resulting in respiratory failure: a case report. Pathol Res Pract 2010; 206: 116-120.
22. Szumera-Cieckiewicz A, Olszewski WT, Piech K, *et al*. Endobronchial metastasis from hepatocellular carcinoma - a case description with literature review. Int J Clin Exp Path 2013; 6: 1942-1947.
23. Dong A, Zhao T, Wang Y, *et al*. FDG PET/CT in endobronchial metastases from extrathoracic malignancies. Clin Nucl Med 2014; 39: 446–449.
24. Onofrei C, Patel D, Noor A. An unexpected source of hemoptysis. Chest 2016; 150(4): 682A.
25. Cheung FPY, Russell PA, Alam NZ. Endobronchial metastases from hepatocellular carcinoma: a case report. Asian Cardiovasc Thorac Ann 2019; 27(8): 703-706.
26. Cai Y, Ju S. Endobronchial growth of metastatic hepatocellular carcinoma 15 years after surgery: a case report. Quant Imaging Med Surg 2020; 10(4): 874.
27. Dumortier J, Gérinière L, Atayi E, *et al*. Endobronchial seeding of hepatocellular carcinoma. Digestiv Liver Dis 2021; 53(3): 381-382.
28. Kiryu T, Hoshi H, Matsui E, *et al*. Endotracheal/

endobronchial metastases: clinicopathologic study with special reference to developmental modes. Chest 2001; 119: 768-775.

29. Akoglu S, Ucan ES, Celik G, *et al*. Endobronchial metastases from extrathoracic malignancies. Clin Exp Metastasis 2005; 22: 587-591.
30. Wang GR, Ensor JE, Gupta S, *et al*. Bronchial artery embolization for the management of hemoptysis in oncology patients: utility and prognostic factors. J Vasc Interv Radiol 2009; 20(6): 722-9.
31. Mal H, Rullon I, Mellot F, *et al*. Immediate and long-term results of bronchial artery embolization for life-threatening hemoptysis. Chest 1999; 115(4): 996-1001.
32. Kathuria H, Hollingsworth HM, Vilvendhan R, *et al*. Management of life-threatening hemoptysis. J Intensive Care 2020; 8: 23.
33. Revel MP, Fournier LS, Hennebicque AS, *et al*. Can CT replace bronchoscopy in the detection of the site and cause of bleeding in patients with large or massive hemoptysis? AJR Am J Roentgenol 2002; 179(5): 1217-24.
34. Tsoumakidou M, Chrysofakis G, Tsiligianni I, *et al*. A prospective analysis of 184 hemoptysis cases: diagnostic impact of chest X-ray, computed tomography, bronchoscopy. Respiration 2006; 73(6): 808-14.

Pulmonary Artery Intimal Sarcoma Mimicking Pulmonary Embolism: A Case Report and literature Review for Improvement of Early Diagnosis

Wei-Fan Ou[1], Chung-Chi Wang[2], Yong-Chen Hsu[3], Tsung-Ying Yang[1,4], Jeng-Sen Tseng[1,5,6]

Pulmonary artery intimal sarcoma (PAIS) is a rare disease with a poor outcome. Surgical intervention with complete tumor removal is the mainstay of treatment to prolong survival. However, PAIS has many clinical presentations similar to those of pulmonary embolism (PE), resulting in delayed diagnosis. Herein, we report the case of a 60-year-old man with the initial presentation of recurrent hemoptysis for 2 weeks, accompanied with significant body weight loss, cough, and dyspnea before admission. Based on a filling defect of the left pulmonary artery, as seen on computed tomography (CT) of the chest, the patient was initially diagnosed as having PE. After anticoagulant treatment, the patient felt his symptoms had improved. However, recurrent hemoptysis was still noted. Repeated chest CT showed enlargement of the filling defect, which suggested the possibility of tumor mass. Also, there were 2 nodules in the left lung field that likely represented lung metastasis. Surgical excision biopsy from the left pulmonary artery was performed, and pathology revealed PAIS. This case report can remind clinicians to be alert for a delayed diagnosis of PAIS. Our literature review focused on clinical symptoms, laboratory findings, and image studies to help differentiate PAIS from PE. ***(Thorac Med 2023; 38: 62-68)***

Key words: Pulmonary artery intimal sarcoma; pulmonary embolism; filling defect

[1]Division of Chest Medicine, Department of Internal Medicine, Taichung Veterans General Hospital, Taichung, Taiwan (No. 1650, Sec. 4, Taiwan Boulevard, Taichung, 407 Taiwan), [2]Department of Cardiovascular Surgery, Cardiovascular Center, Taichung Veterans General Hospital, Taichung, Taiwan, [3]Department of Pathology and Laboratory Medicine, Taichung Veterans General Hospital, Taichung, Taiwan, [4]Department of Life Sciences, National Chung Hsing University, Taichung, Taiwan (No. 250, Kuo Kuang Road, Taichung, 402 Taiwan), [5]Institute of Biomedical Sciences, National Chung Hsing University, Taichung, Taiwan (No. 250, Kuo Kuang Road, Taichung, 402 Taiwan), [6]School of Medicine, National Yang Ming Chiao Tung University, Taipei, Taiwan (No. 155, Sec. 2, Linong Street, Taipei, 112 Taiwan)

Address reprint requests to: Dr. Jeng-Sen Tseng, Division of Chest Medicine, Department of Internal Medicine, Taichung Veterans General Hospital, 1650 Taiwan Boulevard Sec. 4, Taichung, Taiwan 40705

Introduction

Pulmonary artery intimal sarcoma (PAIS), usually arising from the pulmonary trunk, is a rare malignancy with an incidence of 0.001-0.03% [1]. PAIS has a dismal outcome, with a median survival of 17 months [2]. Surgical intervention with curative resection remains the mainstay of treatment to prolong survival for patients with PAIS [3]. However, PAIS can be easily misdiagnosed as pulmonary embolism (PE), resulting in delayed diagnosis [4]. Although PAIS and PE share many similar clinical symptoms, laboratory findings, and image characteristics, there are still subtle differences [5]. Herein, we present a patient with a case of PAIS that mimicked PE, and discuss improvement of the diagnosis.

Case Presentation

A 60-year-old man was admitted to our hospital because of recurrent hemoptysis for 2 weeks. Two months before admission, he started to have a dry cough, progressive dyspnea on exertion, and significant body weight loss, from 70 to 64 kg. Physical examination and laboratory tests were unremarkable. The patient's D-dimer level was 0.31 mg/L (< 0.55 mg/L fibrinogen equivalent units [FEU]). The sputum microscopy and culture, including bacteria and mycobacterial tuberculosis, revealed negative findings. Chest computed tomography (CT) at the mediastinal window showed a filling defect within the left main and left interlobar pulmonary artery (Figure 1A and 1B). Echocardiogram revealed a dilated pulmonary artery trunk

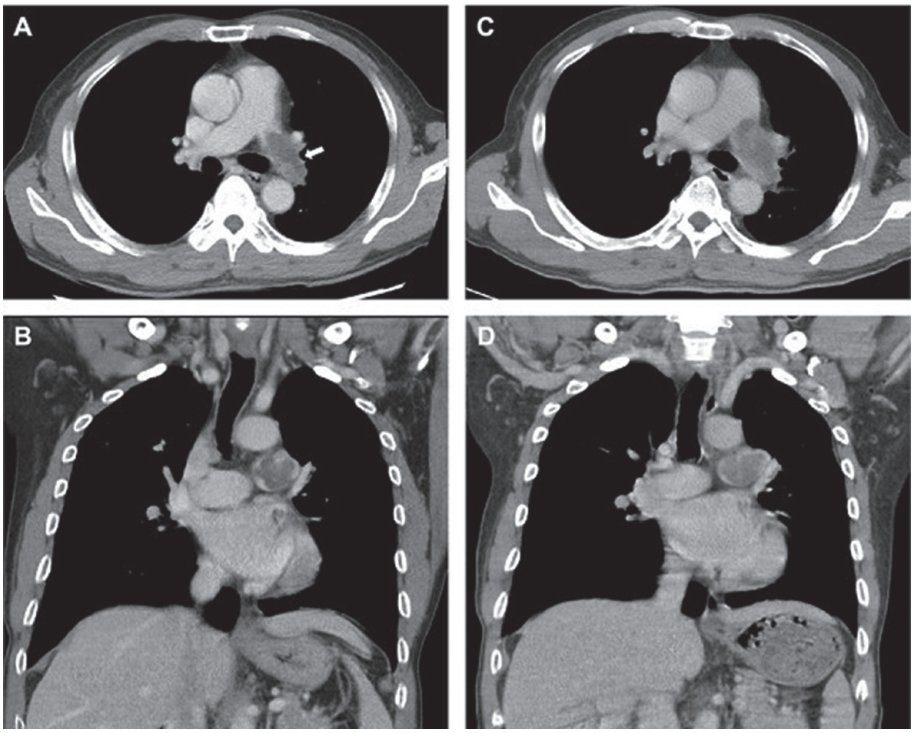

Fig. 1. Initial computed tomography (CT) of the chest revealed a filling defect within the left pulmonary artery. The filling defect obstructed the entire left pulmonary artery, protruded toward the right ventricular outflow tract, and blurred the vascular wall of the left pulmonary artery (arrow), which was compatible with the description of a "wall eclipsing sign" (A and B); repeated CT scans showed enlargement of the intravascular mass lesion. (C and D)

of 2.7 cm with moderate tricuspid regurgitation. Based on the aforementioned findings, the patient was diagnosed with PE involving the left pulmonary artery. After 5 days of enoxaparin treatment, the patient's shortness of breath and hemoptysis showed partial improvement. He was discharged with non-vitamin K antagonist oral anticoagulant (NOAC).

However, the patient had recurrent dyspnea on exertion and hemoptysis 2 weeks later. Repeated chest CT showed mild enlargement of the low-density filling defect within the left pulmonary artery, which suggested the possibility of tumor mass (Figure 1C and 1D). Also, there were 2 nodules in the left lung field that likely represented lung metastasis.

The patient underwent an endarterectomy of the left pulmonary artery mass. The tumor, which occupied the entire left pulmonary artery up to the partial pulmonary trunk, was exposed through a median sternotomy. The distal left pulmonary artery was checked by the scope, which revealed that the tumor was firmly adhesive to the intima of the vessel (Figure 2A). Pathology showed a malignant mesenchymal tumor composed of spindle and epithelioid tumor cell proliferation with nuclear pleomorphism and hyperchromasia (Figure 2B). Tumor necrosis and increased mitotic activity (up to 11 mitotic figures/10 high-power fields) were also observed. Immunohistochemical stains were positive for mouse double minute 2 homolog (MDM2) (Figure 2C), there was scanty expression of anti-pan-cytokeratin antibody (AE1/AE3), and the stains were very focally positive for CD31 and negative for CD117. These findings indicated that the tumor, mimicking a filling defect representing PE, was an intimal sarcoma.

The postoperative course was not satisfactory. Before systemic treatment, repeated chest CT revealed a residual endovascular tumor with mediastinal fat invasion and increased lung metastasis. The patient underwent 3 cycles of chemotherapy with cyclophosphamide, vincristine, doxorubicin, and dacarbazine (CYVADIC). The

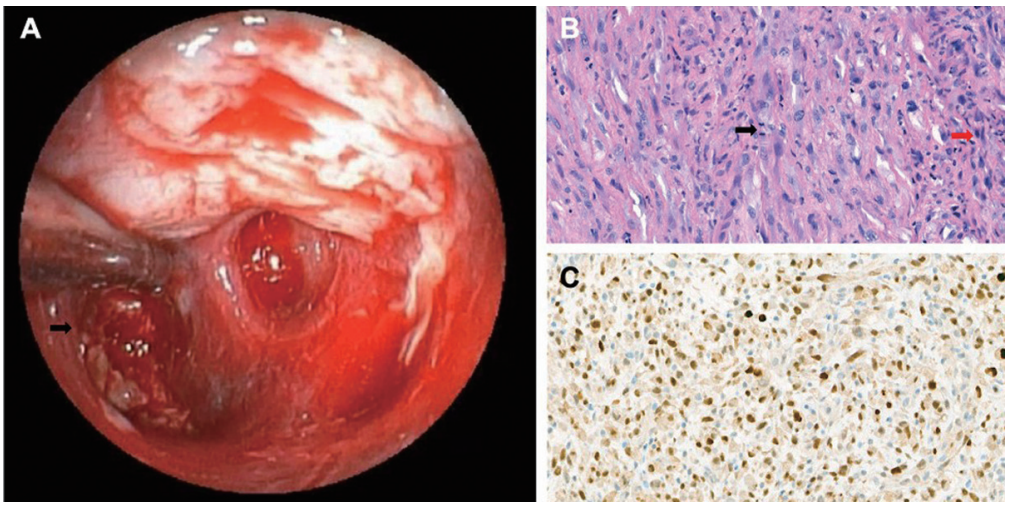

Fig. 2. During the endarterectomy, the distal left pulmonary artery was checked using the scope. The tumor was firmly adhesive to the intima of the distal left pulmonary artery (arrow). (A) The high power view showed spindle and epithelioid tumor cells with nuclear pleomorphism and hyperchromasia (red arrow), and increased mitotic activity (black arrow). (H&E stain, magnification ×400). (B) Immunohistochemical stain of the tumor showed a strong positive for MDM2 (magnification ×400). (C)

follow-up CT scan showed disease progression. Following the poor response to the above treatment, the patient was lost to follow-up.

Discussion and conclusions

PAIS is a rare malignancy and has a dismal outcome. Its overall incidence is 0.001–0.03% [1]. Since Moritz Mandelstamm first described this disease in 1923, there have been only approximately 400 cases reported in the literature up to 2021 [6, 7]. The reports show that the usual age at diagnosis is 45-55 years (range, 13–86 years), and that there is a slightly female predominance (1.3:1) [5, 8].

PAIS has many characteristics similar to those of PE. Bandyopadhyay et al. reported that approximately 47% of PAIS cases were initially misdiagnosed as PE [9]. The clinical presentations of PAIS can range from asymptomatic to decompensated right-side heart failure [10]. The most common symptoms of PAIS include dyspnea, cough, and chest tightness, which are similar to the presentations of PE [9]. A tumor growth can occlude the vascular lumen, and result in the elevation of pulmonary artery pressure. Patients may have leg edema, jugular vein engorgement, hepatosplenomegaly, and cyanosis, which resemble right-side heart failure [11]. Other constitutional symptoms, such as weight loss and fever, are more likely to occur in patients with PAIS, rather than those with PE [5]. Kim et al. reported that patients with PE had a significantly higher D-dimer level than those with PAIS. When using a cut-off value of 2.81 ug/mL FEU, D-dimer showed an 85% sensitivity and a 79% specificity to differentiate PAIS from PE [12].

In the present case, the patient's initial symptoms, such as cough and dyspnea, were nonspecific. With the relapse of symptoms and the enlargement of the intravascular mass in the follow-up chest CT, malignant tumor came into the differential diagnosis. CT pulmonary angiography (CTPA) remains the standard for initial image study for PAIS diagnosis, although the most common finding is a filling defect of the vasculature, which may lead clinicians to misdiagnose PAIS as PE [11].

There are several subtle differences in morphology between these 2 diseases on CTPA. Gan et el. described a specific finding of PAIS called the "wall eclipsing sign", which is defined as the presence of the following 3 findings: almost complete obstruction of the pulmonary trunk and its branches by a low-density mass; protrusion of the proximal end of this mass toward the right ventricular outflow tract; and eclipsing of 1 or both walls of the pulmonary trunk and its branches by this lesion. This sign was not observed in any acute or chronic PE cases [8, 13]. The presence of local invasion to the mediastinum and distant metastasis, usually spreading to the ipsilateral lung, is also a strong hint indicating a PAIS diagnosis, although these manifestations represent an advanced stage [9, 11]. In addition, an increase of 25 housefield units (HU) in density after contrast enhancement at the venous phase also suggests a diagnosis of PAIS [14]. However, nearly 5% of patients with PAIS have the burden of a large thrombus simultaneously surrounding the tumor on histopathology, which may make a differentiation between PAIS and PE more difficult through CTPA alone [9].

Using different imaging modalities, including positron emission tomography (PET) and magnetic resonance imaging (MRI), may lead to a more accurate diagnosis of PAIS [15]. Fluorodeoxyglucose (FDG)-PET scanning can help

distinguish between tumor and thrombus. In the study by Ito et al., the mean maximum standardized uptake value (SUVmax) of PAIS was significantly higher than that of PE (7.63 ± 2.21 vs. 2.31 ± 0.41) [16]. Gan et al. also suggested that if CTPA revealed a wall eclipsing sign or other morphology indicating PAIS, FDG-PET or surgical intervention should be arranged to confirm the diagnosis [13]. Also, FDG-PET possesses an advantage in detecting distant metastasis [11]. However, FDG-PET would yield a false negative if PAIS had low cellularity and was rich in myxoid tissue [17]. Because of advances in techniques, cardiac MRI (CMR) now plays a more critical role in the diagnosis of PAIS than before [11]. The classic CMR findings of PAIS are detectable tissue perfusion and heterogenous enhancement on late CMR imaging based on differences in tumor cellularity [18]. Also, CMR can observe the floating of PAIS tumors in response to changes in blood flow between the pulmonary diastole and systole. Although CMR is a powerful imaging study to confirm PAIS, many patients with PAIS suffer from dyspnea and have difficulty holding their breath long enough to allow CMR scanning, which limits its clinical usefulness in the diagnosis of PAIS [19].

In the present case, the initial CT images showed a low-density mass occluding almost the entire left pulmonary artery and protruding toward the right ventricular outflow tract. The low-density mass lesion also blurred the vascular wall of the left pulmonary artery (Figure 1A). These manifestations were compatible with the "wall eclipsing sign" described above. The follow-up CT scan revealed lung metastasis, which also supported the diagnosis of a malignancy. Besides, the patient had significant body weight loss and a normal level of d-dimer in the initial presentation, which was not typical for PE. Clinicians should keep PAIS in mind if the clinical, laboratory, and radiological findings are not typical for PE.

The definitive diagnosis of PAIS remains tissue biopsy and histopathological presentations, which could be revealed through endobronchial ultrasound-guided fine-needle aspiration, CT-guided transthoracic needle biopsy, or surgical biopsy. Intimal sarcoma is considered a malignant mesenchymal tumor, developing within the lumina of the great vessels, mostly in the pulmonary trunk. Under microscopic examination, intimal sarcoma usually consists of poorly differentiated or undifferentiated spindle or epithelioid cells, with various degrees of pleomorphism, mitotic activity, and necrosis. Sometimes, the tumor may have the heterologous components of rhabdomyosarcoma, osteosarcoma, and angiosarcoma. The classic immunohistochemistry stain of intimal sarcoma would be positive for MDM2 [8, 12, 15, 20].

Surgery remains the mainstay of treatment for PAIS. Blackmon et al. reported that patients receiving curative resection had a longer median survival of 36.5 ± 20.2 months, compared to the 11.0 ± 3.0 months for those undergoing incomplete resection [3]. Bandyopadhyay et al. also reported that patients receiving complete resection had a favorable outcome [9]. Surgical approaches include pneumonectomy, radical tumor resection with pulmonary artery reconstruction, and palliative pulmonary endarterectomy, based on the location and invasion severity of PAIS [21, 22]. The role of postoperative adjuvant chemotherapy or radiotherapy remains controversial [2, 23]. For those who are not suitable for surgery or have metastatic disease, chemotherapy combining anthracycline and ifosfamide is the most effective therapy, with a

response rate of approximately 50%-60% [24]. Several targetable mutations have been found, including amplification of *platelet-derived growth factor receptor α (PDGFRA), epidermal growth factor receptor (EGFR), and MDM2* in PAIS. Imatinib has been used to treat metastatic PAIS with a *PDGFRA* mutation [25]. After progression to chemotherapy, pazopanib, a multitargeted tyrosine kinase inhibitor, is a second-line therapy that can be used for soft tissue sarcoma [26]. Since our patient was diagnosed at an advanced stage with lung metastasis, complete surgical resection was not possible, which implied a poor outcome.

In conclusion, although PAIS is a rare disease and easily mimics the presentation of PE, there are still subtle differences among clinical symptoms, images, and laboratory studies. Multimodality studies, including FDG-PET and MRI, are recommended for cases suspected of being PAIS. For treatment, early aggressive surgical intervention should be considered, since complete resection can prolong survival. For patients with metastatic disease, or those unsuitable for surgical intervention, chemotherapy or targeted therapy can be treatment options.

References

1. Mussot S, *et al*. Retrospective institutional study of 31 patients treated for pulmonary artery sarcoma. Eur J Cardio-Thorac Surg 2013; 43(4): 787-793.
2. Wong HH, *et al*. Presentation and management of pulmonary artery sarcoma. Clin Sarcoma Res 2015; 5(1): 3.
3. Blackmon SH, *et al*. Management of primary pulmonary artery sarcomas. Ann Thorac Surg 2009; 87(3): 977-84.
4. El-Sayed Ahmed MM, *et al*. Pulmonary artery sarcoma mimicking pulmonary embolism. Tex Heart Inst J 2014; 41(5): 515-7.
5. Assi T, *et al*. A comprehensive review on the diagnosis and management of intimal sarcoma of the pulmonary artery. Crit Rev Oncol Hematol 2020; 147: 102889.
6. Mandelstamm M. Über primäre neubildungen des herzens. Virchows Archiv für pathologische Anatomie und Physiologie und für klinische Medizin 1923; 245(1): 43-54.
7. Bai X, Ruan L. A case report of primary pulmonary artery intimal sarcoma. Eur J Med Res 2021; 26(1): 89.
8. Moguillansky NI, *et al*. Pulmonary artery sarcoma: Case report and review of the literature. Respir Med Case Rep 2019; 27: 100857.
9. Bandyopadhyay D, *et al*. Primary pulmonary artery sarcoma: a close associate of pulmonary embolism -- 20-year observational analysis. J Thorac Dis 2016; 8(9): 2592-2601.
10. Lu P, Yin BB. Misdiagnosis of primary intimal sarcoma of the pulmonary artery as chronic pulmonary embolism: A case report. World J Clin Cases 2020; 8(5): 986-994.
11. Xu R, *et al*. Pulmonary intimal sarcoma involving the pulmonary valve and right ventricular outflow tract: a case report and literature review. Medicine (Baltimore) 2020; 99(3): 18813.
12. Kim C, *et al*. Pulmonary artery intimal sarcoma versus pulmonary artery thromboembolism: CT and clinical findings. Korean J Radiol 2018; 19(4):792-802.
13. Gan HL, *et al*. The wall eclipsing sign on pulmonary artery computed tomography angiography is pathognomonic for pulmonary artery sarcoma. PLoS One 2013; 8(12): e83200.
14. Attinà D, *et al*. Pulmonary artery intimal sarcoma. Problems in the differential diagnosis. La Radiologia Medica 2013; 118(8): 1259-1268.
15. Nakrani R, *et al*. Pulmonary artery intimal sarcoma: a diagnostic challenge using a multimodal approach. Case Rep Med 2020; 2020: 6795272.
16. Ito K, *et al*. Diagnostic usefulness of 18F-FDG PET/CT in the differentiation of pulmonary artery sarcoma and pulmonary embolism. Ann Nucl Med 2009; 23(7): 671-676.
17. Lee D-H, *et al*. Pulmonary artery intimal sarcoma: poor 18F-fluorodeoxyglucose uptake in positron emission computed tomography. J Cardiothorac Surg 2013; 8(1): 40.
18. Attinà D, *et al*. Pulmonary artery intimal sarcoma. Problems in the differential diagnosis. Radiol Med 2013;

118(8): 1259-68.
19. Pu X, *et al*. Clinical and radiological features of pulmonary artery sarcoma: a report of nine cases. Clin Respir J 2018; 12(5): 1820-1829.
20. Sebenik M, *et al*. Undifferentiated intimal sarcoma of large systemic blood vessels: report of 14 cases with immunohistochemical profile and review of the literature. Am J Surg Pathol 2005; 29(9): 1184-93.
21. Obeso Carillo GA, *et al*. Primary pulmonary artery sarcoma: a new surgical technique for pulmonary artery reconstruction using a self-made stapled bovine pericardial graft conduit. Eur J Cardio-Thorac Surg 2014; 47(1): 188-190.
22. Grazioli V, *et al*. Surgical treatment of primary pulmonary artery sarcoma. J Thorac Cardiovasc Surg 2014; 148(1): 113-8.
23. Mussot S, *et al*. Retrospective institutional study of 31 patients treated for pulmonary artery sarcoma. Eur J Cardiothorac Surg 2013; 43(4): 787-93.
24. Manso L, *et al*. Primary pulmonary artery sarcoma: report of three cases and review of the literature. Clin Lung Cancer 2007; 8(4): 277-81.
25. Van Dievel J, *et al*. Single-center experience with intimal sarcoma, an ultra-orphan, commonly fatal mesenchymal malignancy. Oncol Res Treat 2017; 40(6): 353-359.
26. van der Graaf WT, *et al*. Pazopanib for metastatic soft-tissue sarcoma (PALETTE): a randomised, double-blind, placebo-controlled phase 3 trial. Lancet 2012; 379(9829): 1879-86.

Prone Positioning in Severe ARDS under Extracorporeal Membrane Oxygenation Support-A Case Report

Ta-Wei Chao[1], Ching-Han Lai[2], Wei-Chieh Lin[3]

Acute respiratory distress syndrome (ARDS) is a critical illness with high mortality, even if appropriate therapies, such as protective lung strategies, prone positioning (PP), and venovenous extracorporeal membrane oxygenation (VV-ECMO), are applied. PP, a natural lung recruitment maneuver, has fewer complications than other salvage therapies; however, the combination of PP and VV-ECMO support is uncommon, not only because of the risk of catheter dislodgement, but also because of the understaffing of healthcare facilities. Herein, we present the case of a patient with severe ARDS who had difficulty weaning from VV-ECMO, but was successfully treated with PP during VV-ECMO support. ***(Thorac Med 2023; 38: 69-76)***

Key words: acute respiratory distress syndrome (ARDS), prone positioning (PP), lung recruitment maneuver, extracorporeal membrane oxygenation support (ECMO).

Background

Acute respiratory distress syndrome (ARDS) is an acute inflammatory lung injury associated with diffused alveolar damage, resulting in increased pulmonary vascular permeability. Based on the Berlin definition of 2012, ARDS is characterized by acute refractory hypoxemia (PaO_2/FiO_2 ≤300 mmHg) occurring within a week, accompanied by bilateral lung opacities that cannot be fully explained by cardiac failure or fluid overload. In patients with a minimum of 5 cmH_2O of positive end-expiratory pressure (PEEP), the severity of ARDS is classified based on the PaO_2/FiO_2 (P/F) ratio: mild (200 <PaO_2/FiO_2 ≤300 mmHg); moderate (100 <PaO_2/FiO_2 ≤200 mmHg); and severe (PaO_2/FiO_2 ≤100 mmHg) [1].

ARDS constituted 10.4% of total intensive care unit (ICU) admissions and resulted in 23.4% of all patients requiring mechanical ventilation (MV). Furthermore, ARDS has a

[1]Division of Respiratory Therapy, Department of Internal Medicine, National Cheng Kung University Hospital, College of Medicine, National Cheng Kung University, [2]Division of General Medicine, Department of Internal Medicine, National Cheng Kung University Hospital, College of Medicine, National Cheng Kung University, [3]Division of Critical Care Medicine, Department of Internal Medicine, National Cheng Kung University Hospital, College of Medicine, National Cheng Kung University
Address reprint requests to: Dr. Wei-Chieh Lin, Division of Critical Care Medicine, Department of Internal Medicine, National Cheng Kung University Hospital, No.138, Sheng Li Road, Tainan, Taiwan 704, R.O.C

hospital mortality of more than 40%, despite the application of a low tidal volume strategy, high PEEP, and prone positioning (PP). Veno-venous extracorporeal membrane oxygenation (VV-ECMO) is a rescue therapy used in cases of severe ARDS [3].

PP is rarely performed during VV-ECMO because hypoxemia/hypercapnia can improve with VV-ECMO alone, and many healthcare facilities are understaffed. PP is undoubtedly beneficial because it leads to better lung recruitment and oxygenation; however, whether PP is advantageous for ARDS patients treated with VV-ECMO support is still unknown.

Case Report

A 59-year-old man with a medical history of hypertension presented to National Cheng-Kung University Hospital (NCKUH) because of productive cough. A few days before this presentation, he went to a local clinic due to a cough with yellowish sputum; however, his cough did not resolve, and he developed shortness of breath. Therefore, he was referred to the emergency department at NCKUH on 20 December 2020 with a fever up to 38.9°C, and right upper lobe and right lower lobe pneumonia that was revealed on chest X-ray (CXR) (Figure 1A). Laboratory data showed leukocytosis (white blood cell count of 10.4 × 103/μL), but urinalysis revealed no pyuria; other laboratory test results are shown in Table 1. Viral, bacterial, and fungal culture reports were all negative. The electrocardiogram and echocardiography were not remarkable. He was admitted to the general ward initially, for he was suspected of having community-acquired pneumonia (CAP). After admission, he was tested for urine pneumococcus antigen, legionella antigen, and mycoplasma IgM, all of which came back negative. Sputum culture revealed normal

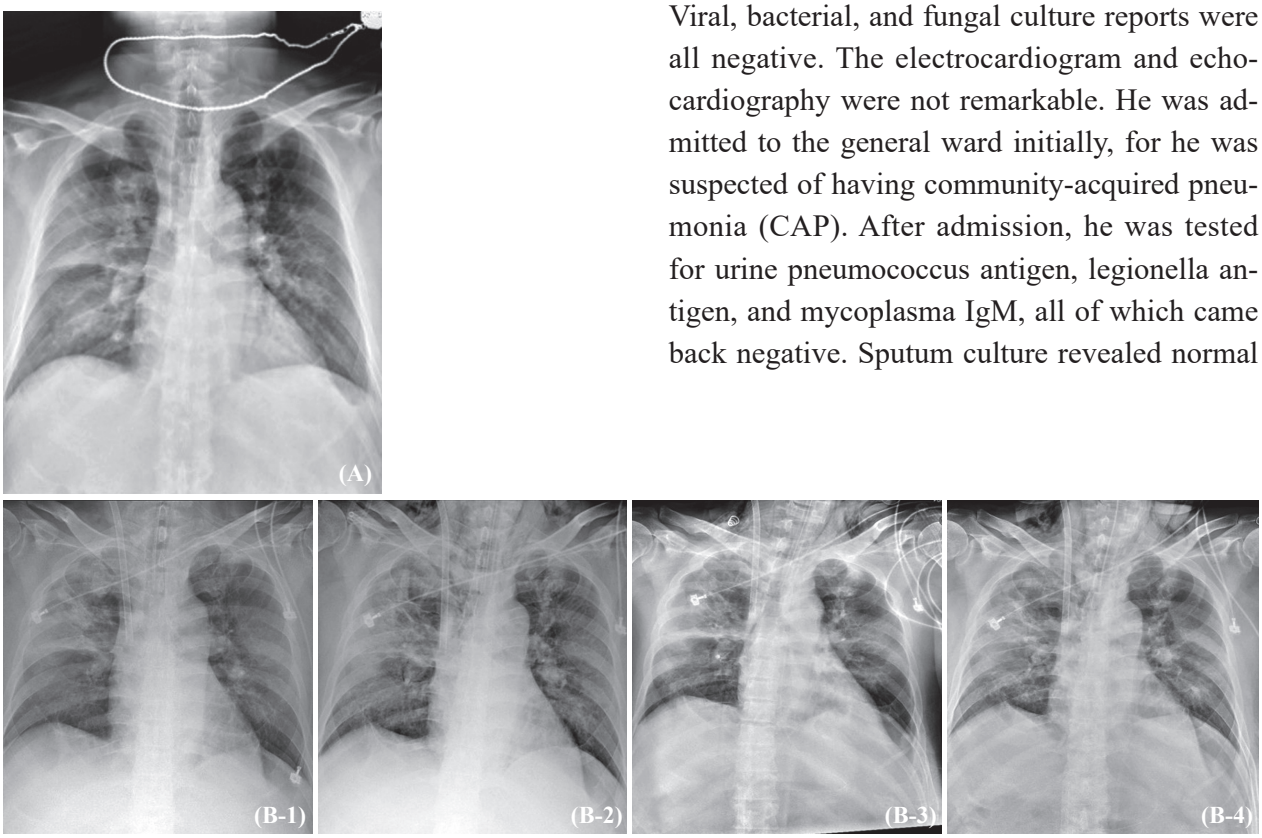

Fig. 1. CXRs at the Emergency Department (A) and before and after the 1st and 2nd LRM (B). (A) The CXR showed bilateral pneumonia patches with a right-side predominance. (B) A series of CXRs were taken: 1. Before the 1st LRM; 2. After the 1st LRM; 3. Before the 2nd LRM; 4. After the 2nd LRM.

Table 1. Laboratory Data on Initial Arterial Blood Gas, Blood Chemistry, Hemogram, and Coagulation

Arterial blood gas		**Biochemistry examination**		**Hemogram**		**Coagulation**	
pH	7.49	K (mmol/L)	3.4	WBC (10^3/μL)	10.4	APTT (sec)	26.5
PCO_2 (mmHg)	37	NA (mmol/L)	133	Hb (g/dL)	12.7	MNAPTT (sec)	32.6
PO_2 (mmHg)	47	CREA (mg/dL)	0.75	Plt (10^3/μL)	299	PT (sec)	17.1
HCO_3- (mmol/L)	28.2	ALT (U/L)	27	Seg (%)	81.3	PT (MNPT)(secs)	10.8
BEb (mmol/L)	4.7	Glucose (random)(mg/dL)	174	Eos (%)	1.9	PT (INR)(secs)	1.58
BEecf (mmol/L)	4.9	hs-cTnT (ng/L)	15.6	Baso (%)	0.2		
SO_2 (%)	86.2	NTproBNP	1086	Mono (%)	8.5		
		CRP (mg/L)	297.5	Lymph (%)	8.1		
		LACTATE (mmol/L)	1.2				

flora. Empirical ceftriaxone was administered for CAP treatment. Nonetheless, his symptoms progressed, and desaturation developed soon afterward. CXR revealed progressive bilateral patches, and ARDS induced by CAP was suspected. The empirical antibiotic therapy was escalated with the addition of piperacillin/tazobactam and doxycycline. Consequently, the patient was intubated with MV support and transferred to the medical ICU (MICU) on 27 December 2020.

At the MICU, the patient's ventilator setting was pressure-controlled ventilation with 100% FiO_2, a pressure control level of 16 cmH_2O, and PEEP of 12 cmH_2O. However, the hypoxemia (PaO_2: 42 mmHg) and respiratory acidosis ($PaCO_2$: 81 mmHg; pH: 7.15) were still overwhelming. Thus, a low tidal volume (VT) strategy (6 ml/kg predicted body weight) with a high level of PEEP, sedation and total paralysis, and PP were applied. Despite the above strategies, the severe hypoxemia (PaO_2: 50 mmHg) and hypercapnia ($PaCO_2$: 90 mmHg) did not improve. Hence, VV-ECMO was performed for this patient in a supine position on the first day of MICU admission.

The hypoxemia and hypercapnia improved after the initiation of VV-ECMO (Table 2). Nevertheless, improvement in the P/F ratio stopped at around 130, as we tried to wean the patient from the VV-ECMO. Considering the high risks and possible complications of PP during VV-ECMO, we first tried a lung recruitment maneuver (LRM) with incremental pressure-controlled ventilation, according to the ART trial [14], as rescue therapy on the 7th day of MICU stay, while the optimal PEEP was set at 13 cmH_2O (optimal PEEP defined as the PEEP associated with the best compliance plus 2 cm H_2O). The detailed parameters are shown in Table 3. However, the P/F ratio, tidal volume, and CXR (Figure 1B) did not show improvement as expected.

Based on the chest computed tomography

Table 2. Ventilator Parameters and Arterial Blood Gas Analysis in Supine/Prone/Supine + VV-ECMO/Prone + VV-ECMO

Day of MICU stay	1st day ventilator only	1st day PP	1st day SP + VV-ECMO	9th day SP + VV-ECMO	10th day 09:15 PP + VV-ECMO	10th day 17:20 PP + VV-ECMO	11th day 09:08 *SP + VV-ECMO	11th day 17:30 PP + VV-ECMO	13th day +18:25 PP
Ventilator parameters									
FiO_2 (%)	100	100	100	50	50	50	50	45	35
PC level/PEEP (cmH_2O)	16/12	14/16	12/12	14/13	16/13	12/13	12/13	12/13	14/13
V_T (ml)/MV (L/min)	410/11.7	380/10.7	400/11.2	420/7.7	480/7.8	410/7.1	465/5.5	410/5.6	450/8.1
Peak airway pressure (cmH_2O)	29	31	33	27	30	25	25	25	28
Mean airway pressure (cmH_2O)	18	22	23	17	18	17	16	16	18
Driving pressure (cmH_2O)	16	14	15	13	15	10	12	11	9
Compliance (mL/cmH_2O)	25.6	27.1	26.7	32	32	41.3	38.3	36.3	51.1
VV-ECMO parameters									
FiO_2 (%)	-	-	100	60	60	50	30	21	-
Pump speed	-	-	2514	1705	1705	1705	1697	1695	-
Blood flow (L/min)	-	-	3.5	2.1	2.12	2.04	2.05	2.03	-
Gas flow (L/min)	-	-	3	1	1	1.5	2	1	-
Arterial blood gas									
pH	7.15	7.12	7.35	7.46	7.52	7.42	7.51	7.46	7.45
$PaCO_2$ (mmHg)	81	90	41	47	42	49	36	47	51
PaO_2 (mmHg)	42	50	116	65	69	83	64	94	118
HCO_3^- (mmol/L)	28.2	29.3	22.6	33.4	34.3	31.8	28.7	33.4	35.4
BE (ecf)(mmol/L)	-0.7	0	-3	9.6	11.4	7.3	5.7	9.6	11.4
P/F ratio	42	50	116	130	138	166	172	209	295

PP: prone positioning, SP: supine positioning.

*Prone positioning was kept for 24 h, with supine positioning once a day for nursing care +VV-ECMO was removed in the morning (09:43).

Table 3. Lung recruitment Maneuver (LRM) According to the Protocol of the ART Trial

	Total PEEP (cmH_2O)	Intrinsic PEEP (cmH_2O)	Tidal volume (ml)	Plateau pressure (cmH_2O)	Driving pressure (cmH_2O)	Compliance (mL/cmH_2O)
1st LRM	23	0	280	37	14	20
	20	0	350	33	13	27
	17	0	450	31	14	32
	14	0	540	27	13	41
	11	0.2	630	23	12	52
			Optimal PEEP: 11+2=13 cmH_2O			
2nd LRM	23	0.6	308	37	14	22
	20	0	372	34	14	27
	16	0	463	31	14	33
	14	0.3	534	28	14	38
	11	0.1	600	24	13	46
			Optimal PEEP: 11+2=13 cmH_2O			

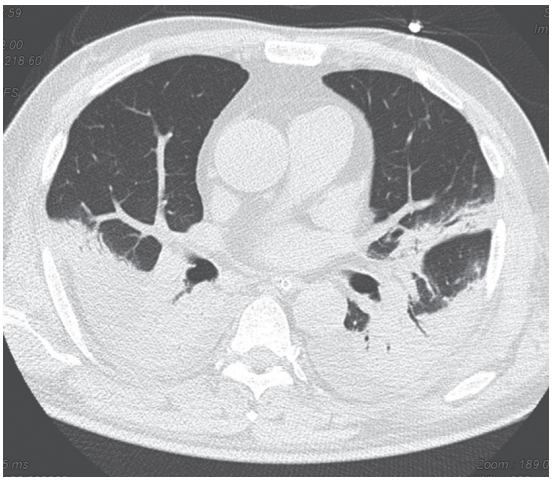

Fig. 2. Chest CT before prone positioning during VV-ECMO support. The chest CT showed pulmonary consolidations with air-bronchogram in both lungs; the lesions were mostly at the dependent parts.

(CT), which showed significant lung consolidation and atelectasis at bilateral dorsal sites (Figure 2), we added PP while the patient was on the 10th day of VV-ECMO support in the MICU. To prevent complications, the whole PP process was closely monitored and performed by our MICU staff and the ECMO team (at least 5 people were involved each time). The staff assignments included: 1 for securing the location of the airway/endotracheal tube, 1 for the ECMO cannulation, and 3 for moving the patient's position.

The P/F ratio on the 1st day of combined PP and VV-ECMO increased slightly to 160. Consequently, the ECMO FiO_2 could be gradually reduced to 21%, which resulted in the P/F ratio being increased significantly, from 140 to over 200 on the 2nd and 3rd days of combined PP with VV-ECMO (Table 2). The VV-ECMO was removed on the 4th day of combined treatment (on the 13th day of MICU admission) (Table 2). The patient was extubated successfully on the 19th day of MICU admission.

Discussion

Our patient had severe ARDS caused by CAP, which is known as the most common di-

rect risk factor for lung injury [4]. ARDS is an inflammatory process of the lungs that induces non-hydrostatic protein-rich pulmonary edema [5]. The immediate consequences that result in hypoxemia and hypercapnia include decreased lung compliance, increased intrapulmonary shunting, and an increase in pulmonary dead space. Special interventions or procedures, such as a neuromuscular blockade agent, PP, and VV-ECMO, may be needed to solve those undesirable problems.

As a salvage therapy for refractory hypoxemia, early PP (within 48 h) for at least 16 h per day can improve oxygenation and improve the survival rate of patients with moderate to severe ARDS (P/F ratio <150 mmHg) [6]. In the PROSEVA trial, the investigators reported a significant reduction in 28-day and 90-day mortality in patients treated with PP [7]. PP can naturally recruit the lung through mechanisms that include reduced ventilator-induced lung injury, increased lung homogeneity, increased compliance, and better oxygenation, resulting in improved survival [7-9].

VV-ECMO is also a rescue therapy for more severe ARDS. In a meta-analysis study which included 2 randomized controlled trials (RCTs) (CESAR and EOLIA) of individual patients with severe ARDS, 90-day mortality was significantly lower in the ECMO group compared with conventional management (77 of the 214 [36%] ECMO group and 103 of the 215 [48%] control group patients had died) [10]. In addition to improving hypoxemia and hypercapnia, VV-ECMO provides the patient with total lung rest during the acute phase. In our patient, hypercapnia improved significantly (pH: 7.12 to 7.32; $PaCO_2$: 90 to 41 cmH_2O) after initiation of VV-ECMO; however, severe hypoxemia did not improve as expected (P/F <150), which did not allow us to wean the patient from VV-ECMO. The tidal volume also did not significantly improve as we titrated PC levels.

The chest CT revealed large regions of bilateral consolidation and atelectasis in the dependent parts of the lungs, which theoretically made PP an ideal way to manage intrapulmonary shunting. However, this procedure is difficult, and when it is performed during VV-ECMO, it has high risks, such as low-grade pressure sores, unexpected drop in VV-ECMO flow, accidental decannulation, endotracheal tube displacement, or accidental extubation. Therefore, we first used an LRM, before combined treatment with PP and VV-ECMO. However, some studies have demonstrated the safety of PP during VV-ECMO when performed by an experienced medical team [11-12]. One systematic review and meta-analysis reported that PP during VV-ECMO appeared safe with a cumulative survival of 57%. The most common complication related to PP is the development of low-grade pressure sores (PP complications in 12 out of 24 patients), whereas accidental tube decannulation, endotracheal tube displacement, or accidental extubation were not reported in any study [13].

There is no evidence that the routine use of LRM and PEEP titration in patients with moderate to severe ARDS could improve survival or increase the number of ventilator-free days. The ART trial reported that LRM might increase 28-day all-cause mortality, decrease the number of ventilator-free days during the first 28 days, increase the risks of pneumothorax requiring drainage and barotrauma, increase the use of vasopressors, and increase the occurrence of hypotension [14]. In addition, a post-hoc analysis showed that LRM might be harmful in ARDS patients with pneumonia or in those re-

quiring vasopressor support [15]. Our patient's blood pressure was stable without any vasopressor support during his first week of MICU stay while on VV-ECMO support. Thus, we considered LRM as a rescue therapy to improve oxygenation and "keep the lungs open."

Some retrospective or observational studies have reported the use of PP during VV-ECMO. In some medical centers, the decision to perform PP during ECMO support was based on the clinician's judgment or specific indications such as an unsuccessful ECMO weaning attempt, refractory hypoxemia under ECMO support, persistent high plateau pressure, and more than 50% lung consolidation [11, 16-19]. In contrast, PP in other facilities was routinely performed or encouraged to be used on patients without hemodynamic instability or contraindication [20-21]. Although PP and VV-ECMO are both well-known suggested treatments for severe ARDS, the benefits of the combined use of PP and VV-ECMO are still unclear. Rilinge et al. reported that the timing of PP was an independent predictor of survival. Early initiation of PP (<17 h on Youden's Index) after ECMO cannulation was strongly associated with better survival compared to late or no PP (81.8% vs. 33.3%, $p = 0.02$) [16]. Guervilly *et al*. reported that PP during ECMO support increased the P/F ratio. The P/F ratio was also increased significantly 6 h after PP ($p = 0.03$), and this persisted for 1 h ($p = 0.017$) and 6 h ($p = 0.013$) after returning the patients to the supine position [17].

In our patient, the critical reason for refractory hypoxemia, even under VV-ECMO, was the large portion of pulmonary shunting (collapsed lungs) on the dependent parts, which can theoretically benefit from PP. Although previous studies emphasized the advantages of performing PP in early-stage ARDS, the dependent parts of the lungs tend to collapse in both early and late stages of ARDS, making PP potentially beneficial even in late-stage ARDS. Therefore, we decided to use PP 9 days after VV-ECMO support, and this improved lung compliance from 32 ml/cmH_2O to 41 ml/cmH_2O, consequently allowing us to wean the patient from VV-ECMO on the 4th day of adding PP treatment.

Conclusion

We reported a patient with CAP with a severe ARDS complication, who was treated with VV-ECMO for refractory hypoxemia and hypercapnia. Due to the difficulty in weaning the patient from the ventilator, we applied PP during VV-ECMO support and had an excellent outcome. However, future large RCTs are needed to verify whether the combination of PP and ECMO treatment is more beneficial than treatment without PP.

References

1. Ranieri VM, Rubenfeld GD, Thompson BT, *et al*. Acute respiratory distress syndrome: the Berlin definition. JAMA 2012; 307(23): 2526-33.
2. Bellani G, Laffey JG, Pham T, *et al*. Epidemiology, patterns of care, and mortality for patients with acute respiratory distress syndrome in intensive care units in 50 countries. JAMA 2016; 315: 788-800.
3. Wu M-Y, Huang C-C, Wu T-I, *et al*. Venovenous extracorporeal membrane oxygenation for acute respiratory distress syndrome in adults. Medicine (Baltimore) 2016; 95(8): e2870.
4. Bauer TT, Ewig S, Rodloff AC, *et al*. Acute respiratory distress syndrome and pneumonia: a comprehensive review of clinical data. Clin Infect Dis 2006; 43(6): 748-756.
5. Acute Respiratory Distress Syndrome Network. Ventilation with lower tidal volumes as compared with

traditional tidal volumes for acute lung injury and the acute respiratory distress syndrome. N Engl J Med 2000; 342: 1301-8.

6. Scholten EL, Beitler JR, Prisk GK, *et al*. Treatment of ARDS with prone positioning. Chest 2017; 151(1): 215-224.
7. Guérin C, Reignier J, Richard J-C, *et al*. Prone positioning in severe acute respiratory distress syndrome. N Engl J Med 2013; 368: 2159-2168.
8. Galiatsou E, Kostanti E, Svarna E, *et al*. Prone position augments recruitment and prevents alveolar overinflation in acute lung injury. Am J Respir Crit Care Med 2006; 174(2): 187-97.
9. Albert RK, Keniston A, Baboi L, *et al*. Prone position-induced improvement in gas exchange does not predict improved survival in the acute respiratory distress syndrome. Am J Respir Crit Care Med 2014; 189(4): 494-6.
10. Combes A, Peek GJ, Hajage D, *et al*. ECMO for severe ARDS: systematic review and individual patient data meta-analysis. Intensive Care Med 2020; 46: 2048-2057.
11. Kimmoun A, Roche S, Bridey C, *et al*. Prolonged prone positioning under VV-ECMO is safe and improves oxygenation and respiratory compliance. Ann Intensive Care. 2015;5(1):35.
12. Kipping V, Weber-Carstens S, Lojewski C, *et al*. Prone position during ECMO is safe and improves oxygenation. Int J Artif Organs 2013; 36(11): 821-32.
13. Poon WH, Ramanathan K, Ling RR, *et al*. Prone positioning during venovenous extracorporeal membrane oxygenation for acute respiratory distress syndrome: a systematic review and meta-analysis. Crit Care 2021; 25(1): 292.
14. Cavalcanti AB, Suzumura ÉA, Laranjeira LN. Effect of lung recruitment and titrated positive end-expiratory pressure (PEEP) vs low PEEP on mortality in patients with acute respiratory distress syndrome: a randomized clinical trial. JAMA 2017; 318(14): 1335-1345.
15. Zampieri FG, Costa EL, Iwashyna TJ, *et al*. Heterogeneous effects of alveolar recruitment in acute respiratory distress syndrome: a machine learning reanalysis of the alveolar recruitment for acute respiratory distress syndrome trial. Br J Anaesth 2019; 123(1): 88e95.
16. Rilinger J, ZotzmannV, Bemtgen X, *et al*. Prone positioning in severe ARDS requiring extracorporeal membrane oxygenation. Crit Care 2020; 24:397.
17. Guervilly C, Hraiech S, Gariboldi V, *et al*. Prone positioning during veno-venous extracorporeal membrane oxygenation for severe acute respiratory distress syndrome in adults. Minerva Anestesiol 2014; 80(3): 307-13.
18. Garcia B, Cousin N, Bourel C, *et al*. Prone positioning under VV-ECMO in SARS-CoV-2-induced acute respiratory distress syndrome. Crit Care 2020; 24(1): 428.
19. Guervilly C, Prud'homme E, Pauly V, *et al*. Prone positioning and extracorporeal membrane oxygenation for severe acute respiratory distress syndrome: time for a randomized trial? Intensive Care Med 2019; 45(7): 1040-2.
20. Giani M, Martucci G, Madotto F, *et al*. Prone positioning during venovenous extracorporeal membrane oxygenation in acute respiratory distress syndrome: a multicentre cohort study and propensity-matched analysis. Ann Am Thorac Soc 2020; 6: 66.
21. Schmidt M, Hajage D, Lebreton G, *et al*. Extracorporeal membrane oxygenation for severe acute respiratory distress syndrome associated with COVID-19: a retrospective cohort study. Lancet Respir Med 2020; 8(11): 1121-31.

Prolonged Spontaneous Pneumothorax in Patients with Pleuroparenchymal Fibroelastosis – Report of 2 Cases

Hsin-Jung Hsieh[1], Ping-Hung Kuo[1]

Pleuroparenchymal fibroelastosis (PPFE) is a rare interstitial lung disease, characterized by pleural and subpleural parenchymal fibrosis, predominantly in the upper lobes. Around 60% of patients with PPFE develop spontaneous pneumothorax during the disease course. Previous studies, however, rarely addressed the natural course and duration of pneumothorax in these patients. Here, we reported 2 patients with PPFE who developed spontaneous pneumothorax lasting for more than 6 months. Serial chest images and pulmonary function tests were also provided. It was notable that both patients could still perform the forced expiratory maneuver during spirometry without further lung collapse, probably due to thickening and fibrosis of the visceral pleura and subpleural lung parenchyma. Our experience with these 2 cases suggests that prolonged pneumothorax can develop in patients with PPFE, due to its unique pathophysiology. ***(Thorac Med 2023; 38: 77-82)***

Key words: interstitial lung disease; pleuroparenchymal fibroelastosis; pneumothorax; respiratory function tests

Introduction

Pleuroparenchymal fibroelastosis (PPFE) is a rare interstitial lung disease that was first reported in 2004 by Frankel et al [1]. It is characterized by fibrosis involving the visceral pleura and fibroelastotic changes, predominately in the subpleural lung parenchyma [2]. Common presentations include progressive breathlessness, cough and non-specific chest discomfort. Many patients with PPFE develop platythorax due to upper lobe volume contraction and progressive weight loss during the disease course [3]. Due to pleural involvement, pneumothorax is a common complication in patients with PPFE [3]. Previous reports, however, rarely described the clinical course and duration of pneumothorax in these patients. Here, we report 2 patients with PPFE, who developed spontaneous pneumothorax lasting for more than 6 months.

[1]Department of Internal Medicine, National Taiwan University Hospital and National Taiwan University College of Medicine, Taipei, Taiwan
Address reprint requests to: Dr. Ping-Hung Kuo, Department of Internal Medicine, National Taiwan University Hospital and National Taiwan University College of Medicine, No. 7, Zhongshan S. Rd., Zhongzheng Dist., Taipei, 100, Taiwan

Case Report

CASE 1

A 67-year-old man presented to our outpatient clinic with dry cough and exertional dyspnea for 4 years. He was a non-smoker. His past history was notable for hepatocellular carcinoma with complete remission after treatment. Physical examination revealed slightly decreased breathing sounds in the right lung and diffuse crackles in both lungs. Significant decrease in the anteroposterior diameter of the chest wall (platythorax) was also noticed. Chest radiograph showed patchy subpleural consolidations and pleural thickening in bilateral upper lungs. Chest computed tomography (CT) disclosed pleural thickening, subpleural consolidations, reticulation and mild bronchiectasis in bilateral upper lungs (Fig.1). The autoimmune and microbiology profiles were unremarkable. Pulmonary function tests revealed a forced vital capacity (FVC) of 75.6% of the predicted value, and a diffusing capacity for carbon monoxide (DLCO) of 57.5% predicted (Table 1).

Six months after the initial visit, right pneumothorax was incidentally noticed on the follow-up chest CT (Fig.1). The patient did not experience exacerbation of chest tightness or dyspnea. He could still perform the forced expiratory maneuver during spirometry, and pulmonary function results remained stationary (Table 1). Suggestions of lung transplantation and intervention for his pneumothorax were declined. Off-label use of nintedanib 150 mg twice per

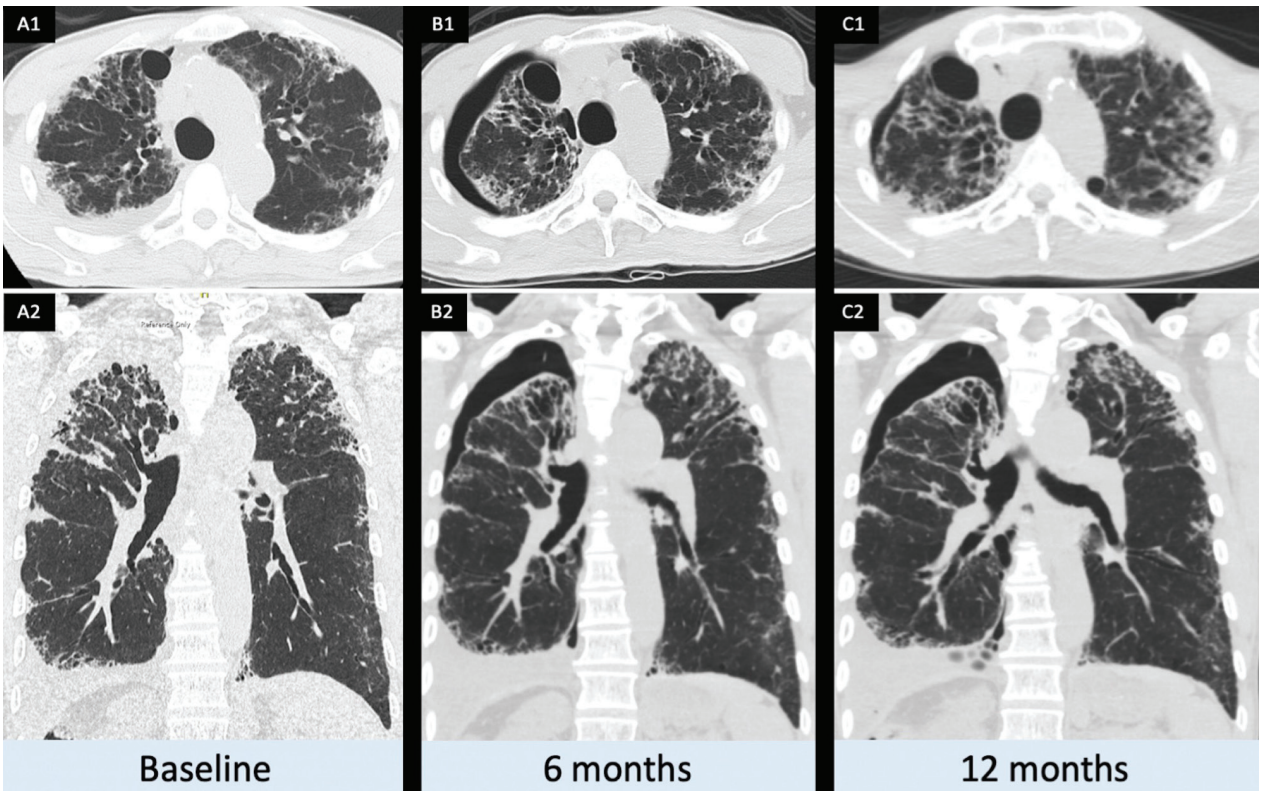

Fig. 1. Chest computed tomography serial axial and coronary views for case 1 at baseline (A1, A2), and at 6 months (B1, B2) and 12 months (C1, C2) after diagnosis of persistent pneumothorax.

day was initiated thereafter, and the follow-up chest images revealed no significant progression of pneumothorax (Fig.1). Unfortunately, the patient did not respond well to the antifibrotic therapy and passed away due to chronic respiratory failure 2 years later.

CASE 2

An 18-year-old man presented with persistent cough, exertional dyspnea and recurrent bilateral pneumothorax for 3 years when visiting the clinic. He had received tube drainage at another hospital due to recurrent pneumothorax. During the serial image follow-up at the other hospital, pneumothorax remission was found to be not satisfactory after tube removal. Due to the above symptoms, he came to our clinic for a second opinion. He was a non-smoker, and had a past medical history of right post-auricular neuroblastoma in childhood, with complete remission when he was 15 years old. Physical examination revealed diffuse crackles in both lungs and platythorax. Chest CT disclosed bilateral pleural thickening and volume reduction in the upper lungs. Imaging also revealed bilateral pneumothorax, with the right side more severe than the left side (Fig. 2). The pathologic report of the pleuroscopic biopsy of the parietal pleural at the previous hospital revealed chronic inflammation and fibrosis. The autoimmune profiles, tumor markers and microbiology studies were all negative. Pulmonary function tests revealed a FVC of 770 mL (17.1% of the predicted value) (Table 1). Based on the image findings, the patient was diagnosed with PPFE

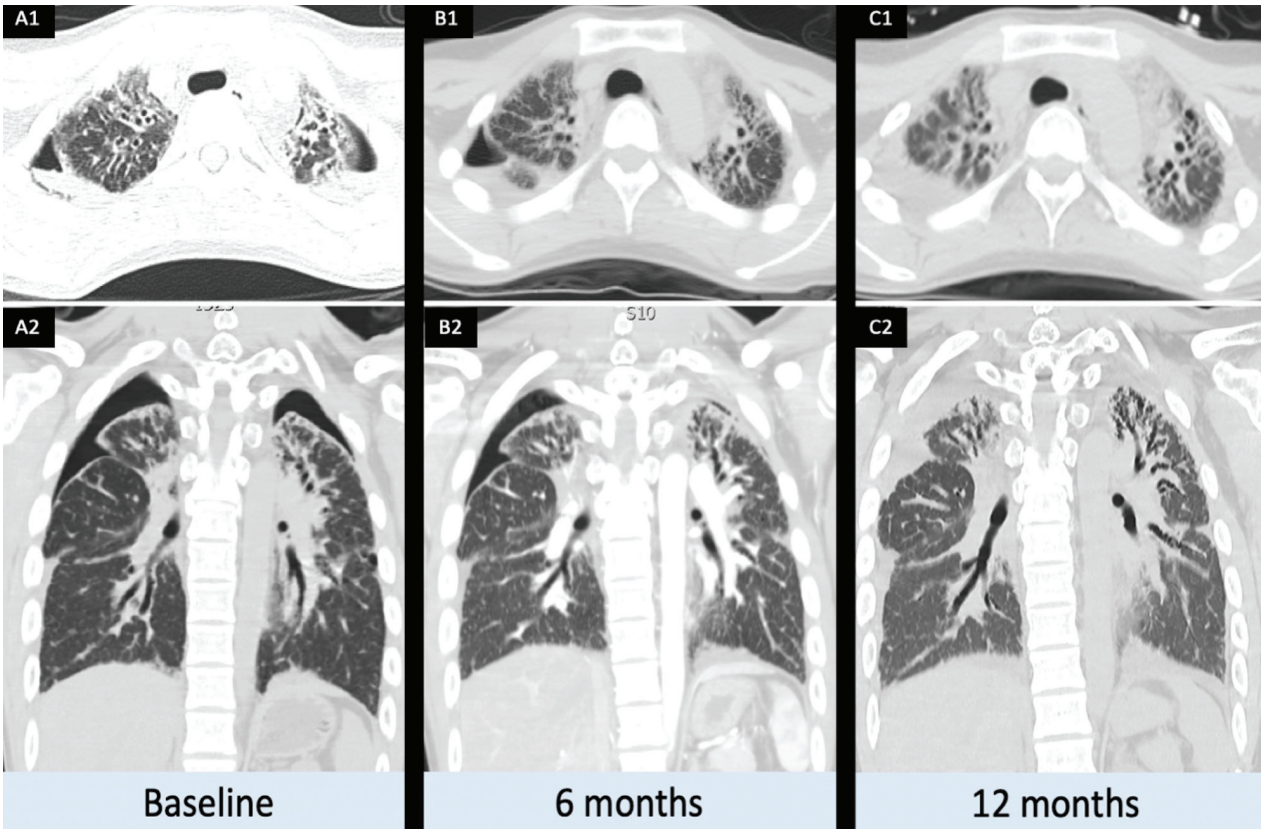

Fig. 2. Chest computed tomography serial axial and coronary views for case 2 at baseline (A1, A2), and at 6 months (B1, B2) after diagnosis of persistent bilateral pneumothorax, which resolved 12 months (C1, C2) after diagnosis.

Table 1. Summary of Baseline Demographic Characteristics and Serial Pulmonary Function Testing Results of the 2 Cases

	Case 1			Case 2		
Age and sex	67-year-old man			18-year-old man		
Height (cm)	170.5			172.6		
Body weight (kg)	58.5			54.2		
Body mass index (kg/m^2)	20.24			18.32		
Ratio of chest wall AP to the transverse diameter	57.2%			37.1%		
	Baseline	6 months	12 months	Baseline	6 months	12 months
FVC (% predicted)	75.6	74	63.3	17.1	14.4	9.5
FEV1 (% predicted)	89.1	86.6	78.1	18.6	16.1	10.6
FEV1/FVC (%)	94.1	93.2	98.1	97.4	100.0	100.0
TLC (% predicted)	76.02	N/A	74.8	N/A	25.9	N/A
DLCO (% predicted)	57.5	72.5	65.4	Undetectable due to small FVC		

Acronyms: AP, anteroposterior; DLCO, diffusing capacity for carbon monoxide; FEV1, forced expiratory volume in 1 second; FVC, forced vital capacity; N/A, not applicable; TLC, total lung capacity.

and was admitted for further management.

During the admission course, a pigtail catheter was placed on the right side for pneumothorax management. After partial remission of pneumothorax, the drainage tube was removed. The residual pneumothorax gradually resolved during the following 2 years (Fig. 2). Nonetheless, his FVC rapidly declined, even under medical treatment (Table 1). He eventually passed away due to respiratory failure as the disease progressed.

Discussion

In this report, we described the serial chest imaging and pulmonary function testing results of 2 patients with PPFE complicated with spontaneous pneumothorax lasting more than 6 months. To our knowledge, few previous studies have reported these findings of this unique phenomenon in PPFE patients.

In our patients, the diagnosis of PPFE was not confirmed by surgical lung biopsy. Enomoto et al. proposed that PPFE can be diagnosed if the following criteria were met: classical image findings, radiologic confirmation of disease progression, and exclusion of other lung diseases [2]. In a retrospective study of 89 patients diagnosed based on modified criteria, only 14 (15.7%) cases were confirmed pathologically [4]. The clinical manifestations, radiological features and natural course were consistent with those reported in patients with typical PPFE.

Spontaneous pneumothorax is a common complication in patients with PPFE [2, 4, 5]. According to a recent largescale retrospective study that included 89 patients with idiopathic PPFE, the incidence of pneumothorax was around 60%, and the recurrence rate of pneumothorax was 56.6% [4]. The risk factors in these patients included male sex, a history of receiving steroid treatment, and a higher value

for the residual volume/total lung capacity ratio. Furthermore, the incidence of pneumothorax in patients with PPFE is higher than that in patients with other interstitial lung diseases. Kano et al. reported that the 3-year cumulative incidence of pneumothorax in patients with PPFE was 53.9%, but only 17.7% in patients with idiopathic pulmonary fibrosis [4]. In addition, those patients with pneumothorax have a poorer survival rate than patients without [4]. Therefore, when treating patients with PPFE, we emphasize that serial images should be followed regularly to monitor the occurrence of pneumothorax.

Based on its etiologies, PPFE can be classified as idiopathic in form (without a known cause) or secondary in form (with a known cause). Previous studies have shown that radiotherapy, chemotherapy, autoimmune disease, hematopoietic stem cell transplantation (HSCT) and lung transplantation are related to secondary PPFE [6]. A retrospective analysis revealed that the prevalence rate was 0.28% in HSCT recipients and 7.54% in lung transplant recipients [7]. In our case 1, the patient was classified as having idiopathic PPFE, since no related condition was noticed. In case 2, we presumed that the patient might have secondary PPFE due to the history of chemotherapy related to neuroblastoma. The difference between idiopathic and secondary PPFE is not only in etiology, but also in age at disease onset. A retrospective study conducted by Oda et al. found that patients with secondary PPFE tended to be younger than those with idiopathic PPFE. However, there were no differences in the incidence of pneumothorax and the survival rate between the 2 groups [6].

Up to the present, there is no treatment specific to pneumothorax with PPFE. Management of pneumothorax in PPFE should follow general principles of treatment. Symptoms, severity of pneumothorax and underlying conditions should be taken into account. Around 70% of events of pneumothorax in patients with PPFE were small in size and asymptomatic. Therefore, providing conservative oxygen therapy with close monitoring should be sufficient. Since the remaining 30% of pneumothorax events were large in size and symptomatic, they required tube drainage. Nonetheless, despite receiving tube drainage, more than half of them still had a prolonged air leak [4]. Management of a prolonged air leak included medical pleurodesis (autologous blood patch, minocycline, talc, etc.), bronchial occlusion and surgical intervention [4]. In both of our cases, the pneumothorax was small in size and with prolonged duration. Without further intervention, the pneumothorax remained stationary, and in case 2, the pneumothorax resolved spontaneously 1 year after diagnosis. At present, there is no study discussing which treatment is more effective in managing prolonged pneumothorax, or which is able to reduce the recurrence of pneumothorax. Therefore, clinical physicians should closely follow the treatment response of the patient.

In clinical practice, the presence of a recent pneumothorax is usually considered as a contraindication for performing the forced expiratory maneuver during pulmonary function testing, to avoid the risk of further lung collapse [8]. Nevertheless, it is interesting that our 2 patients could still tolerate serial pulmonary function testing without deterioration of oxygen saturation and chest imaging after the procedure. We speculate that the limited progression of pneumothorax was related to the natural course of pleural fibrosis and adhesion, and therefore prevented lung collapse during expiration.

In conclusion, we have described 2 cases of PPFE with prolonged spontaneous pneumothorax, and with serial images and PFT. The pathophysiology of prolonged pneumothorax remains unknown and requires further investigation.

References

1. Frankel SK, Cool CD, Lynch DA, *et al*. Idiopathic pleuroparenchymal fibroelastosis: description of a novel clinicopathologic entity. Chest 2004; 126: 2007-13.
2. Enomoto Y, Nakamura Y, Satake Y, *et al*. Clinical diagnosis of idiopathic pleuroparenchymal fibroelastosis: a retrospective multicenter study. Respir Med 2017; 133: 1-5.
3. Chua F, Desai SR, Nicholson AG, *et al*. Pleuroparenchymal fibroelastosis. A review of clinical, radiological, and pathological characteristics. Ann Am Thorac Soc 2019; 16: 1351-9.
4. Kono M, Nakamura Y, Enomoto Y, et al. Pneumothorax in patients with idiopathic pleuroparenchymal fibroelastosis: incidence, clinical features, and risk factors. Respiration 2021; 100: 19-26.
5. Lee JH, Chae EJ, Song JS, *et al*. Pleuroparenchymal fibroelastosis in Korean patients: clinico-radiologic-pathologic features and 2-year follow-up. Korean J Intern Med 2020; 36: S132-41.
6. Oda T, Sekine A, Tabata E, *et al*. Comparison of clinical characteristics and outcomes between idiopathic and secondary pleuroparenchymal fibroelastosis. J Clin Med 2021; 10: 846.
7. Mariani F, Gatti B, Rocca A, *et al*. Pleuroparenchymal fibroelastosis: the prevalence of secondary forms in hematopoietic stem cell and lung transplantation recipients. Diagn Interv Radiol 2016; 22: 400-6.
8. Cooper BG. Republished review: an update on contraindications for lung function testing. Postgrad Med J 2011; 87: 724-33.

Crouzon Syndrome with Severe Obstructive Sleep Apnea and Restrictive Ventilatory Impairment -a Case Report and Literature Review

Lun-Yu Jao[1,2], Yao-Kuang Wu[1,2], Mei-Chen Yang[1,2], Chih-Wei Wu[1,2], Chung Lee[1,2], Li-Ping Tsai[2,3*], Chou-Chin Lan[1,2]

Crouzon syndrome is a rare autosomal-dominant genetic disorder characterized by premature fusion of the cranial sutures. Clinical features include midface hypoplasia, maxillary hypoplasia, and prognathism, which can lead to difficulty breathing. Patients with Crouzon syndrome are reported to have a high prevalence of obstructive sleep apnea syndrome (OSAS). Non-cranial orthopedic deformities such as kyphoscoliosis are also reported. We reported the case of a 41-year-old female with exophthalmos, midface hypoplasia, and mandibular prognathism. She was diagnosed with severe kyphoscoliosis with restrictive ventilatory impairment. Surgical treatment was not recommended due to her very poor lung function. However, she developed dyspnea and edema of the legs 5 years later. A cardiac echogram revealed cor pulmonale. Owing to pneumonia and respiratory failure, intubation with an invasive mechanical ventilator was initiated. She was successfully extubated after 1 month on mechanical ventilation and was maintained on noninvasive bilevel positive airway pressure (BiPAP). Due to the typical facial appearance, Crouzon syndrome was suspected and confirmed by genetic analysis. Polysomnography revealed severe OSAS with an apnea-hypopnea index score of 105.8/h with prominent desaturation. The apnea-hypopnea and desaturation were significantly improved after non-invasive positive pressure ventilation. Due to severe OSAS and the above problems, she was maintained on long-term BiPAP. Although subsequent polysomnography and pulmonary function testing revealed some decline in the apnea-hypopnea index and lung function, she continues to maintain a good quality of sleep and daily activities under BiPAP. ***(Thorac Med 2023; 38: 83-91)***

Key words: Crouzon syndrome; kyphoscoliosis; obstructive sleep apnea; restrictive ventilatory impairment

[1]Division of Pulmonary Medicine, Taipei Tzu Chi Hospital, Buddhist Tzu Chi Medical Foundation, New Taipei City, Taiwan, [2]School of Medicine, Tzu-Chi University, Hualien, Taiwan, [3]Department of Pediatrics, Taipei Tzu Chi Hospital, Buddhist Tzu Chi Medical Foundation, New Taipei City, Taiwan

Address reprint requests to: Dr. Chou-Chin Lan, Division of Pulmonary Medicine, Taipei Tzu Chi Hospital, Buddhist Tzu Chi Medical Foundation, 289, Jianguo Road, Xindian City, New Taipei City 23142, Taiwan, Republic of China

Introduction

Crouzon syndrome is a rare autosomal-dominant genetic disorder characterized by premature fusion of the cranial sutures [1]. The syndrome has a highly variable phenotype [1]. There is premature synostosis of the coronal and sagittal sutures leading to facial dysmorphism, skull deformities, and exophthalmos. The features of Crouzon syndrome include craniosynostosis, exophthalmos, brachycephaly, midface hypoplasia, maxillary hypoplasia, prognathism, hypertelorism, strabismus, and a shallow nasal septum [2]. Cognitive ability of patients with Crouzon syndrome is typically normal; however, mental retardation has been reported [3]. Hearing loss is common, with an incidence of 55% [2].

Patients with Crouzon syndrome are prone to obstructive sleep apnea syndrome (OSAS), due to anatomical facial abnormalities [4]. Spinal abnormalities leading to kyphoscoliosis have been reported in these patients. Severe kyphoscoliosis leads to restrictive ventilatory impairment [3]. Surgical treatment is usually recommended for midface hypoplasia and kyphoscoliosis. However, some patients have a high risk of complications following surgery or anesthesia. We present here, the report of a patient with Crouzon syndrome who had OSAS and kyphoscoliosis with severe restrictive ventilatory impairment. Surgical treatment was not recommended because of very poor lung function; however, she was successfully treated with non-invasive positive pressure ventilation using bilevel positive airway pressure (BiPAP) for many years.

We reviewed reports on the management of patients with Crouzon syndrome and OSAS. Because of the high prevalence of OSAS in patients with Crouzon syndrome and the possibility of sudden death in childhood or infancy, we recommend attention to and evaluation of sleep-related breathing disorders in these patients.

Case Presentation

The patient was a 41-year-old female presenting with exophthalmos, midface hypoplasia, and mandibular prognathism. She had a short stature with a weight of 34.5 kg, height of 133.5 cm, and a body mass index of 19.4 kg/m^2. She reported that her father and 2 sisters had similar physical appearances.

In 2007, she first visited our orthopedic department for severe kyphoscoliosis. X-ray (Fig 1A) and CT scan (Fig. 1B) images revealed severe kyphoscoliosis of the thoracolumbar (T-L) spine. Her pulmonary function test (PFT) revealed forced expiratory volume in 1 second (FEV1)/forced vital capacity (FVC) of 81%, FVC of 1.13 L (49% of predicted value), and FEV1 of 0.92 L/min (44% of predicted value). Surgical treatment for the severe kyphoscoliosis was not recommended due to her severe restrictive ventilatory impairment, which put her at a high risk of complications following surgery or anesthesia. However, her symptoms of dyspnea were not prominent at that time.

In 2013, she visited our chest outpatient department with the complaints of significant dyspnea and edema of the legs for 3 months. She also had wheezing, nasal obstruction, rhinorrhea, and sore throat. The chest X-ray (Fig 2A) images revealed severe dextroscoliosis of the T-L spine. Due to her severe dyspnea, she was admitted to the hospital. At admission, her body temperature was 36.8°C, pulse rate was 102 beats/min, and blood pressure was 136/86 mmHg. Her respiratory rate was 28 breaths/

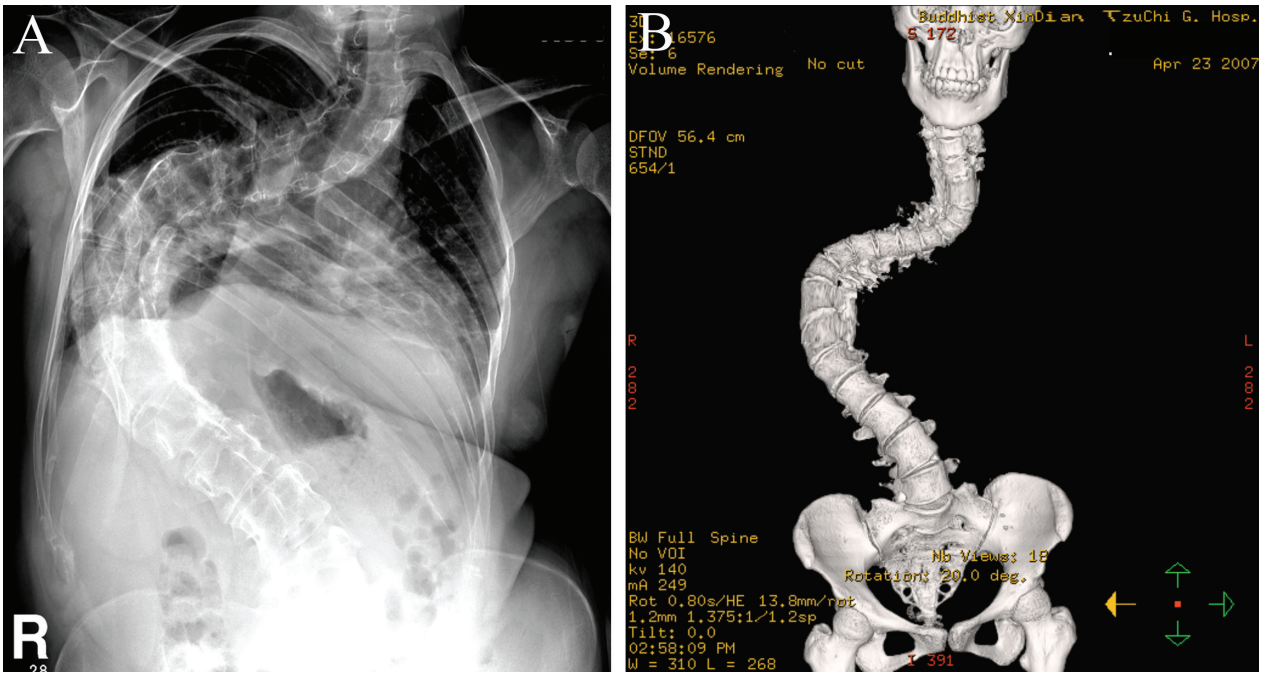

Fig. 1. X-ray and CT scan of the thoracolumbar spine

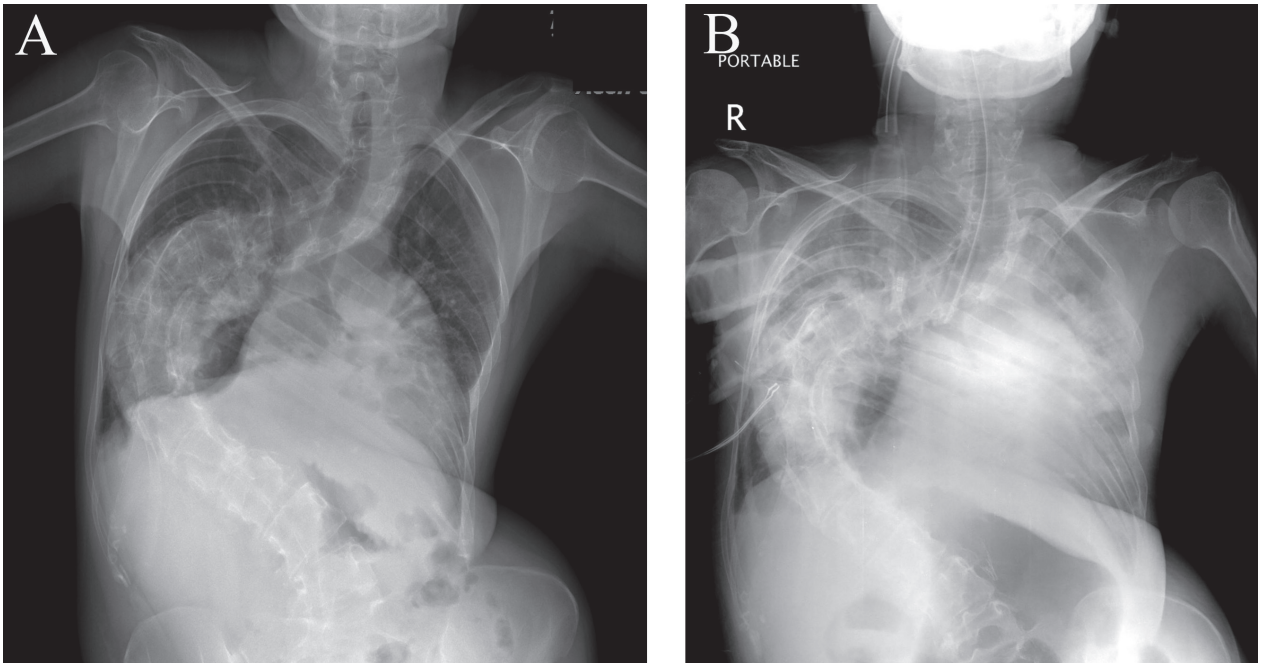

Fig. 2. Chest X-ray during admission

min with a mildly rapid breathing pattern, and oxygen saturation was 95% in ambient air. Lab examination results revealed a white blood cell count of 6780 /uL, hemoglobin of 11.3 g/dL, normal renal function (blood urea nitrogen 15 mg/dL, creatinine 0.6 mg/dL), and mildly elevated liver enzymes (aspartate aminotransferase 53 IU/L, aspartate aminotransferase 82

IU/L). Intravenous injection of furosemide and inhaled Atrovent and Bricanyl were prescribed for the leg edema, dyspnea, and wheezing. A cardiac echogram revealed moderate pulmonary hypertension and cor pulmonale, suspected of being due to severe kyphoscoliosis with severe restrictive ventilatory impairment. After admission and treatment as above, edema of the legs persisted. Lung auscultation revealed rhonchi in the lower lobes, bilaterally. Her symptoms aggravated with progressive dyspnea and drowsiness. Arterial blood gas analysis revealed pH 7.302, PaO_2 166.1 mmHg, $PaCO_2$ 88.9 mmHg, HCO_3 43.1, and SaO_2 99.3%. Invasive mechanical ventilation (MV) through endotracheal intubation was initiated. The chest X-ray (Fig 2B) images revealed pneumonic patches in the lower lobes, bilaterally. Parenteral antibiotic therapy with piperacillin/sulbactam 4.5 g every 6 hours was administered. She was then transferred to the intensive care unit (ICU).

Following treatment with antibiotics, the pneumonic patches seen in the bilateral lower lobes improved. However, weaning her off MV was difficult because of severe kyphoscoliosis with severe restrictive ventilatory impairment. We suggested a tracheostomy after 2 weeks of MV, but the patient refused and her mother agreed with her decision. Following respiratory training with pressure support and T-piece training, she was successfully extubated after 1 month of MV use. Noninvasive BiPAP then was initiated due to her very poor lung function. Initially, BiPAP use throughout the day was recommended. Following progressive improvement in her respiratory function, only nocturnal BiPAP was recommended. We suggested long-term nocturnal use of BiPAP since she had chronic respiratory failure with cor pulmonale. She then was transferred to the general ward and was discharged in stable condition.

Owing to her unusual appearance with exophthalmos, midface hypoplasia, and mandibular prognathism, we had a high degree of suspicion of Crouzon disease and performed genetic analysis. The gene test revealed a fibroblast growth factor receptor 2 (FGFR2) mutation, which was diagnostic of Crouzon disease. She then underwent a series of studies on Crouzon disease. Computed tomography (CT) images of her head revealed midface hypoplasia (Fig 3A), mandibular prognathism, sinusitis, exophthal-

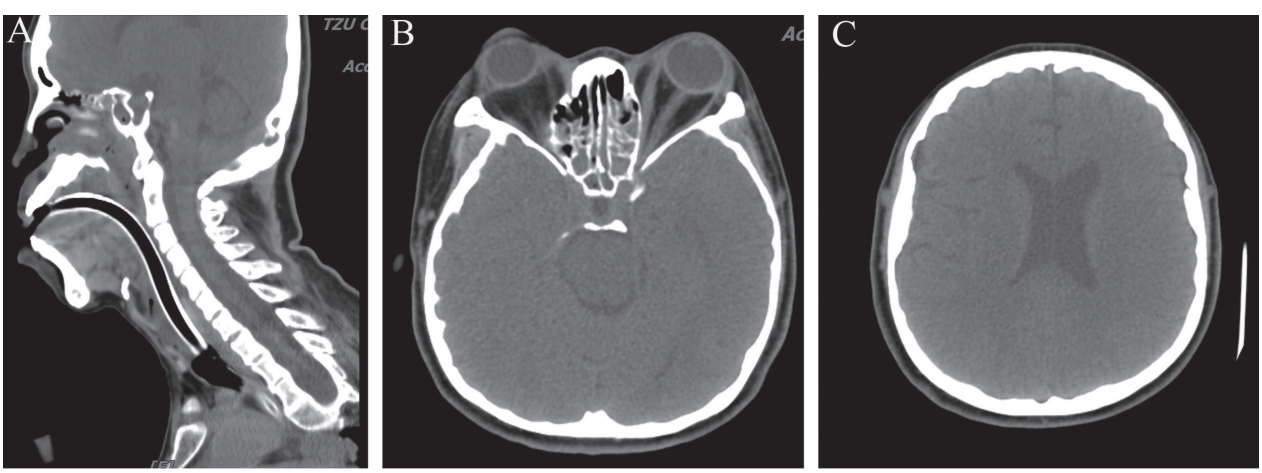

Fig. 3. CT scan of the skull and brain

mos (Fig 3B), and an absence of hydrocephalus (Fig 3C). Polysomnography (PSG) revealed an obstructive-type apnea-hypopnea index (AHI) of 105.8/h, a mean oxygen saturation on pulse oximeter (SpO_2) of 55%, and a minimum SpO_2 of 30% without continuous positive airway pressure (CPAP) use. CPAP titration results suggested her CPAP level was 13 cmH_2O with a minimum SpO_2 of 94% and a mean SpO_2 of 95.2%. However, her reported Epworth Sleepiness Scale (ESS) was only 1.

Since she had OSAS combined with severe restrictive ventilatory impairment, we recommended continued use of BiPAP at night. The patient tolerated BiPAP well and her compliance with BiPAP remained good. A PSG (Table 1) in the following year revealed an improvement in AHI to 66.8/h, mean SpO_2 of 89%, and minimum SpO_2 of 60% without CPAP use. The suggested CPAP level was 12 cmH_2O with minimum SpO_2 of 94.1% and mean SpO_2 of 95.0%. Her ESS was 2. The PSG in 2020 showed AHI of 98.6/h, mean SpO_2 of 89%, and minimum SpO_2 of 80% without CPAP use. The suggested CPAP level was 13 cmH2O with a minimum SpO_2 of 94.0% and mean SpO_2 of 95.0%. Her ESS was 0. Although the AHI increased from 66.8/h to 98.6/h during this period, her subjective sleep quality was stable with maintenance on night BiPAP. For evaluation of the severe restrictive ventilatory impairment, a PFT (Table 2) was performed. Although there was some decline in FVC and FEV1, her respiratory condition was stable with mild exertional dyspnea. Her dyspnea has been under control and without any acute exacerbation since 2013.

Table 1. Polysomnography in the Following Years

Year	2013	2014	2020
Total AHI (/h)	105.8	66.8	98.6
DI (/h)	114.2	63.8	98.6
Mean SPO_2 (%) without CPAP	55%	89%	89%
Minimum SPO_2 (%) without CPAP	30%	60%	80%
Suggested CPAP level (cmH_2O)	13	12	14
Mean SPO_2 (%) with suggested CPAP	95.2%	95.0%	95.0%
Minimum SPO_2 (%) with suggested CPAP	94.1%	94.1%	94.0%
ESS	1	2	0

Acronyms: AHI: apnea-hypopnea index; DI: desaturation index; SpO_2: oxygen saturation on pulse oximeter; ESS: Epworth Sleepiness Scale

Table 2. Pulmonary Function Test in the Following Years

Year	2007	2009	2010	2013	2014	2015	2018	2019
FVC (L)	1.13	0.98	1.06	1.01	1.12	1.05	1.10	0.97
FVC (%)	49%	34%	32%	31%	41%	39%	39%	34%
FEV1 (L/min)	0.92	0.80	0.90	0.83	0.93	0.88	0.96	0.82
FEV1 (%)	44%	32%	31%	30%	40%	38%	39%	33%

Acronyms: FVC: forced vital capacity; FEV1: forced expiratory volume in 1 second

Discussion

In 1912, Dr. Crouzon first described an autosomal dominant syndrome of craniofacial dysplasia in a mother-daughter family, with the triad of cranial deformities, facial abnormalities, and proptosis [5]. Our patient presented with the typical triad of features of Crouzon syndrome. She also had a family history, with her father and sisters having similar facial appearances. She was diagnosed as having Crouzon syndrome after a genetic analysis. The patient also presented with severe OSAS and kyphoscoliosis with severe restrictive ventilatory impairment. She was even admitted to the ICU due to respiratory failure.

Over the years, she has been successfully treated with BiPAP and has maintained a good quality of sleep and daily life. Her PSG data showed that SpO_2 at baseline (without BiPAP) was 30%, and that it increased to 60% and 80% after using BiPAP for a long time. This may be related to the residual effect of using BiPAP [6, 7]. In previous studies, some patients with good compliance with BiPAP use had better SpO_2 or AHI when BiPAP was temporarily discontinued [6, 7]. This effect is possibly related to improvement in the mucosal edema of the pharyngeal airway and an increase of the upper airway size [6, 7]. However, the residual effect lasts several days only, and the patient still has to use BiPAP regularly. This case indicates that BiPAP therapy is a useful treatment option for OSAS combined with severe restrictive ventilatory disorders in patients with Crouzon syndrome.

Crouzon syndrome is usually diagnosed during labor or during the prenatal period through clinical and physical evaluation [2]. Experienced obstetricians can identify signs of premature closure of the cranial sutures on ultrasound scanning [2]. Proptosis and shallow eye sockets are diagnostic features of Crouzon syndrome, and are seen in almost all cases. Plain radiography and CT scan of the skull might help in the diagnosis and evaluation of Crouzon syndrome [2]. Some patients also have hydrocephalus, which can be detected on a CT scan of the brain [2].

OSAS is common in patients with Crouzon syndrome, with a prevalence of 40-85% [4]. The causes of the high prevalence of OSAS in these patients are multifactorial, including midface hypoplasia, adenotonsillar hypertrophy, mandibular hypoplasia, and others [8]. Midface hypoplasia with retraction and subsequent soft-tissue abnormalities are believed to be the major causes of upper airway obstruction leading to OSAS [8, 9]. An abnormal shape of the head with brachycephaly, maxillary hypoplasia, and a small nasal cavity can also lead to upper airway obstruction and OSAS [9].

There are many approaches to treating patients with OSAS, such as noninvasive CPAP therapy, an oral appliance, and surgical treatment, based on the severity or causes of OSAS [10-14]. However, in patients with Crouzon syndrome, oral appliances are not suitable, due to the major problems of midface hypoplasia. Furthermore, procedures such as tonsillectomy or adenectomy do not lead to a significant improvement [15]. Unlike patients with OSAS only, those with Crouzon syndrome have additional complications secondary to mid-facial hypoplasia and other anatomic abnormalities. Since midface hypoplasia is the main cause of OSAS in Crouzon syndrome patients, midface advancement is the treatment of choice [8, 15]. Le Fort III osteotomy with distraction osteogenesis advancement is recommended for increasing the cross-sectional area of the nasopharyn-

geal airway in treating OSAS in children and teenagers with Crouzon syndrome [8]. However, the decision regarding the degree of midface advancement and the timing of surgery requires comprehensive analysis. Although mid-face advancement seems to be a good option to treat a compromised airway, Bannink et al. reported that only 55% of patients showed good results following Le Fort III distraction, and that some patients might relapse in long-term follow-up [15]. Since patients with Crouzon syndrome often have multiple anatomical abnormalities and multiple levels of airway obstruction, Le Fort III advancement does not lead to improvement in all Crouzon patients who have OSAS. It might be possible to treat the obstructions at other levels using other procedures, such as widening the palate to enlarge the nasopharynx and mandibular advancement to create more space. Moreover, long-term follow-up is important because OSAS might relapse after surgery in these patients [15].

Noninvasive CPAP at night is effective in preventing upper airway collapse and relieving symptoms of disturbed sleep in patients with OSAS; it is also a good option for treating patients with Crouzon syndrome and OSAS [15, 16]. Bannink et al. reported that some Crouzon syndrome patients with moderate or severe OSAS underwent midface advancement and were under long-term CPAP dependence [15, 16]. Our patient, who had Crouzon syndrome with OSAS, and who was at high risk for post-surgical complications, was successfully treated with nocturnal BiPAP for OSAS.

Some non-cranial orthopedic deformities associated with Crouzon syndrome have been reported. Umezu et al. reported that 18% to 40% of patients have a cervical spine deformity, 18% have an elbow deformity, and 7% have deformities of the fingers [3]. The reports of thoracic and lumbar spine deformities with kyphoscoliosis in such patients are limited [1, 3]. Harde M et al. reported patients with kyphoscoliosis with severe restrictive lung functions and atlantoaxial dislocation [17]. Surgical treatment with spinal fusion is often recommended to correct spinal abnormalities. However, performing surgery in patients with Crouzon syndrome with craniofacial deformities is very challenging, owing to difficult airway management. This is due to a high-arched palate, limited neck extension, narrowing of the nasopharynx, and a tracheal ring abnormality [17]. Moreover, surgery in patients with severe spinal deformity requires a longer operative duration and prolonged intubation under general anesthesia in the prone position. Therefore, it is challenging to administer anesthesia and perform surgery in patients with Crouzon syndrome [9, 17]. Umezu et al. described the case of a patient having Crouzon syndrome with severe thoracic kyphoscoliosis who underwent surgical correction [3]. The patient developed serious postoperative respiratory complications with pneumonia and respiratory failure. Tracheostomy was finally performed with this patient. The report concluded that a comprehensive evaluation is needed prior to surgical treatment for kyphoscoliosis [3].

Since surgical treatment for severe kyphoscoliosis poses a high risk for patients with Crouzon syndrome, a non-surgical treatment option is necessary. The orthopedic surgeon did not recommend surgery for the severe kyphoscoliosis and severe restrictive ventilatory impairment in our patient. Hence, we used BiPAP therapy. In patients with chronic respiratory failure secondary to severe kyphoscoliosis, BiPAP is the treatment of choice [18]. Long-term BiPAP therapy improves daytime blood

gas levels, respiratory muscle performance, and hypoventilation-related symptoms, reduces hospital readmissions, and increases survival in patients with severe kyphoscoliosis [18, 19]. Our patient was therefore suggested to continue long-term BiPAP therapy for the severe OSAS and severe kyphoscoliosis.

Conclusions

Crouzon syndrome is a rare autosomal-dominant genetic disorder characterized by midface hypoplasia, maxillary hypoplasia, and prognathism. Patients with Crouzon syndrome are reported to have a high prevalence of OSAS. Some patients also have kyphoscoliosis. We reported the case of a patient with severe OSAS and severe kyphoscoliosis, and with severe restrictive ventilatory impairment presenting with respiratory failure and cor pulmonale. She was successfully treated with non-invasive BiPAP after respiratory failure. She continues to maintain good sleep quality and daily activity after long-term BiPAP use. We suggest that non-invasive BiPAP ventilation is a useful treatment option for OSAS combined with severe restrictive ventilatory disorders in patients with Crouzon syndrome.

Conflict of Interest

The authors declare that there are no conflicts of interest that could be perceived as prejudicial to the impartiality of the reported research.

References

1. Lin M, Lu Y, Sui Y, et al. Extremely severe scoliosis, heterotopic ossification, and osteoarthritis in a three-generation family with Crouzon syndrome carrying a mutant c.799T>C FGFR2. Mol Genet Genomic Med 2019; 7(9): e843.
2. Al-Namnam NM, Hariri F, Thong MK, et al. Crouzon syndrome: genetic and intervention review. J Oral Biol Craniofac Res 2019; 9(1): 37-39.
3. Umezu T, Fujita N, Yagi M, et al. Surgical correction of severe kyphoscoliosis associated with Crouzon syndrome with serious postoperative respiratory problems: a aase report. JBJS Case Connect 2017; 7(4): e98.
4. Inverso G, Brustowicz KA, Katz E, er al. The prevalence of obstructive sleep apnea in symptomatic patients with syndromic craniosynostosis. Int J Oral Maxillofac Surg 2016; 45(2): 167-169.
5. Crouzon O. Dysostose cranio-faciale héréditaire. Bulletins et Mémoires de la Société Médicale des Hôpitaux de Paris 191; 33: 545-555.
6. Fiz JA, Abad J, Ruiz J, *et al*. nCPAP treatment interruption in OSA patients. Respir Med 1998; 92(1): 28-31.
7. Hers V, Liistro G, Dury M, *et al*. Residual effect of nCPAP applied for part of the night in patients with obstructive sleep apnoea. Eur Respir J 1997; 10(5): 973-976.
8. Lu X, Forte AJ, Park KE, *et al*. Airway growth in preoperative patients with Crouzon syndrome. Facial Plast Surg Aesthet Med 2021; 23(3): 191-197.
9. Ganeriwal V, Dey P, Gore B, *et al*. Anesthesia challenges in a case of Crouzon syndrome for corrective rigid external distraction frame insertion. Indian Anaesth Forum 2019; 20: 42-45.
10. Akashiba T, Inoue Y, Uchimura N, *et al*. Sleep apnea syndrome (SAS) clinical practice guidelines 2020. Respir Investig 2022; 60(1): 3-32.
11. Kent D, Stanley J, Aurora RN, *et al*. Referral of adults with obstructive sleep apnea for surgical consultation: an American Academy of Sleep Medicine clinical practice guideline. J Clin Sleep Med 2021; 17(12): 2499-2505.
12. Patil SP, Ayappa IA, Caples SM, *et al*. Treatment of adult obstructive sleep apnea with positive airway pressure: an American Academy of Sleep Medicine clinical practice guideline. J Clin Sleep Med 2019; 15(2): 335-343.
13. Ramar K, Dort LC, Katz SG, *et al*. Clinical practice guideline for the treatment of obstructive sleep apnea and snoring with oral appliance therapy: an update for 2015. J

Clin Sleep Med 2015; 11(7): 773-827.
14. Tan HL, Kheirandish-Gozal L, Abel F, *et al*. Craniofacial syndromes and sleep-related breathing disorders. Sleep Med Rev 2016; 27: 74-88.
15. Bannink N, Nout E, Wolvius EB, *et al*. Obstructive sleep apnea in children with syndromic craniosynostosis: long-term respiratory outcome of midface advancement. Int J Oral Maxillofac Surg 2010; 39(2): 115-121.
16. Kyprianou C, Chatzigianni A. Crouzon syndrome: a comprehensive review. Balk J Dent Med 2018; 22:1-6.
17. Harde M, Varsha S, Chhatrapati S, *et al*. Crouzon syndrome: an anesthetic challenge. Ain-Shams J Anaesthesiol 2015; 8: 683-685.
18. Adıgüzel N, Karakurt Z, Güngör G, *et al*. Management of kyphoscoliosis patients with respiratory failure in the intensive care unit and during long-term follow-up. Multidiscip Respir Med 2012; 7(1): 30.
19. Buyse B, Meersseman W, Demedts M. Treatment of chronic respiratory failure in kyphoscoliosis: oxygen or ventilation? Eur Respir J 2003; 22(3): 525-528.

Multimodality Treatment for a Huge Anterior Mediastinal Seminomas: A Case Report

Tzu-Lung Lai[1], En-Kuei Tang[1], Yen-Chiang Tseng[1]

Huge anterior mediastinal seminomas are rare mediastinal tumors. The diagnosis is usually delayed because there are only a few initial symptoms; most of the seminomas were large and bulky at the time of diagnosis with tumor compression of the lung, trachea, or heart. We present the case of a 29-year-old man who complained of progressive dyspnea and cough. Chest radiography revealed a huge mediastinal tumor, and mediastinal seminoma was diagnosed by computed tomography-guided biopsy. Induction chemotherapy with cisplatin, etoposide, and ifosfamide was administered for 4 courses, leading to remarkable tumor shrinkage. Surgical intervention was recommended by the multidisciplinary team, since a residual viable tumor was noted on the positron emission tomography/computed tomography scan. Complete R0 resection was achieved. As of this writing, the patient is alive with a good performance status. ***(Thorac Med 2023; 38: 92-95)***

Key words: mediastinal seminoma, anterior mediastinal tumor

Introduction

Anterior mediastinal seminoma is uncommon, accounting for 2%-4% of mediastinal tumors [1]. Anterior mediastinal seminomas have no specific symptoms, such as cough and dyspnea, and therefore are mostly diagnosed after compression symptoms of the bronchus, lungs, heart, or great vessels appear. In this report, we present the case of a 29-year-old man with a huge mediastinal seminoma who underwent induction chemotherapy followed by complete surgical resection.

Case Description

A 29-year-old man with underlying hypertension without regular medication control was diagnosed with gastroesophageal reflux disease at a local clinic. He visited our hospital because of symptom progression despite medication, and that he had dyspnea while lying down. His vital signs were normal, and he had no fever, chest pain or consciousness disturbance. Chest radiography (CXR) revealed mediastinal widening and complete consolidation of left hemithorax. Computed tomography (CT) scan of the

[1]Division of Thoracic Surgery, Department of Surgery, Kaohsiung Veterans General Hospital, Kaohsiung, Taiwan
Address reprint requests to: Dr. En-Kuei Tang, Division of Thoracic Surgery, Department of Surgery, Kaohsiung Veterans General Hospital, No.386, Dazhong 1st Rd., Zuoying Dist., Kaohsiung City 813, Taiwan (R.O.C.)

chest revealed a huge anterior mediastinal tumor, measuring 20x15 cm, with pericardial invasion and moderate pericardial effusion(Fig. 1). Levels of tumor markers were measured. The beta-human chorionic gonadotropin (beta-HCG) and alpha-fetoprotein (AFP)levels were within a normal range, but the lactate dehydrogenase (LDH) level was elevated(3799U/L, normal range: 140-271U/L). An anterior mediastinal tumor biopsy was performed, and yielded a diagnosis of germ cell tumor (GCT).

The tumor's morphology led to a consideration of seminoma, and most immunomarkers were also compatible with this tumor, including positive for SALL4, CD117, and OCT3/4. Induction chemotherapy was administered with cisplatin, ifosfamide and etoposide (a VIP regimen) for 4 courses. After chemotherapy, the LDH level was down to 137U/L, and re-staging CT scan of the chest revealed a residual anterior mediastinal tumor, measuring 7.5 cm in maximum diameter(Fig. 2). Median sternotomy was performed to completely remove the anterior mediastinal tumor (Fig. 2),with partial resection of the invaded pericardium and left upper lobe of the lung. Pathology revealed a GCT resembling a seminoma (faint staining of SALL4 and OCT3/4 in the tumor necrosis area), status post-induction chemotherapy without residual tumor. The mediastinal tumor was finally staged as ypT0Nx. The patient recovered well post-operation, and had no recurrence in the 6-month follow-up.

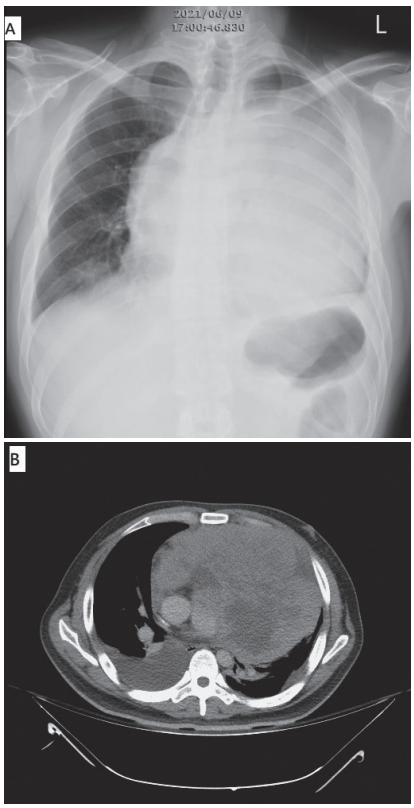

Fig. 1. Anterior mediastinal tumor with pericardial invasion before treatment.(A)Chest radiography; (B)Computed tomography of the chest.

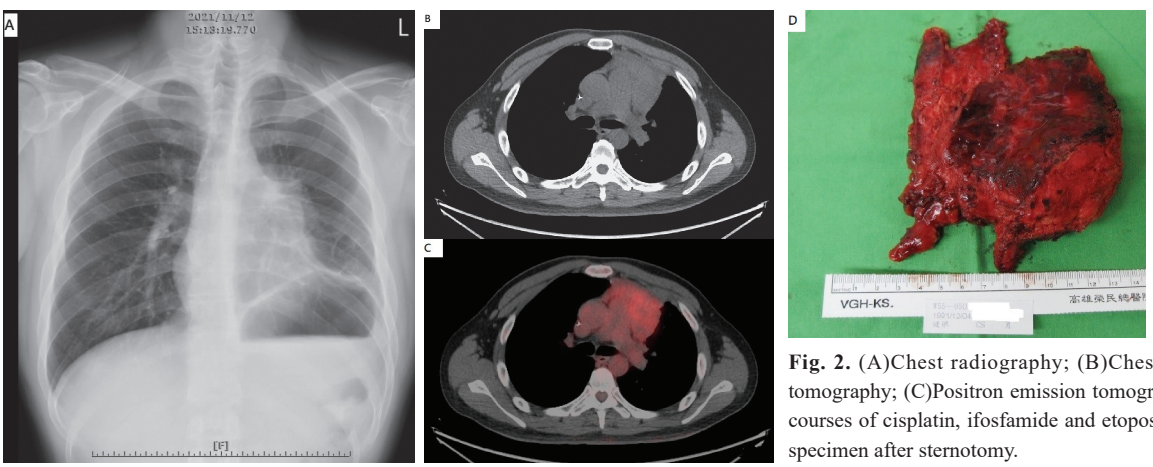

Fig. 2. (A)Chest radiography; (B)Chest computed tomography; (C)Positron emission tomography after 4 courses of cisplatin, ifosfamide and etoposide;(D) The specimen after sternotomy.

Discussion

Primary anterior mediastinal seminoma is always initially asymptomatic. Mediastinal seminoma is a slow-growing tumor that is usually diagnosed after mass compression of the great vessels, bronchus, or the heart. Approximately 39% of patients complain of chest pain, 29% have dyspnea and 22% experience cough at the time of diagnosis[2]. Anterior mediastinal seminoma commonly occurs in men aged 20-40 years with testicular tumors, usually with peritoneal lymph node metastasis [3]. Testicular palpation and sonography are necessary to assess the GCT. If a testicular tumor is detected, orchiectomy should be performed. In the differential diagnosis of anterior mediastinal tumor, seminoma or non-seminomatous GCT requires needle or open biopsy for confirmation. Seminomas do not produce AFP. Thus, an elevated serum AFP is inconsistent with the diagnosis of a pure seminoma and indicates that nonseminomatous elements are present, even if the histopathologic diagnosis is pure seminoma. Such tumors are treated as nonseminomatous GCTs.

Seminomas are sensitive to radiotherapy and chemotherapy. It is essential to identify distant metastasis because pulmonary metastasis and non-pulmonary metastasis have different outcomes, with extra-thoracic metastases associated with a poorer prognosis.

Most centers prefer chemotherapy rather than radiotherapy for patients with mediastinal seminoma, even when disease is limited to the mediastinum. This is due to concern about an increased risk of cardiovascular events, secondary malignancies, and other toxicity following mediastinal radiotherapy.

Efficacies of chemotherapy, radiotherapy and surgery have not been evaluated in randomized controlled trials, and treatments are still based on small case series and retrospective studies. First-line chemotherapy usually involves 4 courses of bleomycin, etoposide, and cisplatin. If patients cannot tolerate bleomycin, a non-bleomycin regimen should be chosen[4, 5].

Mediastinal radiotherapy should be carefully monitored to avoid radiotoxicity to other organs. Mediastinal radiotherapy is associated with coronary artery disease, lung fibrosis, and endocrine dysfunction[5].Most patients who receive primary radiotherapy are cured, but have a higher distant metastasis rate; thus, patients who relapse following primary radiotherapy can undergo salvage chemotherapy. In the study by Napieralska *et al*. [6], 5-, 10- and 15-year overall survival was 100%, 91% and 91%, respectively, after chemoradiotherapy. In our patient , a residual viable tumor was noted on the follow-up PET/CT scan after induction chemotherapy; thus, the multidisciplinary team recommended surgical resection for the remaining viable tumor, but no residual tumor in the pathology examination. At the 6-month follow-up, there was no recurrence noted on the CT scan of the chest. Whether the prognosis of mediastinal seminomas in all cases is as good with chemotherapy followed by surgical intervention is unclear; further research on the optimal treatment of mediastinal seminomas is still needed.

References

1. Bokemeyer C, Nichols CR, Droz JP, *et al*. Extragonadal germ cell tumors of the mediastinum and retroperitoneum: results from an international analysis. J Clin Oncol 2002;20: 1864-73.
2. Moran CA, Suster S, PrzygodzkiRM,*et al*.Primary germ cell tumors of the mediastinum: II. Mediastinal seminomas--a clinicopathologic and

immunohistochemical study of 120 cases. Cancer1997;80: 691-8.

3. DulmetEM, Macchiarini P, SucB,etal.Germ cell tumors of the mediastinum. A 30-year experience. Cancer 1993;72: 1894-901.
4. SamuelsML, Johnson DE, HoloyePY,*et al*. Large-dose bleomycin therapy and pulmonary toxicity: a possible role of priorradiotherapy. JAMA 1976;235: 1117-20.
5. Cameron RB, LoehrerPJSr, Thomas CR Jr. Neoplasms of themediastinum.In: DeVita VT Jr, Hellman S, Rosenberg SA, eds. Cancer: Principles andPractice of Oncology, Sixth Edition. Philadelphia: Lippincott-Raven Publishers, 2000: 1019-36.
6. Napieralska A, Majewski W, Osewski W, *et al*. Primary mediastinal seminoma. J Thorac Dis 2018 Jul; 10(7): 4335-4341.